University of Alberta

The Role of the Endothelial Cytoskeleton in Mediating Lymphocyte Transendothelial Migration

by

Amer Muhammad Hussain ©

A thesis submitted to the Faculty of Graduate Studies and Research in partial fulfillment of the

requirements for the degree of ***Master of Science***

in

Experimental Medicine

Department of ***Medicine***

Edmonton, Alberta

Fall 2004

Library and
Archives Canada

Published Heritage
Branch

395 Wellington Street
Ottawa ON K1A 0N4
Canada

Bibliothèque et
Archives Canada

Direction du
Patrimoine de l'édition

395, rue Wellington
Ottawa ON K1A 0N4
Canada

Your file Votre référence
ISBN: 0-612-95772-1
Our file Notre référence
ISBN: 0-612-95772-1

The author has granted a non-exclusive license allowing the Library and Archives Canada to reproduce, loan, distribute or sell copies of this thesis in microform, paper or electronic formats.

The author retains ownership of the copyright in this thesis. Neither the thesis nor substantial extracts from it may be printed or otherwise reproduced without the author's permission.

L'auteur a accordé une licence non exclusive permettant à la Bibliothèque et Archives Canada de reproduire, prêter, distribuer ou vendre des copies de cette thèse sous la forme de microfiche/film, de reproduction sur papier ou sur format électronique.

L'auteur conserve la propriété du droit d'auteur qui protège cette thèse. Ni la thèse ni des extraits substantiels de celle-ci ne doivent être imprimés ou aturement reproduits sans son autorisation.

In compliance with the Canadian Privacy Act some supporting forms may have been removed from this thesis.

While these forms may be included in the document page count, their removal does not represent any loss of content from the thesis.

Conformément à la loi canadienne sur la protection de la vie privée, quelques formulaires secondaires ont été enlevés de cette thèse.

Bien que ces formulaires aient inclus dans la pagination, il n'y aura aucun contenu manquant.

Canadä

"It is He Who has created you from dust, then from a sperm-drop, then from a leech-like clot; then does he get you out (into the light) as a child: then lets you (grow and) reach your age of full strength; then lets you become old, - though of you there are some who die before; - and lets you reach a Term appointed; in order that ye may learn wisdom."

Sura Mu-min (The Believer): Verse 67

"Education is our passport to the future, for tomorrow belongs to the people who prepare for it today."

Malcolm X

ACKNOWLEDGMENTS

I owe an immense debt of gratitude to my supervisor, Dr. Allan Murray. His help, guidance and support have been vital throughout my thesis project. Your passion for research has inspired me and shown me the true meaning of a scientist. Thank you for the skills you have given me.

Sincere thanks to all of my supervisory committee members, Dr. Larry Guilbert and Dr. John Elliott, and my external examiner, Dr. Barbara Ballermann, for your interest and advice. Luis, Qiu-Xia and Kathleen, thank you for all of the time you spent guiding me through the lab, your expertise was greatly appreciated. Thanks to Shazam, Saud, Sahar and Sana for your help in the preparation and revisions of my thesis.

To all of my family and friends that have stuck with me over the past two years and those that were willing to let me draw blood, I will always be grateful. Mom and Dad, thank you for you support, patients and advice. Mummy and Papa, thanks for the comforting words you have shared with me, you have made the past two years very enjoyable. Thanks to Cash Money whose companionship throughout my master will never be forgotten.

Finally to my wife Saba, I will never forget the time and sacrifices you gave for me to achieve all of my goals. Your love, understanding and belief in me helped get me through the trying times. I could not have done it without you by my side.

TABLE OF CONTENTS

CHAPTER 1. RATIONALE, HYPOTHESES AND LITERATURE REVIEW ___ 1

1.1 RATIONALE **1**

1.2 HYPOTHESES **2**

1.3 LYMPHOCYTE TRAFFICKING **4**

1.4 LEUKOCYTE ADHESION CASCADE **5**

1.4.1 Selectins *5*

1.4.2 Rolling *6*

1.4.3 Chemokines *9*

1.4.4 Activation *11*

1.4.5 Integrins *13*

1.4.6 Firm Adhesion and Locomotion *14*

1.5 TRANSENDOTHELIAL MIGRATION **17**

1.5.1 Overview *17*

1.5.2 Static Systems Used Studying TEM *19*

1.5.3 Shear Dependence *20*

1.6 ENDOTHELIUM **22**

1.7 ENDOTHELIAL CYTOSKELETON **23**

1.7.1 Composition *23*

1.7.2 F-actin *24*

1.8 ENDOTHELIAL INVOLVEMENT IN LEUKOCYTE TEM **26**

1.8.1 Remodelling of Endothelial Adherens Junctions 26
1.8.2 Remodelling of Endothelial Cytoskeletal Structures 28
1.8.3 Calcium Signalling Events 29
1.9 ENDOTHELIAL RESPONSES TO SHEAR STRESS **31**
1.9.1 Shear Stress Sensors in EC 31
1.9.2 Shear Stress Effect on Endothelial F-actin and Shape 33
1.9.3 Shear Stress Effect on New Gene Synthesis 34
1.10 CALPAIN **36**
1.10.1 Calpain's Structure and Regulation 36
1.10.2 Calpain's Biological Functions 38
1.11 SUMMARY **41**
CHAPTER 2. MATERIALS AND METHODS ________ **46**
2.1 GROWTH MEIDA AND ANTIBIOTICS **46**
2.2 SOLUTIONS AND BUFFERS **46**
2.3 REAGENTS AND ANTIBODIES **47**
2.4 CELL CULTURE **48**
2.4.1 Lymphocytes 48
2.4.2 Endothelial Cell Culture 49
2.4.3 Cell Viability Assay 52
2.5 ANALYSIS OF LYMPHOCYTE MIGRATION UNDER SHEAR FLOW **53**
2.5.1 Parallel Plate Laminar Flow Apparatus Setup 53
2.5.2 Lymphocyte Motion Analysis 55
2.6 RETROVIRAL INFECTION OF ENDOTHELIAL CELLS **56**

2.7 CONFOCAL FLUORESCENCE IMAGING 57

2.8 ANALYSIS OF CALPAIN ACTIVITY 58

2.8.1 Static Calpain Activity Assay 58

2.8.2 Calpain Activity Under Shear Flow Conditions 59

2.9 ICAM-1 LABELLING EXPERIMENTS 60

2.9.1 ICAM-1 Antibody Labelling 60

2.9.2 Adhesion Cup Assay System 61

2.9.3 Analysis of ICAM-1 Cup Formation 62

2.10 IMMUNOCYTOCHEMISTRY 63

2.10.1 F-actin Staining 63

2.10.2 Calpain Staining 64

2.11 FLOW CYTOMETRY 65

2.12 WESTERN BLOT ANALYSIS 65

2.12.1 F-actin/G-actin in vivo Assay 65

2.12.2 Cell Lysis 66

2.12.3 Immunoblotting 67

2.13 STATISTICS 68

CHAPTER 3. RESULTS ________ 69

3.1 PILOT STUDIES - OPTIMIZATION OF EXPERIMENTAL CONDITIONS .. 69

3.1.1 TNF-α is Required for Leukocyte Adhesion 69

3.1.2 Lymphocyte Cell Population 70

3.1.3 Determination of Appropriate Shear Conditions 72

3.1.4 SDF-1α and Binding Media are Required 72

3.2 EC F-ACTIN CYTOSKELETAL INVOLVEMENT IN LYMPHOCYTE TEM. 74

3.2.1 EC F-actin Remodelling is Required for Lymphocyte TEM............... 74

3.2.2 EC F-Actin Condenses Around the Migration Pore 75

3.3 EC CALCIUM FLUX IS REQUIRED FOR LYMPHOCYTE TEM 76

3.4 EC PI KINASES PARTICIPATE IN LYMPHOCYTE TEM........................... 78

3.4.1 Optimization of Experimental Conditions.. 78

3.4.2 PIK's Role in Lymphocyte TEM 79

3.5 EC CALPAIN'S ROLE IN LYMPHOCYTE TEM 80

3.5.1 Levels of μ- and m-Calpain in HUVECs 80

3.5.2 EC Calpain is Inhibited by Pretreatment with Calpain Inhibitors....... 81

3.5.3 EC Calpain is Required for Lymphocyte TEM 82

3.5.4 Calpain Activity is Increased in ECs Involved in TEM 83

3.5.5 μ-Calpain is Increased Around Areas of TEM 84

3.5.6 EC Calpain Inhibition Limits EC ICAM-1 Distribution........................ 84

3.6 AGENTS USED HAVE NO EFFECT ON LYMPHOCYTES 86

CHAPTER 4. GENERAL DISCUSSION ________________________________ 112

CONCLUSIONS 122

BIBLIOGRAPHY 123

APPENDIX A: FUTURE EXPERIMENTS ____________________________ 141

A.1 RATIONALE 141

A.2 PRELIMINARY RESULTS 142

A.2.1 EC ROCK's Involvement in Lymphocyte TEM 142

A.2.2 CNF-1 Rho Mobility Shift Assay.. 142

LIST OF TABLES

Table 3.1 Calpain inhibitions decreases ICAM cup formation around adherent lymphocytes 109

LIST OF FIGURES AND VIDEOS

Figure 1.1 The leukocyte adhesion cascade 42

Figure 1.2 Structure of the selectins 43

Figure 1.3 F-actin formation 44

Figure 1.4 Calpain strucure 45

Figure 3.1 TNF-α is required to allow lymphocyte interaction with HUVECs 88

Figure 3.2 HUVECs surface adhesion molecule expression in response to TNF-α treatment 89

Figure 3.3 Lymphocyte subpopulations 90

Figure 3.4 Higher concentrations of lymphocytes create increased interactive events between the endothelium and lymphocytes 92

Figure 3.5 SDF-1α and complete media affect lymphocyte TEM 93

Figure 3.6 Disruption of the endothelial F-actin cytoskeleton inhibits lymphocyte TEM 94

Figure 3.7 Jasplakinolide stabilizes the endothelial F-actin cytoskeleton 95

Figure 3.8 Endothelial F-actin localizes around the migration pore 96

Figure 3.9 Endothelial F-actin condenses around the migration pore 98

Figure 3.10 Lymphocyte TEM is dependent on endothelial Ca^{2+} 100

Figure 3.11 Effect of various wortmannin concentrations and incubation times in treated HUVECs on lymphocyte TEM and HUVEC viability 101

Figure 3.12 Endothelial PIK inhibition decreases lymphocyte TEM 102

Figure 3.13 Endothelial PI4K inhibits lymphocyte TEM.................................... 103

Figure 3.14 Robust expression of μ-calpain in HUVEC lysates 104

Figure 3.15 HUVECs possess constitutive calpain activity which is inhibited by ALLN and PD 150606 105

Figure 3.16 Endothelial calpain activity is required for efficient PBL TEM 106

Figure 3.17 Calpain activity is increased in HUVECs that participated in TEM 107

Figure 3.18 Endothelial μ-Calpain appears to localize around transmigrating lymphocytes 108

Figure 3.19 Calpain inhibitions decreases ICAM cup formation around adherent lymphocytes.. 110

Figure 3.20 Various agents have no affect on PBLs.. 111

Figure A.1 Endothelial ROCK inhibition decreases lymphocyte TEM 144

Figure A.2 CNF-1 stimulated Rho A activation 145

Video B.1 Lymphocyte are able adhere to the HUVEC monolayer but efficient TEM is absent 146

Video B.2 Efficient lymphocyte TEM requires SDF-1α pretreatment of HUVECs 146

Video B.3 Stabilization of the EC F-actin cytoskeleton inhibits lymphocyte TEM 146

Video B.4 EC F-actin localizes to areas of lymphocyte TEM.......................... 147

Video B.5 Cytoplasmic clumping around the migration pore is absent........... 147

Video B.6 Endothelial calpain activity is required for lymphocyte TEM. 147

LIST OF SYMBOLS AND ABBREVIATIONS

The following abbreviations, definitions and units have been used throughout this thesis.

Ab	antibody
ADP	adenosine diphosphate
AJ	adherens junction
ANOVA	analysis of variance
ATP	adenosine triphosphate
BAEC	bovine aortic endothelial cells
BAPTA-AM	1,2-bis(2-aminophenoxy)ethane-N,N,N',N'-tetraacetic acid
BHQ	2,5-di-tert-butyl-1,4-benzo-hydroquinone
BOC	tert-butoxycarbonyl-L-leucyl-L-methionineamide-7-amino-4-chloromethylcoumarin
BSA	bovine serum albumin
CD	cytochalasin D
CLA	cutaneous lymphocyte-associated antigen

CMFDA	cell tracker green
CMTMR	cell tracker orange
CNF-1	cytotoxic necrotizing factor-1
CR	consensus repeats
ddH_2O	double-distilled deionized water
E-selectin	endothelial selectin
EC	endothelial cell
ECGS	endothelial cell growth supplement
EDTA	ethylenediaminetetraacetic Acid
EGF	epidermal growth factor
ERM	ezrin, radixin, moesin
F-actin	filamentous actin
FBS	fetal bovine serum
FRET	fluorescence resonance energy transfer
g	gram
G-actin	globular actin
GDP	guanine diphosphate
GlyCAM-1	glycosylation-dependent cell adhesion molecule 1

GTP	guanine triphosphate
HBSS	Hank's balanced salt solution
HEV	high endothelial venules
HLA	human leukocyte antigen
HRP	horseradish peroxidase
HUVEC	human umbilical vascular endothelial cell
ICAM-1	intercellular adhesion molecule-1
IL-8	interleukin 8
IP_3	inositol 1-4-5 trisphosphate
JAM	junction adhesion molecule
JAS	jasplakinolide
kDa	kiloDaltons
L	litre
L-selectin	leukocyte selectin
LAD-1	leukocyte adhesion deficiency type 1
LFA-1	leukocyte function associated antigen 1
LN	lymph nodes
LPS	lipopolysaccharide

M	moles/litre
MAdCAM-1	mucosal-associated cell adhesion molecule 1
MCP-1	monocyte chemoattractant protein 1
MHC	major histocompatibility complex
MLCK	myosin light chain kinase
P-selectin	platelet selectin
P/S	penicillin/streptomycin
PBL	peripheral blood lymphocytes
PBS	phosphate buffered saline
PECAM	platelet endothelial cell adhesion molecule
PFA	paraformaldehyde
PI	phosphatidylinositol
PIK	phosphatidylinositol kinases
PI3K	phosphatidylinositol 3-kinase
PIP_2	phosphatidylinositol 4,5-bisphosphate
PLC	phospholipase C
PMS	phenazine methosulfate
PMSF	phenylmethylsulfonyl fluoride

PNAd	peripheral node addressin
PSGL-1	P-selectin glycoprotein ligand 1
PVDF	polyvinylidene difluoride
ROI	region of interest
RT	room temperature
S1P	sphingosine-1-phosphate
S1PRs	sphingosine-1-phosphate receptors
SDC	sodium diethyldthiocarbamate
SDF	stromal derived factor
SDS	sodium dodecyl sulfate
SDS-PAGE	sodium dodecyl sulfate-polyacrylamide gel electrophoresis
SEM	standard error of the mean
sER	superficial endoplasmic reticulum
SERCA	sarco/endoplasmic reticulum Ca^{2+}-ATPase
TEM	transendothelial migration
TNF	tumour necrosis factor
VCAM-1	vascular cell adhesion molecule-1
VE-cadherin	vascular endothelial cadherin

VEGFR-2	vascular endothelial growth factor receptor 2
VLA-4	very late antigen 4
XTT	2,3-bis(2-methoxy-2-nitro-5-sulfophenyl)-2H-tetrazolium-5-carboxanilide
YFP	yellow fluorescent protein
°C	degrees Celsius

Mathematical prefixes

m.................. .... milli (10^{-3})

μ.................. .... micro (10^{-6})

n.................. .... nano (10^{-9})

CHAPTER 1. RATIONALE, HYPOTHESES AND BACKGROUND

1.1 *RATIONALE*

Lymphocyte movement from the blood to the tissue is a fundamental feature of many inflammatory reactions such as allograft rejection [1]. ECs play an active role in lymphocyte recruitment to the inflammatory site. For example, ECs regulate the display of adhesion molecules on their cell surface which allows differential recruitment of specific leukocyte subpopulations to the tissue. Moreover, previous work indicates that ECs remodel their actin cytoskeleton and matrix adhesion structures to facilitate leukocyte recruitment and tissue infiltration [2]. Although in the recent years there have been considerable advances in deciphering the process of leukocyte TEM, the molecules which participate in TEM in ECs and leukocytes still remain poorly defined.

Evidence has accumulated to implicate leukocyte-stimulated reorganization of EC cytoskeletal structures in promoting leukocyte TEM. Adhesion of leukocytes to ECs stimulates calcium-dependent myosin light chain phosphorylation and increased endothelial contractility [3, 4]. TEM may be prevented by inhibition of these events or by depolymerization of endothelial F-actin [5]. Furthermore, structures linked to the cytoskeleton, such as the interendothelial adherens junctions (AJs) are remodelled during leukocyte diapedesis [6-8]. Therefore, this thesis investigated the role of the EC cytoskeleton in mediating lymphocyte TEM under physiological shear-stress conditions.

1.2 HYPOTHESES

As mentioned in the rationale, the EC cytoskeleton plays an important role in lymphocyte trafficking and can mediate lymphocyte TEM. A limitation of previous work studying the final phase of lymphocyte TEM has been the use of non-physiologic conditions and timeframes to analyse the outcomes. The focus of the project is to characterize the endothelial remodelling event and some of the molecules required for efficient lymphocyte TEM under shear stress conditions in vitro. The general hypothesis is that *endothelial cytoskeletal reorganization is required to support leukocyte transendothelial migration.*

Specific hypothesis, aims and experimental approach are described below:

Specific hypothesis: *EC reorganize F-actin structures at the interendothelial cell junctions.*

This project has the following aims:

Aim 1: To develop an in vitro model system of lymphocyte-EC interactions under flow conditions suitable for real time video and fluorescence microscopy. ***Experimental approach 1***: Previously published techniques in studying lymphocyte-EC interaction under a laminar flow system will be adapted to optimize for use in our system.

Aim 2: To characterize the dynamics of endothelial F-actin reorganization during lymphocyte TEM under shear stress conditions. ***Experimental approach 2***: EC will be treated with inhibitors of F-actin remodelling and placed into the laminar flow system. Real time images will then be collected and analysed to determine changes in lymphocyte TEM. Second, ECs will be transduced with a YFP-Actin construct and then placed into the laminar flow system to visualize cytoskeletal changes.

Aim 3: To identify the regulatory molecules involved in endothelial F-actin reorganization during lymphocyte TEM under shear stress conditions. ***Experimental approach 3***: Pharmacological inhibitors of various signalling pathways and regulatory molecules in EC will be implemented to assess their roles in lymphocyte TEM. Treated endothelial monolayers will again be subjected to the laminar flow system and analysed for changes in lymphocyte TEM.

1.3 LYMPHOCYTE TRAFFICKING

Lymphocyte movement from the blood into tissues is a key feature of inflammatory reactions such as allograft rejection [9]. Recruitment of leukocytes to the inflammatory site involves the active participation of EC. A series of discrete interaction between the leukocyte and the EC during leukocyte extravasation have been identified [9]. First the lymphocyte loosely adheres to adhesion molecules displayed by the venular endothelium to allow the leukocyte to sample the surface of the endothelium for a migration signal. Next, in response to a soluble chemoattractant, or solid-phase chemokine signal the lymphocyte β2 and β1 integrins are 'activated' to mediate firm adhesion to the endothelium via their EC ligands, intercellular adhesion molecule-1 (ICAM-1) and vascular cell adhesion molecule-1 (VCAM-1). Finally, the adherent leukocyte moves to a nearby junction. This locomotion step is required before diapedesis can occur [10]. Although much is know about these early steps of leukocyte recruitment, the molecular mechanisms involved in the final TEM step, remain poorly characterized. Interactions between the leukocyte and endothelium, and the specific adhesion molecules involved in these events are summarised in Figure 1.1.

1.4 ***LEUKOCYTE ADHESION CASCADE***

1.4.1 Selectins

The initial contact between a leukocyte and the endothelium is mediated by lymphocyte selectins and vascular endothelial addressins [11, 12]. Named for their cell-specific surface expression, selectins make up a family of carbohydrate-binding glycoproteins [13, 14]. Selectins are made up of an N-terminal extracellular domain followed by an epidermal growth factor like domain, and two to nine consensus repeats [15]. The selectins posses a short cytoplasmic tail and are inserted into the membrane via a hydrophobic transmembrane domain (Figure 1.2). The known selectin ligands are sulfated, fucosylated mucins containing clusters of sialic acid-rich-O-linked carbohydrate side chains [16]. Adhesion of the selectin to its ligand is independent of an activation signal [17].

There are three selectins, leukocyte (L-), endothelial (E-), and platelet (P-) selectin. The interaction of the selectins and their ligands are implicated in the trafficking specificity of various PBL subpopulations. L-selectin, present on lymphocytes, is involved with homing of naïve cells [18], whereas endothelial selectins, E and P are involved in leukocyte trafficking to inflamed endothelium [19, 20].

E-selectin is upregulated on inflamed ECs in response to treatment with inflammatory cytokines [21]. Cutaneous lymphocyte-associated antigen (CLA) is the ligand for E-selectin and is expressed by a subset of PBLs during naive to memory transition [22]. P-selectin is the largest of the selectins and is stored in Weibel-Palade bodies in EC [23-25] and in α-granules of activated platelets [23]. P-selectin is rapidly mobilized to the cell surface following stimulation with inflammatory mediators such as histamine, thrombin, or H_2O_2 [25, 26]. The ligand for P-selectin is P-selectin glycoprotein ligand 1 (PSGL-1). PSGL-1 is constitutively expressed on all lymphocytes, monocytes, eosinophils, and neutrophils [27]. P-selectin interacts with specific carbohydrate motifs on PSGL-1's surface [28].

1.4.2 Rolling

The result of the initial attachment of a leukocyte to the endothelium is a slower downstream movement of the leukocyte along the endothelium via transient, reversible, adhesive interactions. This process is referred to as rolling. As stated above the initial attachment of leukocytes from the blood stream to the EC is mediated mainly by the selectin family. However this process is not exclusively mediated by selectins since VCAM and VLA-4 interactions have the ability to support both capture and rolling [29]. All of the selectins are able to mediate rolling given the appropriate conditions.

The rolling stage of the cascade can be broken down into the initial capture of the leukocyte and then the rolling event. The process known as capture describes the first contact of a leukocyte with the endothelium. Once a leukocyte moves away from the central blood stream and closer to the endothelium, capture of the leukocyte can occur. EC activation increases adhesion molecules on the surface of the endothelium that are required to initiate capture. The primary adhesion molecule and ligand required for capture and the initiation of rolling is P-selectin, on the EC, and PSGL-1, on the leukocyte [30]. Although, PSGL-1 not present in high amounts on leukocytes, its high-affinity for P-selectin expressed on ECs makes it essential for capture and rolling to occur [31]. P-selectin's and PSGL-1's orientation on the surface of the endothelium and leukocyte respectively is thought to be the key feature of the molecules that aids in their interaction. PSGL-1 is concentrated on microvillus tips [30] and the binding domains of P-selectin and PSGL-1 are highly extended and project above the EC surface glycocalyx [31, 32], thus allowing specific interactions between the molecules to occur. L-selectin has also been suggested to play an important role in leukocyte capture [33, 34]. Since L-selectin is expressed on the tips of PBL microvilli, rather than on the cell body [35], the PBL is able to interact with the endothelium without becoming tightly adherent.

After leukocytes are captured they begin to roll. The velocity of rolling cells must be at or below that of the freely flowing cells, like erythrocytes, in the same vessel and the same radial position. The hydrodynamic force of the bloodstream acting on the adherent cell is the driving force for rolling [36]. Among the selectins, E- and P-selectin are the crucial selectins required for rolling. However, L-selectin is also involved in rolling. When E- and P-selectin is absent, trauma-induced rolling becomes L-selectin dependent, but the average leukocyte rolling velocity is three to five times faster in this case [34]. This increase in velocity implies that L-selectin is much less efficient than P-selectin in mediating rolling. Still, L-selectin is necessary for the normal capture and rolling functions.

In the absence of L-selectin, P-selectin can support both capture and rolling [37]. The critical role of P-selectin in the rolling phase of the adhesion cascade is supported in experiments done on gene-targeted mice. There is an absence of trauma-induced leukocyte rolling in mice lacking P-selectin [38]. These studies indicate that P-selectin is required to remove the leukocytes from the bloodstream and allow them to roll along the venular endothelium.

In contrast to L-selectin, E- and P-selectin appear to be functionally redundant in mediating leukocyte rolling on cytokine-activated endothelium [39]. E-selectin's specific role is mediating slow rolling [40]. The slow rolling aids the contact time a leukocyte makes with the inflammatory microenvironment of the endothelium. E-selectin is thought to facilitate the conversion of rolling leukocytes to enter into the firm adhesion stage of the cascade. Studies show that in response to local chemoattractant [41] or cytokine stimulation [42], E-selectin deficient mice have a reduced number of firmly adherent leukocytes. The lack of firmly adherent leukocytes is most likely related to the increased rolling velocities in the absence of E-selectin [40]. Although the selectins are the primary molecules that support capture and rolling, the α4-integrins have also been shown, both in vitro and in vivo, to be able to support capture and rolling [29, 43-45]. The rolling step is crucial for the leukocyte to proceed to the next stage in the cascade where a leukocyte can come in contact with the chemoattractant signal required to activate and target the leukocyte to proper area.

1.4.3 Chemokines

The chemokines are a superfamily of chemoattractant small secreted proteins that bind to and signal through receptors expressed on leukocytes. The chemokine receptors contain seven transmembrane loops and signal through heterotrimeric G proteins [46, 47]. Chemokines are transported and become immobilized on the surface of vascular endothelial cells on the endothelial glycocalyx. The endothelial glycocalyx consists of membrane-bound proteoglycans and glycoproteins that will bind the chemokines, preventing them from being released into the blood stream [48]. The bound chemokines then activate the leukocyte via the specific receptors present on the various leukocyte subsets. Chemokines also possess a chemotactic property, that allows the chemokine to direct the movement of a leukocyte to areas of increasing concentration of the chemokine where the leukocyte would be able to transmigrate [49].

There are four main classes of chemokines: C, CC, CXC and CXXXC. Chemokine amino acid sequences contain 20 to 70 percent homology. The class divisions arise from the relative position of their cysteine residues. C chemokines have only two cysteines, CC chemokines have the first two cysteine residues adjacent to each other, CXC chemokines have the first two cysteine residues separated by a single amino acid and CXXXC chemokines have three amino acids separating the first two cysteines [49]. There are greater than 40 chemokines classified based on their N-terminal cysteine residues [50-52].

The chemokine receptors are G-protein-coupled receptors that are expressed on the leukocyte. When a chemokine binds to its receptor, the receptor associates with a G-protein, allowing the exchange of guanine diphosphate (GDP) for guanine triphosphate (GTP) [47]. The GTP bound active state results in the disassociation of the Gα, Gβγ protein subunits. Downstream effectors within the cell are then signalled by the disassociated Gα, Gβγ subunits. These effectors include various tyrosine kinases, second messengers and members of the Rho family of small GTPases [53]. Activation of the various signalling cascades can result in actin polymerisation [54], cell shape changes [55], and activation of integrin adhesivity [56, 57].

A potent chemokine that activates a broad spectrum of lymphocytes is CXCL12-α (stromal derived factor (SDF) 1-α) [58-60]. SDF 1-α is widely expressed and was originally isolated in bone marrow stromal cells [61]. SDF 1-α is expressed in ECs from many different tissues including human bone marrow endothelium, skin endothelium and HUVECs [62-65], but is absent in leukocytes [66]. Tumor necrosis factor (TNF-α) is an inflammatory chemokines that can effect chemokine receptor expression. TNF-α can both down-regulate early expression [58, 59] and up-regulate late expression (24 h) of CXCR4, the receptor for SDF 1-α [67]. SDF-1α increases VLA-4 avidity on TNF-α stimulated ECs [68]. The increase in avidity caused by SDF-1α leads to increased numbers of lymphocytes that roll and firmly adhere to the endothelium.

1.4.4 Activation

Chemokines mediate the activation step of the adhesion cascade. They are able to induce rapid but transient increases in adhesion of leukocytes to immobilized integrin ligands [56, 69, 70]. The change in adhesion strength can be regulated via two different mechanisms. One is by upregulation of integrin affinity through conformational changes and the other is changes in integrin avidity which occur through integrin clustering [71-73].

Changes in integrin affinity by soluble chemokines has been observed when measuring the binding of soluble ICAM-1 and VCAM-1 to activated cells, [56, 69, 74] or the binding of antibodies that act as ligand mimetics [74]. The results found are not consistent in different cell types and with different integrins. SDF-1α is able to induce rapid binding of soluble ICAM-1 to lymphocytes [56], while binding to soluble VCAM-1 is minimal [69]. Whereas with regards to monocytes, SDF-1 is able to induce significant increases in the binding of soluble VCAM-1 [69, 74].

Chemokines are able to induce rapid clustering of integrins [56, 70]. An increase in integrin avidity is caused and thus the clustering of low affinity receptors strengthens adhesion to the ligands [75]. To achieve this increase in avidity, a protease-dependent release of integrins from cytoskeletal restraints is required [71, 74]. This will then allow the lateral mobility of integrins in the plasma membrane. It appears that changes in integrin affinity and avidity are regulated through different pathways. Inhibition of phosphoinositide-3 kinase (PI3K) or the Ca^{2+} dependent protease, calpain, can block chemokine induced clustering of LFA-1 ($\alpha L\beta 2$). However these inhibitors have no affect on the ability of chemokine-stimulated lymphocytes to bind soluble ICAM-1 [69].

The use of in vitro laminar flow chamber assays have been essential to studying the ability of chemokines to induce adhesion in the context of the adhesion cascade, since these flow chambers mimic blood flow. One major difference between the static adhesion assays and flow chamber assays is that the selectin-mediated rolling interactions become much more important under flow conditions. Leukocytes will not interact on surfaces coated only with ICAM-1 [74, 76, 77]. The chemokines that induce firm adhesion differ between the various leukocyte subsets. For example, in monocytes, monocyte chemoattractant protein 1 (MCP-1) will trigger the adhesion through CCR2 [78]; interleukin 8 (IL-8) signals neutrophils through CXCR1 and CXCR2 [79]; and eotaxin activates adhesion through CCR3 in eosinophils [80]. Common to all subset of leukocytes is that chemokine activation of integrins leads to the next stage of the adhesion cascade, firm adhesion.

1.4.5 Integrins

Integrins are the adhesion molecules responsible for inciting firm adhesion of the leukocyte to the endothelium [81, 82]. They are large, heterodimeric, transmembrane glycoproteins consisting of noncovalently associated large α (~1,000 a.a.) and small β (~800 a.a.) subunits [83]. Each subunit contains a large extracellular domain, a transmembrane segment and a short cytoplasmic tail [84]. In mammals, eighteen α and eight β subunits non-covalently combine to form 24 integrins [85-87]. Integrins contain binding sites for divalent cations Mg^{2+} and Ca^{2+}, which is a requirement for functional integrin:ligand binding [88]. The α-chains contain a metal ion-dependent adhesion site motif [84] and a β-propeller structure, formed from 7 N-terminal consensus repeat sequences [83], which are also involved in integrin:ligand interactions.

Inside-out and/or outside-in signalling by association of specific molecules with the C-terminal tails is the main mechanism by which the regulation of integrin states is controlled [89]. Arising from the intracellular compartment, inside-out signalling results in a change in integrin conformation in response to an activation signal [83]. Whereas, via an external signal, outside-in signalling results in an intracellular response, as is the case with cytoskeletal reorganisation following integrin:ligand interaction.

1.4.6 Firm Adhesion and Locomotion

Firm adhesion of leukocytes to the EC must have two key features: The conversion to firm adhesion must occur rapidly and adhesive interactions must be strong to resist detachment by disruptive shear flow [9]. Rolling allows the leukocyte to enter into close proximity with EC chemokines and integrin ligands [90]. Chemokine interaction with the leukocyte integrins leads to a rapid increase in integrin avidity [91]. This increase in avidity takes place within fractions of seconds [68]. Arrest can then occur immediately when the integrin avidity become sufficiently strong [77].

Integrins involved in leukocyte trafficking include: CD18 (β2) family (leukocyte function associated antigen 1; LFA-1) and α4β1 (very late antigen 4; VLA-4) [43, 81, 92]. LFA-1 is ubiquitously expressed by lymphocytes and is able to bind to endothelial ICAM-1 and ICAM-2 [93, 94]. ICAM-1 is expressed at low levels on EC, but can be upregulated upon cytokine stimulation. ICAM-2 is constitutively expressed on EC, and is not regulated by cytokines. In many models of inflammation, interfering with β2 integrin function is a very efficient way to prevent leukocyte recruitment. When β2 is absent or non functional, responses to exogenous chemoattractant are drastically reduced [95]. However, cytokine treatment still yields a robust inflammatory response in β2 null mice [96], implying that β2 integrins are not always required to participate in leukocyte arrest. VLA-4 is expressed on eosinophils, monocytes, and many lymphocytes [97], but only under special conditions is it seen on neutrophils [98]. Following PBL stimulation VLA-4 is induced and associates with EC VCAM-1 [81]. EC VCAM-1 is upregulated following cytokine stimulation, and has been show to support both rolling and firm adhesion [99, 100].

Using monocytes, the locomotion step of the adhesion cascade was recently identified as a key step in the pathway. Locomotion occurs when a monocyte moves from a site of firm adhesion to the nearest junction between EC to begin diapedesis [10]. The interaction of LFA-1 and MAC-1 with ICAM-1 and ICAM-2 mediated the locomotion. These results also implicate a greater function for the constitutive expressed molecule ICAM-2. Locomotion was also described previously with B lymphoblasts adhering and moving on planar lipid bilayers containing purified LFA-1 and ICAM-1 [101]. VLA-4-VCAM interactions have also been seen to support lateral migration of monocytes on the endothelium and again it was believed this occurred to allow the leukocyte to migrate to an interendothelial junction [102].

LFA-1 is not only involved in the firm adhesion stage. LFA-1 appears to make a contribution to neutrophil rolling by stabilizing the transient attachment or tethering phase of rolling [103]. Also recently, it was shown that in response to LFA-1 engagement the endothelium forms cup like structures that are enriched in ICAM-1. These structures surround the adherent leukocytes but they did not appear to be important for firm adhesion [104]. This implicates the role of the LFA-1:ICAM-1 interaction in leukocyte transendothelial migration.

1.5 TRANSENDOTHELIAL MIGRATION

1.5.1 Overview

After a leukocytes has become firmly adherent and locomotive it will travel to the EC borders where it will be able to transmigrate through the endothelial monolayer. This is the process referred to as leukocyte TEM or diapedesis (reviewed in [105]). There are two pathways that have been suggested for a leukocyte to travel across the endothelium. It is proposed that leukocyte TEM occurs either at EC borders [105] or by physically passing through the EC [106]. The more commonly followed method of TEM is thought to be that the EC borders are the location of migration. EC are linked laterally through tight junctions and AJs [107]. The junctional proteins, platelet endothelial cell adhesion molecule (PECAM), CD99 and junction adhesion molecule (JAM) -A and –C, have all been reported to play a role in leukocyte TEM.

PECAM-1 is known to be expressed leukocytes and at high levels at EC borders [108, 109]. The leukocyte PECAM interacts with EC PECAM during diapedesis. Interfering with the homophilic interaction in vitro and in vivo leads to a reduction of diapedesis of around 90% [110-112]. Interestingly, PECAM-1 deficient mice leukocyte recruitment varies only slightly from the wild-type animals [113]. These results along with the 10% of diapedesis that still occurs in the interaction interfering experiments suggest that PECAM is not the only molecule required for diapedesis.

CD99 is another molecule suggested as being intimately involved with leukocyte TEM. It is similar in expression to PECAM in that it is expressed on the surface leukocytes and is concentrated in EC borders [114]. Another similarity to PECAM-1 is that CD99 on leukocytes interacts with CD99 on EC during TEM. Using anti-CD99 antibody to block this interaction lead to a decrease in TEM by greater than 90% in vitro [114]. An additive effect is seen when both PECAM-1 and CD99 interactions where blocked, leading to a nearly complete prevention of TEM [114].

Both JAM–A and –C are also though to be involved in diapedesis. JAM–A is found at EC borders [115] and on leukocytes [116]. JAM-C is known to be present in HUVECs, most monocytes, B and T cells [117]. JAM–A involvement in both memory T cells and neutrophils TEM in vitro was seen using a polyclonal antibody for JAM–A [118]. JAM–A is also involved in monocyte TEM [115]. JAM–C has been seen to play a role in lymphocyte TEM [117]. Migration of lymphocytes was prevented when either soluble JAM–C or antibodies against JAM–C were used.

The number of cells located at a junction may also play a role in determining where a leukocyte is likely to transmigrate. Neutrophils preferentially migrate at tricellular junctions, a border where three ECs meet [119, 120]. Accordingly, in vitro adherens junctions appear discontinuous at tricellular junctions. However, it appears that the migration preference at tricellular borders is specific for neutrophils. Studies using a similar in vitro flow model show that monocytes commonly transmigrate between borders at two EC [6]. Also, at these sites AJs disorganize during monocyte migration [7]. The junctions undergo reversible changes and the entire junctional complex is able to reform itself in less than five minutes following diapedesis [6, 7].

1.5.2 Static Systems Used Studying TEM

Until recently, the use of transwell Boyden chamber assays has been the traditional method employed to study leukocyte TEM [121, 122]. In transwell boyden chamber assays, an EC monolayer is plated on a matrix over a filter that separates the surface EC from a well below. The EC would then be activated with inflammatory cytokines [102] and leukocytes would be placed on top. Then following a 1 – 4 h incubation, wells are analyzed to account for leukocytes that have migrated past the EC into the wells below [121, 122]. This method of studying TEM is effective but inefficient. One of the major concerns when using this assay is the inability to closely mimic physiological conditions. Chemokine gradients used to induce TEM are not similar to those found in vivo [65, 123, 124]. Another discrepancy is the use of non-physiological time frames. Work both in vitro [125] and in vivo [126-128] has shown that leukocyte TEM is very rapid taking only a few minutes for a cell to dive under an EC monolayer.

The extended contact times of the leukocyte with the EC cannot be realistically compared to physiological conditions. Long term adhesion signaling and the time required for a leukocyte to sense chemokine gradients are both examples of non-physiological mechanisms that could be at work in these systems [129]. Also transwell assays cannot focus in on the TEM step of the adhesion cascade, since they take into account all of the steps and migration through the filter. If an agent is used and it interferes with any of the stages, it will ultimately effect TEM [105]. It has also been reported that antibodies that were able to inhibit leukocyte TEM in the transwell assay also able to inhibit leukocyte migration through the bare filter [130, 131]. Therefore, use of the transwell Boyden chamber assays does not give an accurate representation of the migratory profile of leukocytes.

1.5.3 Shear Dependence

A newly developed method is currently the new standard used in studying lymphocyte TEM. This new methods differs from the transwell Boyden chamber assays in that a new factor is now considered, shear forces. Studies have shown that shear forces play a significant role in lymphocyte and eosinophil TEM [125, 132-134]. They are able create, in the presence of chemokines, promigratory signals that the lymphocyte and eosinophil use in order to transmigrate [134, 135]. This new factor also decreased the TEM time to more physiological levels [125].

The new assay will be discussed in greater detail in the Materials and Methods chapter. It is reviewed in [129]. Essentially, EC are plated to confluence on cell culture dishes and a parallel plate flow chamber apparatus is placed on top with a narrow gap to allow for leukocyte EC interaction. EC are treated with proinflammatory cytokines, to increase cell adhesion molecule expression, prior to the perfusion of leukocytes over the monolayer. The perfused leukocytes can be tightly regulated to control the shear forces at which they are applied. Interaction throughout the adhesion cascade can then be captured using video microscope in ~20 min time frames. The collected videos can then be analyzed to check for leukocytes undergoing all of the stages from rolling to firm adhesion and TEM. This new flow chamber assay is now an essential technique utilized when studying leukocyte TEM since it incorporates shear forces and allows researchers to differentiate between effects on different steps in the adhesion cascade.

1.6 ENDOTHELIUM

The endothelium is a single layer of cells that line the lumen of the heart, all blood vessels and lymphatics vessels. ECs originate embryologically from the mesoderm [136]. The primary function of EC is maintenance of vessel wall permeability [137]. However, EC are involved in many different functions also such as blood vessel formation, coagulation and fibrinolysis, regulation of vascular tone and as seen above EC play a critical role in inflammatory reactions [138]. An important part of the endothelium is their tight and AJs. These junctions hold the ECs together laterally. At locations in the endothelium where a strict regulation of exchange between the blood and tissue is required, such as the blood-brain barrier, tight junctions are present [139]. The tight junctions' main function at these areas is to rigorously regulate paracellular permeability. The AJs are involved with maintenance EC monolayer stability and also regulation of paracellular permeability [140]. AJs consist of cadherins and catenins. Cadherins are extracellular adhesion molecules that interact via their cytoplasmic tail, with a network of intracellular cytoplasmic proteins, catenins. The catenins then link the AJs to the EC cytoskeleton by interacting with the actin microfilaments [141]. Since the EC cytoskeleton is connected via this junction and transmigrating leukocytes must pass them, it seems likely that with regards to PBL TEM, the endothelium would play an active role.

1.7 ENDOTHELIAL CYTOSKELETON

1.7.1 Composition

The endothelial cytoskeleton has many different functions. The cytoskeleton is known to play a significant role in cell motility, endothelial integrity and repair, cell adhesion and leukocyte TEM [142-144]. It is composed of three kinds of protein filaments, microtubules, intermediate filaments and microfilaments. The focus of the discussion will be on the microfilaments. Microtubules have many different activities in the cell including chromosome segregation during mitosis vesicle transport and directional cell migration [145, 146]. Microtubules are made up of $\alpha\beta$ tubulin heterodimers that self form by adding onto the different ends of the microtubule [147]. The tubulin subunits α and β are highly homologous and stable [146, 147]. Stability is lost when the cap of tubulin GTP at the ends is lost, and once unstabilized the microtubules can depolymerize [146]. The two ends on microtubules are differentiated by the speed at which the ends grow and shorten [148]. The faster end is referred to as the plus end and has a β-tubulin unit exposed while the slower or minus end has an α-tubulin unit exposed [149]. The heterodimers arrange in a linear fashion to create protofilaments which can then form the microtubule wall [148, 150].

Intermediate filaments are made up of many proteins. One of the largest families of genes in the human genome is where the intermediate filaments arise from [151]. There are five different categories of intermediate filaments, types I-IV, which are localized in the cytoplasm and type V which is found in the nucleus [152].

1.7.2 F-actin

The F-actin portion of the EC cytoskeleton is also known as the microfilaments. Microfilaments are made up of monomers of the protein actin (globular or G-actin) which polymerize to form long, thin fibres. F-actin cytoskeleton is has many roles in the cell, including force generation, wound repair, cell motility, signal transduction and maintenance of structural integrity [145, 153-155]. In ECs, F-actin normally forms central stress fibres that can be found centrally throughout the cell and a dense sheet directly under the plasma membrane known as cortical actin [156]. It is also found at the leading edge of motile cells in lamellipodia and filopodia [157, 158].

A key feature of F-actin microfilaments is that they are dynamic, constantly being remodelled within a cell (Figure 1.3). Individual G-actin units form two chains that wind around each other to form F-actin. Like the microtubules, F-actin has a fast plus where assembly occurs quicker than the slower minus end, giving a defined polarity to each actin subunit. The two ends can also be described as the barbed and pointed ends. At the barbed end association of individual G-actin units occurs faster than the pointed end [159]. Polymerization and depolymerization of the filaments is controlled by adenosine triphosphate (ATP). When the actin monomers are bound to ATP, polymerization can occur and then when the ATP is hydrolysed to adenosine diphosphate (ADP) actin depolymerization occurs [160].

F-actin filament formation and remodelling is tightly regulated by a variety of actin binding proteins, including ADF/cofilin, gelsolin, profilin, WASp/Scar and Arp2/3 complex [161]. There are many other proteins involved in the process, however this discussion will focus on the listed proteins. ADF/cofilin promotes phosphate dissociation from ATP-actin filaments and dissociation of ADP-actin form the microfilament ends [159]. It is also able to cap and sever ADP-actin microfilaments. Gelsolin possesses similar features as ADF/cofilin [161]. They both alter the conformation of the actin filament, and sever and cap F-actin. Binding affinities are higher for ADP-G-actin as opposed to ATP-G-actin. Although gelsolin severing action is greater than ADF/cofilin, the preferred regulatory mechanism of microfilament reorganization is ADF/cofilin [162]. Profilin catalyzes the exchange of ADP for ATP in released G-actin subunit [163]. WASp/Scar proteins and Arp2/3 complex function in the formation of new F-actin filaments branching out from the existing filament [159]. Actin monomers and Arp2/3 complex are brought together by activated WASp/Scar proteins. Arp2/3 nucleates the assembly of new actin filaments on the existing F-actin filament [161]. The F-actin cytoskeleton is a very dynamic and highly regulated component of the EC, and thus it is likely that EC F-actin remodelling would play a role in lymphocyte TEM.

1.8 ENDOTHELIAL INVOLVEMENT IN LEUKOCYTE TEM

1.8.1 Remodelling of Endothelial Adherens Junctions

Previous studies have implicated the involvement of the EC cytoskeleton in lymphocyte TEM. Interendothelial AJs, which are linked to the cytoskeleton, are remodelled during leukocyte TEM [6-8]. Vascular endothelial (VE) -cadherin, an integral member of the AJ, was visualized in EC using a VE-cadherin-GFP. During leukocyte adhesion and diapedesis transient gaps between adjacent EC formed. It appeared that VE-cadherin displaced around the transmigrating leukocyte and following diapedesis the AJ was restored [6]. Monocyte TEM also shows a change in vascular EC cadherin complex of AJs. Under flow conditions, a loss in the staining of VE-cadherin and α–, β–catenin and plakoglobin was shown in areas of monocyte TEM. After diapedesis is complete the events were reversed again indicating that a remodelling of the AJ was occurring [7]. In a more recent study with dual immunofluorescence staining and confocal microscopy, it was visualized that when a neutrophil undergoes TEM many AJ components located at the site of diapedesis are lost. Staining of VE-cadherin, α–, β–catenin and plakoglobin was discontinuous only at sites of neutrophil TEM [164].

Proinflammatory mediators such as thrombin cause EC AJs to disassemble thus increasing EC permeability [165]. Signalling cascades in EC are activated by thrombin through protease-activated receptor-1 (PAR-1) [166]. The result of PAR-1 activation is an increase in intracellular Ca^{2+} and stimulation of protein kinase C and MLCK, thus activating EC actin-myosin contraction [167]. EC Rho GTPases are also involved in increasing EC permeability by mediating MLC phosphorylation [168]. Thrombin activates Rho A which induces actin polymerization, stress fiber formation, and cell rounding to cause the increase in EC permeability [169]. VE-cadherin junctions regulate endothelial barrier function. Thrombin's ability to increase EC permeability by disassembly of the AJs is thought to be through disruption of VE-cadherin [170]. The pathway of AJs remodelling may mimic the process of leukocyte TEM due to the similarities of MLCK phosphorylation and disruption of AJs.

The process of VE-cadherin displacement of during leukocyte TEM is currently under debate. One method suggested involves signalling events triggered by leukocyte adhesion causing VE-cadherin destabilization. The disrupted AJs would then form gaps allowing the leukocyte to transmigrate through the EC monolayer [171]. A second possible method of VE-cadherin displacement involves the migrating leukocytes pushing VE-cadherin out of the junction thus allowing their passage through the intercellular gaps [6]. As stated above during leukocyte adhesion and diapedesis transient gaps between adjacent EC formed. VE-cadherin displaced around the transmigrating leukocyte and following diapedesis the AJ was restored. Narrow contact between the leukocyte and EC is seen. The third possible role is that neutrophil elastase degrades components of the VE-cadherin complex [172]. Membrane-bound elastase localizes to the front of the migrating neutrophil and aids in TEM [173]. Also inhibition of elastase attenuates neutrophil TEM [174]. However elastase may not be required for leukocyte TEM since in neutrophil elastase-deficient mice transmigration of neutrophils is unchanged as compared to wild-type mice [175].

1.8.2 Remodelling of Endothelial Cytoskeletal Structures

EC matrix adhesion structures are linked to the EC cytoskeleton. The matrix adhesion of focal adhesion complex mediates association of the EC to the basement membrane. Paxillin, talin and vinculin are all proteins involved in linking the focal adhesion to the actin cytoskeleton [176]. EC focal adhesions are remodelled to facilitate leukocyte recruitment and TEM [2]. Following lymphocyte adhesion to ECs, focal adhesion complexes in EC were seen to be remodelled.

Preventing focal adhesion remodelling by ECs pretreatment with an antibody inhibited lymphocyte TEM. This data strengthens the role of the actin cytoskeleton in mediating leukocyte TEM.

It has also been shown that disruption of EC microfilaments decreases leukocyte TEM [5]. Using a static system of leukocyte EC interactions, ECs were pretreated with CD to destabilize their F-actin cytoskeleton. Microfilament disruption leads to a significant decrease in monocyte TEM. Another recent study has shown a possible role of ICAM-1:LFA-1 interactions in TEM [104]. ECs actively formed ICAM-1 microvilli-like membrane projections that were enriched in actin when ICAM-1:LFA-1 binding occurred. These projections where shown to have no effect on firm adhesion. Interestingly, treatments that prevented the projections included CD, colchicine and BAPTA-AM, all of which can also prevent leukocyte TEM in static systems [3, 104, 177, 178]. Also the time frames shown for their formation correspond to those needed for efficient TEM. Taken together, all of these studies show that the EC cytoskeleton is definitely involved in leukocyte TEM.

1.8.3 Calcium Signalling Events

Leukocyte TEM has also been linked with Ca^{2+} events. Within EC a transient increase in intracellular free Ca^{2+} required to allow a leukocyte to transmigrate

[3]. Maintaining Ca^{2+} levels at resting levels prevented neutrophil TEM but had no effect on adhesion. The increase in calcium concentrations is limited to those ECs that are next to the transmigrating cell [179]. Also, adhesion of leukocytes to the endothelium stimulates a Ca^{2+}-dependent myosin light chain phosphorylation and increased endothelial contractility [3, 4]. Myosin light chain kinase is activated when there is an increase in the intracellular free Ca^{2+} levels. This leads to myosin II unfolding which increases tension on actin filaments near EC borders and thus causing EC retraction from EC borders [4, 105]. When EC myosin light chain kinase is inhibited, in vitro, neutrophil TEM and EC actin cytoskeletal changes are prevented [180]. An increase in EC intracellular Ca^{2+} as a prerequisite for TEM is also seen with monocytes TEM [181]. Monocyte adhesion leads to the increase. When EC are pretreated with BAPTA-AM to chelate intracellular Ca^{2+}, monocyte TEM is reduced. Similar results have also been reported in brain ECs. Chelating intracellular calcium diminishes T lymphocyte TEM again without affecting adhesion [178]. Taken together these results indicate a significant role for Ca^{2+} in mediating leukocyte TEM by cytoskeletal reorganization through myosin light chain dependent contraction.

1.9 ENDOTHELIAL RESPONSES TO SHEAR STRESS

1.9.1 Shear Stress Sensors in EC

ECs are able to respond to shear stress. They accomplish this through putative shear stress receptors present on various regions of the EC. Cell-cell junction molecules, cell-extracellular matrix molecules, membranal structures and the endothelial cytoskeleton all have been implicated in the ability to sense shear stress forces [182]. Some of the molecules thought to play a role in supporting leukocyte TEM have also been identified as shear-stress sensors. For example, PECAM-1 becomes tyrosine phosphorylated rapidly in response to shear stress on the endothelium [183]. Phosphorylated PECAM-1 binds to the cytoplasmic tail of SHP-2. This leads to a signalling cascade that causes ERK 1/2 activation. When inhibiting expression of PECAM-1 or SHP-2, shear stress induced ERK 1/2 activation is blocked. The rapid changes that occur to PECAM-1 in response to fluid shear stress suggest that PECAM-1 can act as a mechanoreceptor [182, 183].

Molecules present in the adherens junctions can sense fluid shear stress. VE-cadherin is able to transfer information intracellularly through interaction with the EC cytoskeleton via linking molecules, such as β-catenin [184, 185]. Following

EC exposure to laminar shear stress, VE-cadherin, β-catenin, and vascular endothelial growth factor receptor 2 (VEGFR-2) form a complex that is linked to the EC cytoskeleton. When VE-cadherin is absent in EC, as in VE-cadherin null ECs, shear stress mediated events, including phosphorylation of Akt and p38, do not occur [186]. These results imply a significant role for VE-cadherin in shear stress transduction.

Integrins are capable of being mechanoreceptors. Previous studies have shown that integrins are able to convert mechanical stimuli into biochemical signals [187]. In coronary arteries, flow induced vasodilatation can be prevented when blocking antibodies to the integrin β3 chain are present [188]. The αvβ3 integrin is involved in the shear stress pathways of IkB kinase activation and phosphorylation of the VEGF receptor Flk-1 [189, 190]. The β2 integrin is suggested to play a role in the shear stress activation of ERK 1/2 [191]. Taken together these results implicate a strong role for the integrins in sensing fluid shear stress.

G proteins are another mechanoreceptor present in ECs. Interfering with G protein function can significantly affect shear stress induced events. Shear stress activation of ERK 1/2 is inhibited when ECs are treated with pertussis toxin [192]. Also, ras-GTPase shear stress induced activity is prevented when ECs are treated with anti-sense oligonucleotides to Gαq [193].

The endothelial cytoskeleton's role in sensing shear flow is thought to be as a common structure that integrates signals or information from all of the shear stress receptors [182, 183]. The EC cytoskeleton is able to bind directly, or indirectly, to all the mechanoreceptors stated above and it can also respond to fluid shear stress. When the actin cytoskeleton is disrupted, shear stress mediated signalling is inhibited [194]. These data imply that the EC actin cytoskeleton is intimately involved with shear stress responses.

1.9.2 Shear Stress Effect on Endothelial F-actin and Shape

EC are able to adapt to shear stress if present for a sustained period of time. ECs change their morphology and align in the direction of flow. This is accomplished by changes in the EC cytoskeleton [182, 183, 195, 196]. Confluent endothelial monolayers exposed to prolonged laminar shear stress causes cortical actin stress fibres to reform in the direction of flow. Actin assembly is virtually absent in static situations. Following flow conditions of 15 dyne/cm^2, at 8 h actin stress fibres extend in random directions. At 16 h, the majority of actin stress fibres extend parallel and are aligned with the direction of shear stress. This causes the cell to extend in the direction of the shear vector. At 48 h the majority of cells are now aligned with the shear vector and actin assembly continues to proceed [197]. The intermediate filaments and microtubules demonstrate similar features in response to shear stress [198].

Along with changes in the actin cytoskeleton, the actin cytoskeleton also has decreased interaction with VE-cadherin and β-catenin, members of the adherens junction [196, 199]. Increased tyrosine phosphorylation of β-catenin, in response to shear stress, causes a disassociation of both VE-cadherin and β-catenin from SHP-2 and α-catenin, the actin anchoring molecule [182, 196]. Thus, in response to shear stress, the EC actin cytoskeleton reorganizes in the direction of the shear vector and separates from the adherens junction.

1.9.3 Shear Stress Effect on New Gene Synthesis

Shear stress at arterial levels can influence gene expression within the EC. There are three patterns of gene expression. The first are genes that are transiently upregulated. Genes in this group include c-Fos [200], platelet derived growth factor A and B [201, 202], early growth response factor 1 [201], ICAM-1 [203] and MCP-1 [204]. Second are genes that have sustained expression in response to flow. Genes in this group include endothelial isoform of nitric oxide synthase, cyclooxygenase 2, superoxide dismutase, and transforming growth factor β [205, 206]. Thirdly are those genes that are down regulated in response to flow. The genes in this group include endothelin and VCAM-1 [207, 208].

Duration of shear stress can also play a role on gene expression in the endothelium. Experiments were run using acute shear application for 2 or 6 h or chronic shear application for 24 h [209, 210]. Three conclusions were drawn from these experiments. First, physiological levels of laminar shear stress regulate perhaps hundreds of EC genes. Second, under the chronic shear application the majority of genes are suppressed. Thirdly, genes that regulate activation of the endothelium are regulated by acute shear application and appear to be affect by the conversion of static to flow states [182]. Under chronic conditions it is reported that many pro-inflammatory genes including MCP-1, ICAM-2 VCAM-1 and PECAM-1, and signalling genes including integrins and VE-cadherin are down regulated. The data here indicates that ECs are greatly influenced by shear stress and that changes in the shear stress expression pattern on the endothelium may play a significant role in vascular inflammation.

1.10 CALPAIN

1.10.1 Calpain's Structure and Regulation

Calpain, a family of Ca^{2+} dependent thiol protease, has been show to play a role in cytoskeletal remodelling, proliferation, motility and apoptosis [211-213]. Calpain is critical for development as shown by calpain regulatory subunit null mice that die with defects in vascular development during embryonic development [214]. There are many forms of calpain that are widely expressed with both ubiquitous and tissue specific isoforms in humans. Calpain consist of two subunits that exist as heterodimers. The small subunit (28 kDa) is a common regulatory subunit (Calpain 4). The large subunit (80 kDa) expresses different isoforms. The two ubiquitously expressed isoforms are μ-calpain (Calpain 1) and m-calpain (Calpain 2). Calpains contain six domains, I-IV in the large subunit and V-VI in the small subunit (Figure 1.4). Domain I and II contain the protease function, domain III is involved with calcium binding, membrane targeting and phospholipid binding [215] and domain IV and VI contains putative Ca^{2+}-binding EF hands [214].

The two ubiquitous isoforms are similar in structure but differ by the calcium concentrations in vitro required for activation, μ-calpain needing micromolar concentrations between 5 and 50 μM and m-calpain requiring millimolar concentration between 0.2 and 1.0 mM [216]. Calpain activation in vivo remains a mystery since calcium concentrations are only around 50 – 400 nM [211, 217-221]. There are many proposed models of calpain regulation, including interaction with phospholipids, membrane localization, autolytic self-activation and binding activator proteins [216, 222]. Phosphatidylinositols (PI) are also thought to be involved in the activation calpain. Phosphatidylinositol 4,5-bisphosphate (PIP_2) has been shown to promote calpain action in physiological calcium ranges [223]. For μ-calpain the Ca^{2+} requirement for activation is reduced to the upper limits of in vivo Ca^{2+}, therefore in response to localized Ca^{2+} spikes calpain could become activated. Calpain exist in cells with its endogenous inhibitor calpastatin. In response to specific stimuli including a rise in intracellular calcium, activation of the v-Src oncoprotein, or ischemic injury, calpain is able to degrade calpastatin, thus disassociating from it and enhance its own activity [224].

Phosphorylation sites for serine, threonine and tyrosine are present on many areas of calpain [211]. Growth factor signaling pathway activation of calpain has shown the physiological relevance of calpain phosphorylation. Epidermal growth factor (EGF) stimulation of cells via the ERK/MAP kinase signaling pathway activates calpain [225, 226]. However, phosphorylation events may also inhibit calpain activation. The chemokine IP-10 inhibits m-calpain through a PKA-dependent phosphorylation pathway [227]. It would appear that regulation by phosphorylation functions cooperatively by having the ability to both activate and inhibit calpain.

Calpain localization is another method of regulation. Active calpain is predominately found at the plasma membrane. In activated T-cells, active calpain was found to localize to the membrane fraction and associate in a complex with membrane associated proteins such as talin and β1-integrin [228, 229]. It is thought that calpain could localized in the area of a Ca^{2+} channel in the plasma membrane thus aiding in the Ca^{2+} requirement for autolysis [211]. Localization to the plasma membrane would also bring calpain into contact with PIP_2, which is located on the plasma membrane [230, 231]. As a whole, the data shown here with regards to calpain activation indicates that tight regulations are in place to guide proper calpain activity.

1.10.2 Calpain's Biological Functions

Calpain has been identified to play a significant role many biological pathways. Generation of calpain knock out animals has been one of the methods used to gain greater understanding into calpain's biological functions. One pathway identified is the ERK/mitogen-activatied protein kinase pathway. Calpain activation is required downstream of the pathway for EGF receptor-mediated fibroblast motility [225, 226]. Fibroblast activation was seen to be specific for m-calpain only. In this pathway, calpain becomes phosphorylated, increasing calpain activity, which then leads to increased cell motility [225].

Calpain is also thought to act in signal transduction at a site upstream of the Rho family [232]. Inhibiting calpain in bovine aortic endothelial cells (BAEC) alters BAEC's ability to form actin filament networks, stress fibres and focal adhesions. By inhibiting calpain, BAEC expressing constitutively active Rho A but not those constitutively expressing Rac1, could still form focal adhesions and stress fibres [232]. BAEC expressing active Rac1 could, form networks of subcutaneous actin fibres and focal complexes [233]. Calpain's involvement in the formation of Rho-mediated stress fibres in calpain $4^{-/-}$ embryonic fibroblasts is contradictive of these results. The embryonic fibroblasts have enhanced formation of filopodia and lamellipodia [213, 214]. The results demonstrate that calpain is involved in Rho family activation but the pathway of activation is still unknown.

Calpain $4^{-/-}$ embryonic fibroblasts are viable, proliferate and have no calpain activity [211]. These fibroblasts are not able to undergo normal remodelling of cytoskeletal/membrane attachments [213]. The calpain $4^{-/-}$ embryonic fibroblast have a loss of central stress fibres, decreased migration rates, enhanced formation of filopodia and lamellipodia and have a decreased number of focal adhesions. They also do not degrade talin, a component of the focal adhesion complex which is degraded in vitro by calpain [211].

One of the most documented roles for calpain is in remodelling cytoskeletal/membrane attachments. Calpain action on the cytoskeleton is thought to be involved with cell spreading, migration, focal adhesion remodelling and rear detachment [212, 225, 228, 232, 234]. Calpain degradation of focal adhesions at both the leading and the rear edges of cells is required for cell spreading and motility [214, 235]. Intergrin-linked focal adhesions are the main links from the actin cytoskeleton to the extracellular matrix [236]. In cell migration calpain is thought to act at the rear of the cell in weakening the intracellular links to integrin. Studies of migrating cells on varying matrix adhesion strengths demonstrate this. Cells that are plated on high adhesive strength matrix are unable to detach the rear of their cell when calpain is inhibited and will leave behind integrin on the surface of the matrix [212, 237]. Ezrin, radixin and moesin (ERM) proteins are known to be putative calpain targets. ERM proteins function in linking the cortical actin cytoskeleton to the membrane [238]. Ezrin is cleaved by calpain during cell motility to allow cytoskeletal reorganization to occur [239]. Taken together, these results suggest that calpain activity functions in altering cytoskeletal structures. It seems likely that calpain would also be involved in other cellular processes that require cytoskeletal remodelling, namely leukocyte TEM.

1.11 SUMMARY

The leukocyte adhesion cascade in inflammation is critical to the understanding of many diseases throughout the body, from allograft rejection to arthritis to periodontal disease. Much work has been done on studying and regulating rolling, activation and firm adhesion, the early steps in the cascade. However, recently research on the final stage, leukocyte TEM, has only recently been increasing. Much of this is due to the recent development of a flow system that incorporates an additional factor, shear stress. The endothelium is emerging as an active part of diapedesis. Cytoskeletal remodelling events and signalling pathways appear to be vital in deciphering the process of TEM.

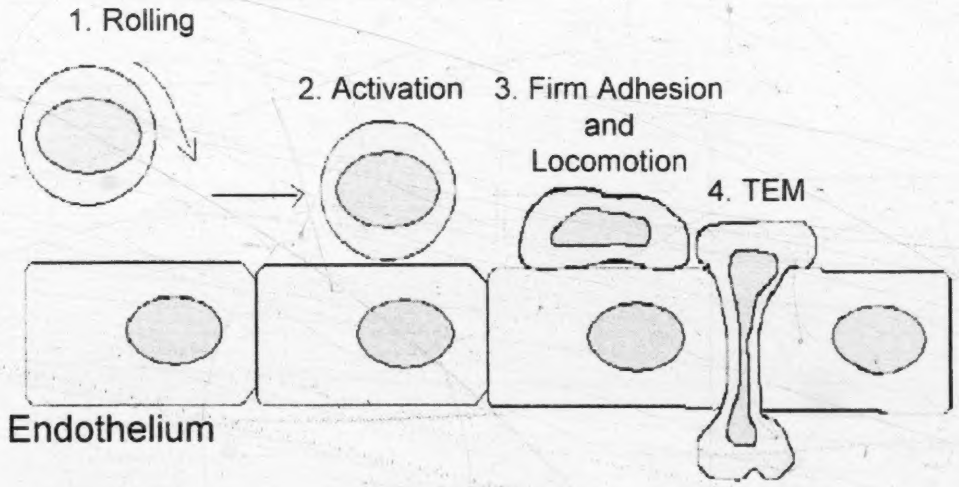

Figure 1.1 The leukocyte adhesion cascade. The sequence of events culminating in Leukocyte TEM is outline. Initially, leukocytes in the blood stream approach the vessel wall and (1) engage in transient interactions with the EC via selectin:addressin interactions. (2) Activation of the leukocyte occurs once the leukocyte comes into contact with a chemokine signal and this facilitates the (3) firm adhesion and locomotion step via integrin:Ig interactions. (4) The final stage, TEM, is the focus of my project. *Adapted from [125]*

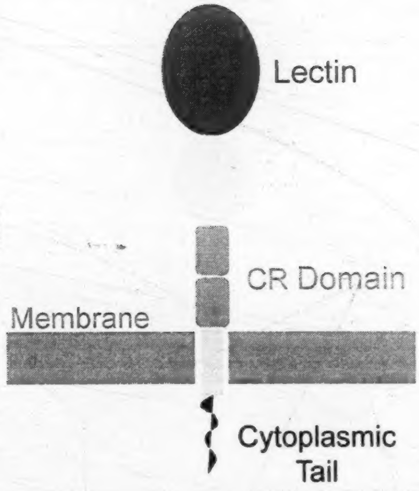

Figure 1.2 Structure of the selectins. Selectins consist of a lectin N-terminal domain (dark blue) followed by an epidermal growth factor like domain (cyan), and two to nine consensus repeats (CR) (red), L-selectin is shown. The selectins posses a short cytoplasmic tail (black) and are inserted into the membrane (grey) via a hydrophobic transmembrane domain (green). Adapted from [240].

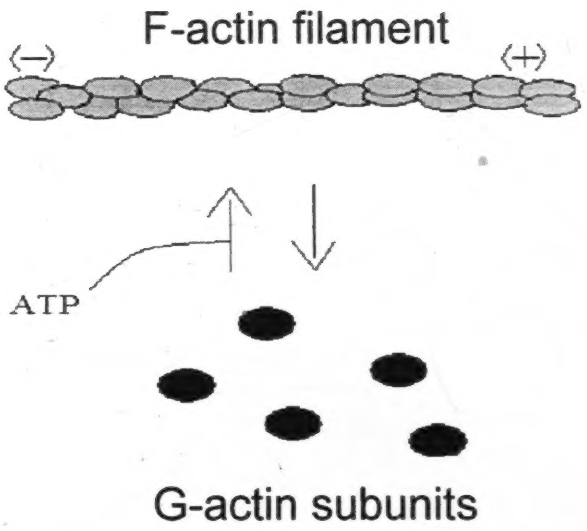

Figure 1.3 F-actin formation. G-actin units bind ATP and become able to polymerize into the two chains that wind around each other to form F-actin. When ATP is hydrolyzed to ADP on the actin monomers in the chain depolymerization can occur. F-actin assembly occurs faster at the plus end. Slower assembly occurs at minus end, defining a polarity to each actin subunit. Adapted from [241]

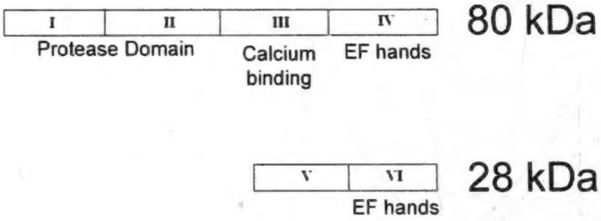

Figure 1.4 Calpain structure. m- or μ-calpain (80 kDa) are shown also with the regulatory subunit (28 kDa). Domains I and II posses the protease function, domain III is involved with calcium binding, membrane targeting and phospholipid binding and domain IV and VI contains EF hands. Adapted from [214]

CHAPTER 2. MATERIALS AND METHODS

2.1 GROWTH MEDIA AND ANTIBIOTICS

M199, RPMI, fetal bovine serum (FBS), bovine serum albumin (BSA), Hank's balanced salt solution (HBSS), Opti-MEM I, penicillin/streptomycin (P/S; 50 U/ml penicillin, 50 µg/ml streptomycin sulfate), glutamine (gln; 2 mM) and trypsin-ethylenediaminetetraacetic acid (0.125% trypsin, 0.5 mM EDTA in HBSS) were purchased from Invitrogen. FBS was heat inactivated and decomplemented by 30 min incubation at 56°C. Cell dissociation solution was from Sigma (St. Louis, MO). EC growth supplement (5 mg/ml ECGS, 10 mg/ml heparin in HBSS) was purchased from Becton Dickinson (Franklin Lakes, NJ).

2.2 SOLUTIONS AND BUFFERS

Solutions were prepared using assured or tissue grade reagents in double-distilled deionized water (ddH_2O). Dulbecco's phosphate buffered saline (PBS) was purchased from Invitrogen. Where PBS containing $CaCl_2$ was used, the solutions were prepared separately in ddH_2O and combined prior to use to prevent precipitation of $Ca_3(PO_4)_2$ crystals. A unique binding media was used in parallel plate laminar flow experiments consisting of cation-free HBSS containing 10 mM HEPES at pH 7.4 and 2 mg/ml of BSA supplemented with Ca^{2+} and Mg^{2+} at 1 mM each as described previously [125].

2.3 REAGENTS AND ANTIBODIES

Matrigel was purchased from Becton Dickinson. Monoclonal Ab mouse anti-human actin and Rho A were purchased from Santa Cruz Biotechnologies (Santa Cruz, CA). JAS, CellTracker green (CMFDA), CellTracker orange (CMTMR), tert-butoxycarbonyl-L- leucyl-L-methionineamide-7- amino-4- chloromethyl- coumarin (BOC) and Alexa fluor 546 monoclonal antibody labelling kit were obtained from Molecular Probes (Eugenem, OR). Donkey serum was obtained from Invitrogen. PD 150606, PD 145305, LY 294002 Wortmannin, BAPTA-AM, U 73122 and U 73343 were from Calbiochem-Cedarlane (Hornby, ON). SDF-1*α* was from Perprotech (Rocky Hill, NJ). TNF-1*α* and anti-ICAM antibody were from Biosource International Inc. (Camarillo, CA). Monoclonal Ab rabbit anti-human actin and F:G actin Kit were from Cytoskeleton Inc. (Denver, CO) FITC-CD4, -CD3, -CD19 and -IgG_{2a} and PE-CD8, -CD49d, -HLA-DR, -CD14 and -IgG_{2a} and anti-CD54 and anti-CD106 were from eBioscience (San Diego, CA). FITC- and Texas Red-conjugated AffiniPure $F(Ab')_2$ fragment goat anti-mouse IgG, FITC-conjugated AffiniPure F(Ab')$_2$ fragment goat anti-rabbit IgG (H+L), horseradish peroxidase (HRP)- AffiniPure goat anti-mouse IgG and goat anti-rabbit (H+L) secondaries were obtained from Jackson Immunoresearch (West Grove, PA). CD31 was from Dako Diagnostics (Glostrup Denmark). Y27632 was a gift from Wilfide Corporation (Japan). CD, ALLN, Nocodazole, 2,5-di-tert-butyl-1,4-benzohydroquinone (BHQ), 2,3-bis (2-methoxy-2-nitro-5-sulfophenyl)-2H-tetrazolium-5-carboxanilide (XTT), phenazine methosulfate (PMS), aprotinin, leupepetin, phenylmethylsulfonyl floride (PMSF), FITC-Phalloidin and monoclonal mouse anti human μ- and m-calpain antibodies were from Sigma.

2.4 CELL CULTURE

2.4.1 Lymphocytes

Human PBL were isolated from healthy donors under a protocol approved by the University of Alberta Health Research Ethics Board. Mononuclear leukocytes were isolated by density separation over a ficol gradient (Lymphoprep, Axis-Shield, Oslo, Norway). Whole blood was diluted 1:2 with HBSS and then Lymphoprep solution was underlayered as per the manufacturer's instructions. The diluted whole blood and ficol solution was then centrifuged in a Beckman GS-6R centrifuge equipped with a GH-3.8 rotor at 1800 rpm for 20 min at 24°C without braking. The peripheral blood mononuclear cells were then removed and resuspended in 30 ml HBSS, and centrifuged for 15 minutes at 1600 rmp. The cells were washed once more by resuspension in 30 ml HBSS and centrifugation at 1200 rpm for 15 min. Contaminating monocyte/macrophages were depleted by incubation in 150 mm x 15 mm plastic petri dishes (Fisher Brand) for 60 min at 37°C in RPMI supplemented with 10% FBS, P/S and gln. The non adherent mononuclear cells were washed off and resuspended in binding media and adjusted to ~1 x 10^7 cells/ml.

In experiments using fluorescently labelled lymphocytes, isolated PBLs were stained with a fluorescent cell tracker (cell tracker red 1 µM, CMTMR or cell tracker green 1 µM, CMFDA) in RPMI supplemented with 10% FBS, P/S and gln by incubation at 37°C for 30 min with frequent agitation. Following staining, PBLs were thoroughly rinsed and then resuspended in binding media for use in experiments.

2.4.2 Endothelial Cell Culture

HUVECs were isolated from several umbilical cords, pooled, and cultured in complete media (M199 with 10% FBS, penicillin, streptomycin, and glutamine) as described previously [242]. The umbilical veins were rinsed with PBS until perfusate was clear. Cord veins were air-purged, distally clamped, and rinsed with PBS. Veins were then injected with collagenase (1 mg/ml) and incubated for

20 min. The ECs were then released by washing with PBS. The collected cells were then centrifuged, resuspended in complete medium (M199 supplemented with 20% FBS, P/S, gln and ECGS). Storage of cells was maintained in a humidified incubator at 37°C, with 5% CO_2.

HUVECs were cultured on a 2 mg gelatin matrix coated 75 cm^2 flasks. The EC were harvested by washing twice with HBSS and then incubation with a nonenzymatic Cell Dissociation Solution until the ECs were seen to lift off the plate. For use in an experiment, the harvested cells were then replated onto matrigel (1 mg/ml) coated 35 mm dishes and incubated at 37°C in complete medium for 24 to 48 h until confluent. EC at passage 2 to 4 were used in experiments.

In select confocal experiments, HUVECs were stained with a cytoplasmic dye (cell tracker green, CMFDA). HUVECs were passaged and split into untreated and treated groups. The treated group was incubated for 30 min with frequent agitation in 5 µM CMFDA that was diluted in complete media. Following staining, HUVECs were thoroughly rinsed and then resuspended in complete media. The untreated group was then mixed with the treated cells and plated onto 35 mm tissue culture dishes coated with 1 mg/ml matrigel.

Where indicated, CD (1 μM) and JAS (300 nM) were diluted in complete medium and added to the HUVECs. After a 1 h incubation at 37°C, the media was removed and discarded. HUVECs were then rinsed three times with fresh binding media. After the final rinse, fresh binding media was applied to the HUVECs.

To chelate intracellular Ca^{2+}, HUVECs were incubated with 20 μM BAPTA-AM for 30 min in Ca^{2+} and Mg^{2+} free binding media, then rinsed and incubated for 1 h in complete media. HUVECs were then rinsed three times and left in binding media for use in an experiment. To collapse the superficial endoplasmic reticulum (sER), HUVECs were pretreated for 16 h with nocodazole (10 μM) diluted in complete medium and added to existing media. To inhibit the sarco/endoplasmic reticulum Ca^{2+}-ATPase (SERCA) HUVECs were pretreated for 30 min with BHQ (15 μM) diluted in complete media. To inhibit phospholipase C (PLC) HUVECs were pretreated for 30 min with U 73122 (5 μM). The inactive enantiomer of U 73122, U 73343 (5 μM; 30 min) was used as a control. After incubation at 37°C, nocodazole, BHQ and U 73122 were removed and discarded. HUVECs were rinsed three times with fresh binding media and then left in fresh binding media for use in an experiment.

To inhibit PIK, HUVECs were pretreated with wortmannin (100 nM; 1h or 10 μM; 30 min) and LY 294002 (30 μM; 1 h) diluted in complete media. After incubation at 37°C, the media was removed and discarded. HUVECs were rinsed three times with fresh binding media and left in fresh binding media for use in an experiment.

To inhibit calpain, HUVECs were pretreated with ALLN (100 µM or 30 µM) or PD 150606 (100 µM) diluted in complete media. The inactive enantiomer of PD 150606, PD 145305 (100 µM) was used as a control. After a 1 h incubation at 37°C, the inhibitors or inactive enantiomer in complete media was removed and discarded. HUVECs were rinsed three times with fresh binding media and left in fresh binding media for use in an experiment.

Inhibition of the serine/threonine kinase effector of Rho A, ROCK, was accomplished by pre-treatment of HUVECs with Y 27632 at 10 µM, 30 µM and 100 µM for 30 min at 37°C. After incubation, the media was removed HUVECs were rinsed three times with fresh binding media and left in fresh binding media for use in an experiment.

2.4.3 Cell Viability Assay

Chemical inhibitors were used at concentrations that maintained HUVEC viability >75% of mock-treated controls as assessed by the XTT assay of mitochondrial activity as described [243]. HUVECs were grown to confluence on C-24 well plates (Falcon) and then in triplicate left untreated or treated with various inhibitors and incubated at 37°C for their desired times. Solutions of XTT (1 mg/ml) and PMS (1.5 mg/ml) were made in DMSO. 5 μL of PMS was added to each ml of XTT solution required. After the desired incubation time, cells were rinsed of the inhibitor three times and 300 μl of the XTT:PMS solution was added to the HUVECs. The HUVECs were then incubated for 2 – 4 h in darkness to allow for significant colour change to occur. The media from each well was then transferred to a 96-well plate (Falcon) in duplicate and the absorbance of each well was read at 450 nm using an UVmax kinetic microplate reader (Molecular Devices, Sunnyvale, CA).

2.5 ANALYSIS OF LYMPHOCYTE MIGRATION UNDER SHEAR FLOW

2.5.1 Parallel Plate Laminar Flow Apparatus Setup

Parallel plate laminar flow adhesion assays were done as described previously [129] with 35 x 15 mm tissue-culture plates (Corning Inc., Corning, NY, USA) as the lower stage of a parallel plate laminar flow chamber (127 μm gap) (Glycotech, Rockville, Maryland, USA). Primary HUVECs (passage 2 to 4) or primary transduced HUVECs were plated at confluence on tissue culture dishes. HUVEC monolayers were stimulated for 20 – 24 h with TNF-*α* (5 ng/ml, 200 U/ml) diluted in complete media in order to mimic an inflamed vessel. Prior to assembly of the parallel plate flow chamber apparatus, HUVECs were rinsed three times with binding media and incubated with SDF-1α diluted in binding media at 100 ng/ml for 5 min. Following incubation HUVECs were extensively washed with binding media to remove any unbound chemokines from the surface of the monolayer.

The parallel plate flow chamber was then primed with binding media in the outflow line and PBLs in binding media in the inflow line and then the lines were clamped. PBLs were stored in a 37°C water bath and the inflow line originated from a tube of fresh binding media also in the 37°C water bath. The outflow line was attached to a 10 cc. syringe (BD, Franklin Lakes, NJ) contained on a flow pump (GENEQ, Montreal, QC). The primed parallel plate flow chamber was then applied to the surface of the HUVEC monolayer and vacuum sealed to ensure firm contact and a definite flow area.

In experiments testing for various agents affect on the PBLs, a modified 2 chamber system was set up. A second chamber was added into the line downstream of the first chamber. HUVECs were used on two 35 mm dishes in the same flow stream. The two primed parallel plate flow chambers were then applied to the surface of the HUVEC monolayers and vacuum sealed to ensure firm contact and a definite flow area. The dish closest to the PBLs was defined as dish A and the dish closest to the flow pump was defined as dish B.

The constructed apparatus was mounted on the stage of an inverted phase-contrast microscope (Leica DM IRB, Leica Microsystems). In the two chamber system dish B was mounted on the stage of the inverted phase-contrast microscope. The clamps were then released from the flow lines and the appropriate shear rates were established by the flow pump pulling the PBLs through the system. PBLs were perfused over the EC monolayer at low physiological shear flow (0.5 dyne/cm^2) and allowed to accumulate on the ECs for 4 min (accumulation phase). The flow rate was then increased to 1 dyne/cm^2 and was kept constant throughout analysis by perfusion of fresh binding medium (shear application phase). PBL:EC interaction were observed through a 20x objective and captured using a CCD camera (Pixelink, Vitana Corporation) and Pixelink software that record images at 12 frames/sec for a 20 min period (shear application phase).

2.5.2 Lymphocyte Motion Analysis

Motion analysis was done manually on all accumulated cells (60-120 cells per high power field, magnification: x20) that were initially attached after the accumulation phase using Quicktime Pro (Apple Computer Inc., Cupertino, CA). Lymphocytes rolling or locomoting into the field of view from upstream fields were not included in the analysis. Throughout the analysis period >90% of cells recruited remained in the field of view. The adherent lymphocytes were categorized into 3 specific groups: **(1) Arrested Lymphocytes;** remained stationary (moving less than one cell body in length) throughout the shear application phase. **(2) Motile Lymphocytes;** both locomotive and transmigrating lymphocytes. Locomotive lymphocytes were described as those cells during the shear application phase that spread and migrated over the EC surface (moving greater than one cell body in length) without detaching or crossing the EC monolayer. **(3) Transmigrating Lymphocytes;** lymphocytes that underwent a phenotypic change from phase light to phase dark. Cell that reappeared on the cell surface after undergoing this change and cell that transmigrated at regions where there was no intact monolayer were not included as Transmigrating Lymphocytes. The three different groups were recorded as a percentage of the originally accumulated lymphocytes.

2.6 RETROVIRAL INFECTION OF ENDOTHELIAL CELLS

The following procedure was performed by our laboratory technician. The peYFP-Actin (Clontech) was digested with restriction enzymes NheI and BamH I, then the eYFP-Actin fragment was blunted at the BamH 1 end using T4 DNA polymerase (Qiagen), and subcloned into the LZRSpBMN-Z oncovirus vector (generously provided by Gary Nolan, Stanford Univ) using standard molecular biology techniques. The insert was sequenced before use in these experiments. Replication-deficient retrovirus was generated in the Phoenix cell line and then used to infect sub-confluent HUVEC on two consecutive days. The transduced HUVEC were then harvested, mixed with uninfected HUVEC and plated at confluence onto 35 mm dishes. The cells were typically used 48 – 72 h after infection for the experiments described.

2.7 CONFOCAL FLUORESCENCE IMAGING

Lymphocytes were stained with a fluorescent cytosolic dye (1 μM CMTMR) for 30 min with frequent agitation and then perfused over the TNF-*α* and SDF-1*α*-treated YFP-actin expressing or CMFDA stained HUVEC monolayer on glass coverslips as described above. YFP-actin cells were imaged in binding medium with a Zeiss LSM 510 confocal inverted microscope system using a Plan-Neofluor 40x objective (NA 1.3) at a Zoom 2.0. The YFP and rhodamine signal of each optical section was acquired sequentially. A z-stack of 10 optical sections was taken at 0.5 μm interval every 2 min over the 20 min period. YFP was excited at 514 nm and the signal was collected with a LP 530 filter. Rhodamine was excited with 543 nm and signal collected with a LP 560 filter. The images acquired were compiled and the various time points were fused together using Quicktime Pro to make videos of the 20 min time interval. Each time point was analysed and a slice about midway through the EC was used to visualize F-actin remodelling events.

2.8 ANALYSIS OF CALPAIN ACTIVITY

2.8.1 Static Calpain Activity Assay

HUVECs grown to confluence on 35 mm glass coverslips were left untreated or pretreated with the calpain inhibitors ALLN (100 μM; 1 h) or PD 150606 (100 μM; 1 h). HUVECs were washed extensively three times with binding buffer and then the BOC (10 μM) was added to the HUVECs and images were immediately recorded. After internalization, BOC is conjugated to thiols. When calpain cleaves the conjugated BOC the thiol-conjugated 7-amino-4-methylcoumarin is released and fluorescence is increased [244]. BOC treated HUVECs were imaged in complete medium with a Zeiss LSM 510 confocal inverted microscope system using a Plan-Neofluor 40x objective (NA 1.3) at a Zoom 2.0. BOC was excited at 351 nm and the signal was collected with a LP 385 filter. For all images, the gain and offset values were set so that no pixel in the images was at saturation or at zero level. Time lapse images were recorded at a time interval of 1 min/image for a total of 20 min. Each time point was analysed using Laser Scanning Microscope 5 Image Browser (Zeiss). Time lapse images were analysed with Zeiss time function where a Region-Of-Interest (ROI) was drawn over the cells of interests. Average pixel intensity of the ROIs was then plotted against time. Intensity levels for 8 cells per field were recorded at the 1 min intervals.

2.8.2 Calpain Activity Under Shear Flow Conditions

HUVECs were grown to confluence on 35 mm glass coverslips and were TNF-α treated as described above. HUVECs were then pretreated with BOC (10 µM) for 20 min. Lymphocytes were stained with a fluorescent cytosolic dye (1 µM CMTMR) for 30 min with frequent agitation and then perfused over the TNF-*α*, SDF-1*α* and BOC-treated HUVEC monolayer on glass coverslips as described in Materials and Methods 2.5.1. HUVECs were imaged in binding medium with a Zeiss LSM 510 confocal inverted microscope using a 40x objective (NA 1.3, F-fluar). The BOC compound was excited at 351 nm and the emission signal was collected using a LP 385 filter. For all images, the gain and offset values were set so that no pixel in the images was at saturation or at zero level. Time lapse images were recorded at a time interval of 2 min/image for a total of 20 min. Each time point was analysed using Laser Scanning Microscope 5 Image Browser (Zeiss). Data was analysed at three different time points: **(1) t = 0**. **(2) Start TEM;** when a PBL begins the transmigration process by entering between ECs in the monolayer. **(3) During TEM;** near the middle to end of the transmigration process. Control HUVECs were those that had no lymphocytes undergo TEM and were assigned a start TEM time (240 sec) and a During TEM time (720 sec). These time points equalled the average start and during times of HUVECs with PBL TEM occurring. Time lapse images were analysed with Zeiss time function where a ROI was drawn over the cells of interests. Average pixel intensity of the ROIs was then plotted against time. Intensity levels for 8 cells per field were recorded at the 2 min intervals.

2.9 ICAM-1 LABELLING EXPERIMENTS

2.9.1 ICAM-1 Antibody Labelling

The non function blocking anti-ICAM-1 antibody (clone # 6.5B5) was directly conjugated to Alexa Fluor 546 as directed by the manufacture at 1 mg/ml. The antibody was diluted 1:10 in 1 M sodium bicarbonate buffer. The protein solution was mixed gently with the Alexa Fluor 546 reactive dye until the dye was fully dissolved and then incubated for 1 h at RT. The mixture was gently inverted every 15 min to increase labelling efficiency. Purification resin was added to a spin column and allowed to settle. The column was centrifuged for 3 min at 1100 x g using a swinging bucket rotor. The mixture was then loaded onto the centre of the spin column and the column was placed in a collecting tube and centrifuged for 5 min at 1100 x g. The labelled ICAM-1 antibody was then collected from the collecting tube.

2.9.2 Adhesion Cup Assay System

HUVECs were grown to confluence on 35 mm glass coverslips and were TNF-α treated as described above. HUVECs were then left untreated or pretreated with the calpain inhibitor ALLN (100 μM; 1 h) or the F-actin stabilizer JAS (300 nM; 1 h). During the last 30 min of incubation with the inhibitors, the Alexa 546 labelled ICAM-1 antibody (1 μg/ml) was added to the surface of the HUVECs. HUVECs were then rinsed extensively and SDF-1α treated as described above. Lymphocytes were stained with a fluorescent cytosolic dye (1 μM CMFDA) for 30 min with frequent agitation and then perfused over the TNF-*α* and SDF-1*α*-treated HUVEC monolayer on glass coverslips as described in Materials and Methods 2.5.1. ICAM-1 labelled HUVECs were imaged in binding medium with a Zeiss LSM 510 confocal inverted microscope system using a Plan-Neofluor 40x objective (NA 1.3) at a Zoom 2.0. The Alexa 546 and CMFDA signal of each optical section was acquired sequentially. A z-stack of 10 optical sections was taken at 0.5 μm interval every 2 min over the 20 min period. Alexa 546 was excited at 543 nm and the signal was collected with a LP 560 filter. CMFDA was excited with 488 nm and signal collected with a BP 500–530 filter.

2.9.3 Analysis of ICAM-1 Cup Formation

ICAM cup projection analysis was done manually on all accumulated cells that were attached to the HUVEC monolayer using Laser Scanning Microscope 5 Image Browser (Zeiss). The adherent lymphocytes were categorized into 3 specific groups: **(1) Complete Cup Formation;** high intensity of ICAM staining surrounding the lymphocyte (comparable to the control condition). **(2) Partial Cup Formation;** medium to low intensity of ICAM staining surrounding the lymphocyte. **(3) No Cup Formation;** virtually no to completely no intensity of ICAM staining surrounding the lymphocyte. Cells that had transmigrated were not included in the analysis. The three different groups were recorded as a percentage of the originally accumulated lymphocytes. Statistics was performed by assigning scores of 1 for complete cup, 2 for partial cup and 3 for no cup formation. The difference between cup formation among all cells for each treatment in two experiments were calculated and tested for statistical significance ($p < 0.05$) by analysis of variance (ANOVA) using SPSS software (SPSS, Chicago, IL).

2.10 IMMUNOCYTOCHEMISTRY

2.10.1 F-actin Staining

In some experiments, PBLs were stained with CMTMR and then perfused over the TNF-*α* and SDF-1*α* stimulated HUVEC monolayer on glass coverslips as described above in Materials and Methods. Shear application phase was limited to 10 min to capture lymphocytes in the process of diapedesis. At 10 min cells were fixed by perfusion with PBS/2% paraformaldehyde (PFA) for 5 min and washed by perfusion with PBS with 1 mM $CaCl_2$ for 5 min, both at 2 dyne/cm^2. The flow chamber was removed and cells were permeabilized with a 0.5% Triton X-100 buffer (20 mM Hepes, 50 mM NaCl, 3 mM $MgCl_2$ and 300 mM sucrose, pH 7.4). The cells were then stained for F-actin by incubation with FITC-phalloidin (2 μg/ml) in PBS and 1% donkey serum for 20 min at room temperature, and then washed three times with PBS with 1 mM $CaCl_2$. Coverslips where washed and then placed on top using Vectashield fluorescence mounting media (4 μl, Vector Labs, Burlingame, CA) and Permount mounting solutions (Fisher Scientific, Pittsburgh, PA). The cells were then analysed using a confocal microscope that fluorescence microscopy (FITC excitation: 488 nm, Rhodamine excitation: 543 nm).

2.10.2 Calpain Staining

PBLs were perfused over the TNF-α and SDF-1α stimulated HUVEC monolayer on glass coverslips as described above in Materials and Methods. Shear application phase was limited to 10 min to capture lymphocytes in the process of diapedesis. At 10 min cells were fixed by perfusion with PBS/2% paraformaldehyde (PFA) for 5 min and washed by perfusion with PBS with 1 mM $CaCl_2$ for 5 min, both at 2 dyne/cm^2. The flow chamber was removed and cells were permeabilized with a 0.5% Triton X-100 buffer (20 mM Hepes, 50 mM NaCl, 3 mM $MgCl_2$ and 300 mM sucrose, pH 7.4). The cells were stained for μ–calpain by incubation with monoclonal human anti-μ-calpain antibody (1 μg/ml) in PBS and 1% donkey serum for 20 min at room temperature, and then washed three times with PBS with 1 mM $CaCl_2$. The cells were labelled with Texas Red-conjugated affinipure F(Ab')$_2$ fragment secondary and stained for F-actin by incubation with FITC-phalloidin (2 μg/ml) in PBS and 1% donkey serum for 20 min at room temperature, and then washed three times with PBS with 1 mM $CaCl_2$. Coverslips where washed and then placed on top using Vectashield fluorescence mounting media (4 μl, Vector Labs, Burlingame, CA) and Permount mounting solutions (Fisher Scientific, Pittsburgh, PA). The cells were then analysed using a confocal microscope with fluorescence microscopy (FITC excitation: 488 nm, Texas Red excitation: 543 nm).

2.11 FLOW CYTOMETRY

Expression of EC surface adhesion molecules and PBL cell types were determined by flow cytometry. ECs were harvested and washed in PBS and suspended in primary antibody or control IgG (5 µg/ml) in 10% donkey serum, for 20 min at 4°C. After the incubation any unbound antibody was wash off the ECs. ECs were then resuspended in FITC-conjugated secondary antibody (15 µg/ml) for 20 min at 4°C. The cells were washed again and fixed with PBS/2% PFA. PBLs were washed in PBS and suspended in FITC- or PE-tagged primary antibody or control IgG (5 µg/ml) in 10% goat serum for 20 min at 4°C. Data was collected with a Becton Dickinson FACScan (San Jose, CA) and analysis was performed using CellQuest software.

2.12 WESTERN BLOT ANALYSIS

2.12.1 F-actin/G-actin in vivo Assay

The ratio of F-actin versus G-actin in cells was analysed using an F-actin/G-actin assay kit (Cytoskeleton Inc., Denver, CO) according to the manufacturer's protocol. HUVECs were either left alone or pretreated with JAS (300 nM) for 1 h and then lysed with a cell lysis and F-actin stabilization (LAS) buffer with or without 7 μM CD and homogenized using 26.5 G syringes. The cell lysates were centrifuged using a Beckman TL-100 Ultracentrifuge with a TLA 100.2 rotor at 100,000xg for 60 min at 37°C. The supernatants (G-actin) were separated from the pellets (F-actin) and were immediately placed on ice. The pellets were resuspended to the same volume as the supernatants using ice cold dH_2O containing 2 μM CD and were incubated on ice for 60 min.

2.12.2 Cells Lysis

In experiments to determine protein expression by western blotting, HUVECs were grown to confluence on 1 mg/ml gelatin-coated dishes. For CNF-1 experiments, HUVECs were pretreated with CNF-1 diluted to various concentrations in complete media for 16 h. Following the incubation, cells were rinsed with HBSS and then lysis buffer (1 M Tris pH=7.5, 10% Triton X-100, 10% sodium dodecyl sulfate (SDS), 10% sodium diethyldthiocarbamate (SDC), 2 M NaCl, 50 mM $MgCl_2$, 2 µg/ml leupeptin, 25 U/ml aprotinin and 1 mM PMSF) was applied to the surface and cells were scraped off using a cell scraper. The cell lysate was collected and centrifuged immediately at 13 000 rpm for 2 min at 4°C. After centrifugation, the supernate was immediately collected and placed on ice.

For calpain level experiments, cells were rinsed with HBSS and then incubated for 10 – 20 min with warm cell disassociation solution at 37°C. EC in suspension were then collected and centrifuged at 1000 rpm for 10 min at 4°C. HUVECs were rinsed with PBS/$CaCl_2$ and centrifuged at 1000 rpm for 10 min at 4°C. The collected cells were resuspended and incubated with lysis buffer for 5 min on ice with vigorous pipetting. The lysate was then centrifuged at 13 000 rpm for 4 min at 4°C. After centrifugation, the supernate was immediately collected and placed on ice.

2.12.3 Immunoblotting

Total protein concentrations were determined with a colormetric modified Lowery, Bio-Rad DC protein assay (Bio-Rad, Hercules, CA). Equal amount of total protein of the samples (400 ng of the G-actin and F-actin fractions, 10 µg of CNF-1 treated HUVECs, 20 – 30 µg of HUVEC lysate) were loaded in each lane and resolved by 7.5% sodium dodecyl sulfate-polyacrylamide gel electrophoresis (SDS-PAGE) in running buffer (0.025 M Tris, 0.192 M glycine, 0.1% sodium dodecyl sulfate, pH=8.3). Kaleidoscope or all blue precision plus protein standards (BioRad) were also loaded onto the gel and used as protein ladders. Protein was blotted onto a polyvinylidene difluoride (PVDF) membrane (Amersham Pharmacia Biotech, Buckinghamshire, England) overnight at 4°C using a Bio-Rad TransBlot with transfer buffer (25 mM Tris, 0.2 M glycine and 20% Ethanol). Following the transfer, the membranes were removed and rinsed with TBS-Tween (TBS-T; 100 mM Tris, 0.9% NaCl, 0.1% Tween 20, pH=7.5) and then incubated with blocking solution (5% BSA in TBS-T) for 4 h at room temperature (RT). The membranes were then rinsed three times with TBS-T for 5 min and various primary mAbs (described in Results) in 2% BSA TBS-T were applied to the membranes. The membranes were incubated for either 1 h at RT or overnight at 4°C. Membranes were washed three times (20 min then two 10 min washes) with TBS-T and then incubated with horseradish peroxidase-(HRP-) secondary in 2% BSA TBS-T for 1 h at RT. Following incubation with the secondary Ab, membranes were washed with TBS-T four times (20 min wash then three 10 min washes). The membranes were developed with chemiluminescence substrate (ECL western blotting detection analysis system, Amersham Pharmacia Biotech, Buckinghamshire, England) and then exposed from 10 – 20 min to Biomax MR X-ray film (Eastman Kodak, Rochester, NY).

2.13 STATISTICS

All experiments were performed at least three times using different pairs of donor lymphocyte and endothelial cells. Data are expressed as mean ± the standard error of the mean (SEM). The difference of the means between treatment and controls among several experiments was calculated and tested for statistical significance ($p < 0.05$) by analysis of variance (ANOVA) using SPSS software (SPSS, Chicago, IL).

CHAPTER 3. RESULTS

3.1 PILOT STUDIES - OPTIMAZTION OF EXPERIMENTAL CONDITIONS

3.1.1 TNF-α is Required for Leukocyte Adhesion

Initially, before specifically studying the role of the EC in lymphocyte TEM, experimental protocols and variables were optimized. Well documented is the need for treatment of HUVECs with an inflammatory cytokine, such as TNF-*α*, to promote leukocyte adhesion to the EC monolayer under static conditions [144, 245]. The use of TNF-*α* to mimic an inflamed vascular endothelium is mainly due to its ability to upregulate ICAM, VCAM and E-Selectin, the major adhesive ligands [246]. We first confirmed the need for TNF-*α* in adhesion of PBLs to HUVECs under shear stress. HUVECs were left untreated or treated with TNF-*α* for 20 h (Figure 3.1). With no TNF-*α* treatment virtually no cells interacted with the monolayer, however with TNF-*α* treatment the desired result was obtained and interaction with the EC monolayer occurred with a significant number of cells interacting that gave us the opportunity to evaluate.

Next we tested for both the upregulation of adhesion molecules (ICAM-1; CD54, VCAM-1; CD106) and the optimal TNF-*α* treatment time required to induce significant effects in our parallel plate flow adhesion assay. HUVECs were treated with TNF-*α* from 0 – 24 h and then flow cytometry was performed to assess levels of the various adhesion molecules. PECAM-1 (CD31) was used as a positive control since it is seen to be constitutively and uniformly expressed on ECs [247, 248]. CD31 levels stayed relatively similar through the various time points (Figure 3.2 A). CD54 and CD106 were both upregulated after the first TNF-*α* time treatment at 8 h and then levels appeared optimal at between 20 – 24 h (Figure 3.2 A). Therefore the 20 – 24 h range was selected as optimal conditions for our flow system. HUVECs were routinely checked for expression of CD54 and CD106, a representative data set is shown at a 20 h treatment (Figure 3.2B)

3.1.2 Lymphocyte Cell Populations

The next step in evaluating our system was to determine the phenotypes of the PBLs that would be interacting with the HUVECs and what concentration of PBLs would be optimal for use in the flow system. Flow cytometry was performed on isolated PBL from whole blood to monitor determine the subpopulations present in each experiment. The data is summarized in Figure 3.3. Both CD8$^+$ and CD4$^+$ T cells were present. The majority of T cells (CD3) expressed the counter receptor for VCAM-1, *α*4 (CD49d) integrin. CD19, a B-cell-specific transmembrane glycoprotein [249] was used along with CD14, the receptor for bacterial lipopolysaccharide (LPS) expressed on monocytes and macrophages [250] and human leukocyte antigen (HLA-) DR, an mAb specific for major histocompatibility complex (MHC) class II and recognizes B cells, monocytes, macrophages, dendritic cells, and activated T cells [251, 252]. Our PBL populations show only a minimal presence of these markers.

Isolated PBLs were next tested for the correct concentration that would give us a significant number of cells interacting with the EC monolayer. Previous studies using a similar system report using 30 – 60 cells per field at 20x magnification [125]. PBLs were diluted to concentrations in the range of 1 x 10^6 – 1 x 10^7 cells/ml. At 1 x 10^6 cells/ml the cell numbers interacting reached an upper range of ~35 cells. We chose to use approximately 1 x 10^7 cells/ml since this gave us between 60 – 120 PBLs interacting with the HUVEC monolayer at 20x magnification. The average number of PBLs interacting with HUVEC monolayer is shown (Figure 3.4).

3.1.3 Determination of Appropriate Shear Conditions

Another variable that needed to be adjusted was the shear rates applied and length of the application phase. Cinamon et. al. reported an accumulation phase of 40 sec at 0.75 dyne/cm^2, and then a shear application phase of 5 dyne/cm^2 [125]. We selected shear rates of 0.5 dyne/cm^2 for the accumulation phase and 1 dyne/cm^2 for the shear application phase since the typical range in the microcirculation of an inflamed vessel is approximately 0.2 – 1.5 dyne/cm^2 [253, 254]. We found that an accumulation phase of 40 s at 0.5 dyne/cm^2 was not efficient for studying PBL TEM due to the lack of adherent PBLs. We chose to increase the accumulation phase to 4 min at 0.5 dyne/cm^2 to obtain an adequate number of events to analyse. Primary studies indicated at least 10% of PBL migrated under optimized conditions. Therefore to observe at least 5 lymphocyte TEM events in the control condition, 20x fields that contained 60 – 120 PBLs were evaluated.

3.1.4 SDF-1*α* and Binding Media are Required

The model of inflamed vascular EC consisted of TNF-*α* stimulated HUVECs, however, TNF-*α* activation of HUVECs does not allow the HUVECs to display functional chemokines to resting PBLs [68]. It was reported that following TNF-*α* activation, PBLs are able to undergo rolling and arrest, but virtually no PBLs undergo TEM, indicating that although TNF-*α* produced subendothelial chemokines that are able to allow some PBLs to transmigrate, their levels are too low to be considered significantly chemotactic [125]. This was resolved by the addition of apical chemokines, which have the ability to induce PBL TEM in flow systems [125]. SDF-1*α* was the chemokine shown previously to induce TEM and also the one we selected to use. Our data confirms these previous results that indicate pretreatment of HUVEC monolayers for 5 min with SDF-1*α* (200 U/ml) can induce PBL TEM under shear conditions (Figure 3.5 Binding Media vs. Binding Media + SDF-1*α*) (Appendix Videos B.1, B.2).

Early experiments produced virtually no PBL TEM. In these experiments all cells were treated and maintained in complete media (M199 with 10% FBS, penicillin, streptomycin, and glutamine). HUVECs pre-treatment with SDF-1*α* and PBLs re-suspension following isolation was done with complete media. Priming of the flow system and the perfusion media consisted of the complete media. These conditions allowed the lymphocytes to adhere to the surface of the endothelium but TEM was rarely observed in contrast to reported levels (Figure 3.5) [125]. Media conditions from similar studies [125] were then mimicked to test for effectiveness of experimental conditions. Perfusion media, priming, SDF-1*α* pre-treatment of HUVECs and resuspension of PBLs was now performed using binding media (HBSS, 10 mM HEPES at pH 7.4, 2 mg/ml BSA, 1 mM Ca^{2+} and 1 mM Mg^{2+}). Using the new conditions we were now able to reproduce similar effects seen previously. TEM was increased significantly when using binding media as compared to conditions using complete media (Figure 3.5). With our system now optimised we were able to begin studying in EC events in PBL TEM.

3.2 *EC F-ACTIN CYTOSKELETAL INVOLVEMENT IN LYMPHOCYTE TEM*

3.2.1 Endothelial F-actin Remodelling is Required for Lymphocyte TEM

To determine if EC cytoskeletal reorganization is involved in TEM, HUVECs were pretreated with CD, to depolymerize F-actin, or JAS, to stabilize endothelial F-actin. The flow chamber apparatus was mounted on the confluent monolayer of HUVECs, and the PBL suspension was perfused through the system. We monitored the PBL population in each experiment as described in Materials and Methods. Both CD and JAS pretreatment of EC were found to decrease the amount of lymphocytes that underwent TEM to 12% ± 5% and 24% ± 11% versus the control respectively, but did not change motility of the surface-adherent PBL (Figure 3.6 A). Sample videos of control (Appendix video B.3 A) and JAS pretreatment of HUVECs (Appendix video B.3 B) demonstrate the decreased TEM in response to endothelial F-actin stabilization. JAS treatment does not completely inhibit PBL TEM; lymphocytes appeared to either arrest on the luminal surface or complete TEM fully. However, even among PBL transmigrating through the JAS-pretreated EC monolayer, the time required for a PBL to complete the migration was significantly increased (Figure 3.6 B).

To confirm that JAS pretreatment of the HUVEC stabilized the F-actin cytoskeleton, control or JAS-pretreated HUVEC were lysed, and then treated with CD in vitro to depolymerize F-actin. Western blots were used to analyze the ratio of F to G-actin levels in the cell lysate. Figure 3.7 demonstrates that JAS protects the EC F-actin from CD-mediated deplomerization. These results indicate that EC require both polymerized F-actin structures and F-actin remodeling to support efficient lymphocyte TEM.

3.2.2 EC F-actin Condenses Around the Migration Pore

Next we sought to visualize the F-actin remodelling event in living ECs. HUVECs were transduced with a YFP-actin construct using a retroviral vector. Confocal fluorescence microscopy was used in the laminar flow system to visualize the incorporation of YFP-actin into organized F-actin structures in transduced HUVECs. First, analysis of the sequential confocal images confirmed that PBLs transmigrate from the luminal to the basal surface of the EC monolayer (Figure 3.8, Appendix Video B.4 A). Second, we observed that YFP-actin condenses around the migration pore as the PBL extends pseudopodia between and under EC (Figure 3.8) (Appendix Video B.4 A, B).

A control experiment was also performed to assess if this apparent YFP-actin polymerization was just simply cytoplasmic clumping around the migration pore. CMFDA stained HUVECs were combined with unstained HUVECs and CMTMR stained PBLs were perfused over the monolayer in our laminar flow system described in Materials and Methods. There was no evidence in any images of cytoplasmic condensation around a migration pore among CMFDA-stained HUVECs (Appendix Video B.5).

This observation was confirmed using immunofluorescence microscopy. The laminar flow system was again used to allow lymphocytes to interact with the HUVEC monolayer. Lymphocytes were fixed as they were in the process of TEM. Cells were then labelled with FITC-phalloidin and visualized using fluorescence microscopy. F-actin again appears to condense around the migration pore of a lymphocyte undergoing TEM (Figure 3.9). These observations support the model that EC cortical and subplasmalemmal F-actin remodelling is associated with TEM.

3.3 EC CALCIUM FLUX IS REQUIRED FOR LYMPHOCYTE TEM

Earlier studies have suggested that lymphocyte adhesion stimulates a Ca^{2+} flux in EC, but only natural killer cell adhesion could be shown to directly induce a

Ca^{2+} signal under static adhesion conditions [255]. We therefore examined the role of an EC Ca^{2+} flux in regulating lymphocyte TEM under shear stress conditions. First, HUVECs were pre-treated with the intercellular Ca^{2+} chelator BAPTA-AM. We observed that PBL TEM was significantly reduced with BAPTA-AM treatment as compared to the control (Figure 3.10 A). BAPTA-AM treatment of the EC decreased PBL TEM to 24% ± 6% of the control condition, thus indicating a role for EC Ca^{2+} signalling during TEM.

Next Ca^{2+} stores, release pathways and transport proteins were targeted. We tested the hypothesis that activation of the IP_3 receptor causes Ca^{2+} release from the ER. HUVECs were treated with either nocodazole, which collapses the sER, BHQ, which inhibits SERCA, to attenuate Ca^{2+} flux from the ER stores or U 73122, which inhibits PLC and prevents inositol 1-4-5 trisphosphate (IP_3) generation.

We observed that nocodazole and BHQ like the BAPTA-AM treatment, significantly inhibited lymphocyte TEM (Figure 3.10 A). Nocodazole decreased the amount of PBLs that underwent TEM to 32% ± 16% and BHQ decreased the amount of PBL TEM to 53% ± 8%. These results indicate Ca^{2+} release from the EC ER facilitates PBL TEM. Furthermore, U 73122 decreased the amount of PBLs that underwent TEM to 60% ± 6%, while U 73122's inactive analogue, U 73343, had no effect on PBL TEM (110% ± 11% of the control condition) (Figure

3.10 B). Cell viability was unaffected by 30 min BHQ (15 μM) treatment (Figure 3.10 C). These data taken together implicate Ca^{2+} signalling as a requirement for efficient PBL TEM.

3.4 EC PI KINASES PARTICIPATE IN LYMPHOCYTE TEM

3.4.1 Optimization of Experimental Conditions

Prior to addressing the effect of EC PIK on PBL TEM, inhibitor concentrations and exposure times needed to be optimized. Wortmannin is a competitive irreversible inhibitor of both PI3 and PI4K, but it is not very stable in solution [256]. Wortmannin's inhibition of PI4K is specific for the different types, since it can prevent the activation type III PI4K at an IC_{50} of 150 nM [256], but not the type II PI4K [257]. Using previously reported concentrations and exposure times we attempted to inhibit PBL TEM. At 30 min incubation time and varying the concentration at 100 nM, 300 nM and 1 μM we saw no change in PBL TEM as compared to the control (Figure 3.11 A). However at 1 h incubation time PBL TEM decreased at 100 nM treatment of wortmannin and the viability of HUVECs was also maintained (Figure 3.11 A, B).

3.4.2 PIK's Role in Lymphocyte TEM

The observation that Ca^{2+} and SERCA inhibition impairs efficient lymphocyte TEM, suggests that ER calcium release is necessary for the EC to enact a structural change during TEM. One stimulus for ER Ca^{2+} release involves the activation of the IP_3 receptor. IP_3 is generated by the action of PLC on PIP_2, which in turn is generated by the activity of PI4K. However, PIP_2 may also be involved in regulation F-actin polymerization through activity on gelsolin or other actin associated proteins. Moreover, PIP_2 or PIP_3 generated by PI3K may act as docking sites for PH-domain proteins such as RhoGEFs, and hence influence F-actin assembly. To inhibit the PIK, HUVECs were pretreated with wortmannin for 1 hr at 100 nM to inhibit PI3K or with wortmannin for 30 min at 10 μM to inhibit both PI3K and PI4K or with the selective PI3K competitive inhibitor LY 294002. We observed that both inhibitors significantly decreased lymphocyte TEM (Figure 3.12). At concentrations inhibiting PI3K, Wortmannin decreased PBL TEM to 44% ± 10% and LY 294002 decreased to PBL TEM to 44% ± 10% of the control condition. To specifically study PI4K we looked at a shorter incubation time with a higher concentration of wortmannin (10 μM). Wortmannin become less specific for PI3K at concentrations above 1 μM and can broadly inhibit PI4K [258, 259]. These higher concentrations of wortmannin, inhibiting both PI3K and PI4K, decreased PBL TEM to 32% ± 4% of the control. This observation suggests that endothelial PI4K, in addition to PI3K activity, is involved in lymphocyte TEM. Comparing the % decrease in PBL TEM it appears that there is a general trend that the decrease in PBL TEM increases with greater PI4K inhibition, however it was not statistically significant (wortmannin 1 h 100 nM and the 30 min 10 μM treatment) (Figure 3.13 A). Cell viability decreased due to the increased levels of dimethylsulfoxide (DMSO) present in 10 μM wortmannin treatment (Figure 3.13 B). However, the equivalent amount of DMSO in binding media had no effect on PBL TEM, implying that the effect on PBL TEM was due to wortmannin.

3.5 EC CALPAIN'S ROLE IN LYMPHOCYTE TEM

3.5.1 Levels of μ- and m-Calpain in HUVECs

Next we tested the hypothesis that calpain proteolytic activity of F-actin-associated targets acts as a downstream effector of the Ca^{2+} signal. We first attempted to determine which form is present in higher levels in HUVECs. Protein determination of whole cell lysates was performed using a modified colormetric Lowry assay. Then equivalent amounts of HUVEC lysates were resolved using SDS-PAGE and transferred to a PVDF membrane. Membranes were blocked and then rinsed. Membranes were incubated overnight with either primary anti-μ- or m-calpain. HRP-conjugated AffiniPure goat anti-mouse IgG (H+L) secondary was then applied for 1 h at RT. The Westerns demonstrate robust expression of μ-calpain in HUVEC lysates (Figure 3.14). Actin (42 kDa) levels in the HUVECs were checked to ensure equivalent loading.

3.5.2 EC Calpain is Inhibited by Pretreatment with Calpain Inhibitors

First we determined if HUVECs exhibited calpain activity in intact cells. ECs were incubated with the membrane-soluble calpain substrate BOC, and then the generation of the specific fluorescent signal was observed, demonstrating that HUVECs exhibit constitutive calpain activity (Figure 3.15).

Second, to ensure that calpain activity would be inhibited by the calpain inhibitors ALLN (100 µM; 1 h) and PD 150606 (100 µM; 1 h), HUVECs were treated with the BOC compound alone or along with either inhibitor as described in Materials and Methods. We observed that both ALLN and PD 150606 inhibited calpain activity levels at 300, 600, 900 and 1200 sec as compared to the control (Figure 3.15). All data is shown as compared to its corresponding treatment at t = 0. At 300 sec control intensity was 149% ± 4%, ALLN intensity was 106% ± 1% (p value = 0.000 vs. control) and PD 150606 intensity was 100% ± 1% (p value = 0.000 vs. control). At 600 sec control intensity was 208% ± 9%, ALLN intensity was 129% ± 1% (p value = 0.000 vs. control) and PD 150606 intensity was 107% ± 2% (p value = 0.000 vs. control). At 900 sec control intensity was 294% ± 15%, ALLN intensity was 155% ± 2% (p value = 0.000 vs. control) and PD 150606 intensity was 120% ± 4% (p value = 0.000 vs. control). AT 1200 sec control intensity was 378% ± 18%, ALLN intensity was 176% ± 3% (p value = 0.000 vs. control) and PD 150606 intensity was 125% ± 5% (p value = 0.000 vs. control).

We were unable to increase calpain activity by treatment with the calcium ionophore, ionomycin 1 μM (data not shown). These observations demonstrate that calpain is constitutively active in confluent HUVEC cultures and that the calpain inhibitors ALLN and PD 150606 inhibit calpain activity.

3.5.3 EC Calpain is Required for Lymphocyte TEM

Calpain is a thiol protease and has been show to play a role in cytoskeletal remodelling [212, 259], and is regulated by Ca^{2+} and PIP_2 [213], and therefore we hypothesized it to would also play a role in PBL TEM. We tested the effect of two inhibitors of calpain activity to determine its role in lymphocyte TEM. HUVECs were pretreated for 1 h with ALLN, PD 150606, or PD 150606's inactive analog PD 145305. We observed that both ALLN and PD 150606 significantly inhibited PBL TEM, while the inactive analog PD 145305 had no effect on PBL TEM. ALLN (Figure 3.16 A) at both 100 μM and 30 μM decreased PBL TEM to 0% ± 0% or 35% ± 9% of the control, respectively. The selective calpain inhibitor, PD 150606 (Figure 3.16 B), treatment of HUVECs at 100 μM showed a significant decrease in the fraction of PBLs that underwent TEM (41% ± 9% of the control condition). The inactive analog showed no significant change in PBL TEM (98% ± 23% of the control condition). Sample videos of control (Appendix video B.6 A) and PD 150606 pretreatment of HUVECs (Appendix video B.6 B) demonstrate the decrease TEM in response to endothelial calpain inhibition. The fraction of adherent lymphocytes that moved on the surface of the endothelial monolayer was not different between PD 150606-treated and PD 145305-treated control groups (Figure 3.16 B). Lymphocytes could be seen moving on PD 150606-treated HUVECs to interendothelial cell junctions, but did not appear to extend pseudopodia between the junctions (Appendix Video B.6 B). This appearance is similar to that of PBL moving on JAS-treated HUVEC monolayers (Appendix Video B.3 B), and indicates that the requirement for both endothelial cytoskeletal reorganization and calpain activity occurs early in the diapedesis step.

3.5.4 Calpain Activity is Increased in ECs Involved in TEM

To determine if EC calpain activity is increased during lymphocyte TEM, HUVECs were pre-incubated with the membrane soluble calpain substrate, BOC (10 μM; 20 min). In a single field of view ECs adjacent to transmigrating PBLs (TEM cells) or nearby ECs that were not involved in TEM (control cells) were analysed as described above. Calpain activity is increased in HUVECs that participate in lymphocyte TEM (Figure 3.17). Control ECs had intensity levels of 99% ± 2% at both the start of TEM and during TEM. In ECs participating in TEM intensity levels were significantly increased at both the start of TEM and during TEM to 115% ± 2% (p value = 0.000 vs. control) and 125% ± 3% (p value = 0.000 vs. control) respectively. Data is shown as compared to t = 0 intensity levels. These results show directly in living ECs that calpain activity is increased in those ECs where PBL TEM is occurring and thus strengthen the hypothesis that calpain activity is required for lymphocyte TEM.

3.5.5 μ-Calpain is Increased Around Areas of TEM

Next we sought to determine if EC μ-calpain localizes to the migration pore of a PBL undergoing TEM. The laminar flow system was used to allow lymphocytes to interact with the HUVEC monolayer. Lymphocytes were fixed as they were in the process of TEM. Cells were then labelled with Texas Red labelled anti-μ-calpain and FITC-phalloidin and visualized using fluorescence microscopy. There appears to be an enhanced calpain signal around the transmigrating PBL (Figure 3.18). However it is difficult to distinguish between EC and PBL calpain. Calpain does appear to be localized up at the cortical membrane and not at the level of focal adhesions or at intercellular junctions. These observations are consistent with the model that calpain is acting in the EC at the same level as cortical and subplasmalemmal F-actin remodelling.

3.5.6 EC Calpain Inhibition Limits EC ICAM-1 Distribution

Next we tested the hypothesis that calpain inhibition affected the assembly of ICAM rich “docking” structures discussed by Sanchez-Madrid and Springer [104, 260]. We fluorescently labelled surface ICAM-1, then the ECs were left untreated or treated the ECs with the calpain inhibitor ALLN (100 μM; 1 h) or the F-actin stabilizing agent JAS (300 nM; 1 h) before the assembly of the laminar flow chamber as described in Materials and Methods. F-actin stabilization treatment was used as a positive control since it would prevent ICAM distribution. Serial confocal fluorescent images were collected of EC ICAM-1 distribution using confocal microscopy. Calpain inhibition significantly decreased the number of ICAM cup projection present on the HUVEC monolayers at the start of the shear application phase and 6 min following the start of the shear application phase (Table 3.1, Figure 3.19). At t = 0 min in the control condition, the percentage of ICAM cup formations associated with adherent PBLs were: 57% complete cup, 20% partial cup and 23% no cup. In response to ALLN treatment at t = 0 min, the percentage of ICAM cup formations associated with adherent PBLs were: 18% complete cup, 46% partial cup and 36% no cup (p value = 0.005 vs. control). In response to JAS treatment at t = 0 min, the percentage of ICAM cup formations associated with adherent PBLs were: 18% complete cup, 39% partial cup and 43% no cup (p value = 0.002 vs. control). At t = 6 min in the control condition, the percentage of ICAM cup formations associated with adherent PBLs were: 59% complete cup, 16% partial cup and 25% no cup. In response to ALLN treatment at t = 6 min, the percentage of ICAM cup formations associated with adherent PBLs were: 21% complete cup, 32% partial cup and 47% no cup (p value = 0.003 vs. control). In response to JAS treatment at t = 6 min, the percentage of ICAM cup formations associated with adherent PBLs were: 24% complete cup, 34% partial cup and 42% no cup (p value = 0.009 vs. control). These results indicate a mechanistic role for calpain in lymphocyte TEM in prevent ICAM cup formation around the adherent lymphocyte.

3.6 AGENTS USED HAVE NO EFFECT ON LYMPHOCYTES

As stated above, the various agents used in studying PBL TEM were all applied to the ECs. However there still was the possibility that the agents could be affecting the PBLs. To study the effect of the various agents on the PBLs a two chamber flow system was set up as described in Materials and Methods. PBLs were perfused through the flow system first encountering dish A and then reaching dish B where PBL:EC interaction were recorded. PBLs were treated to confirm the three major conclusions in our study; actin stabilization with JAS (300 nM; 1 h), Ca^{2+} dependence with BAPTA-AM (20 μM; 30 min) and calpain dependence with ALLN (100 μM; 1 h). A control was also run to check for effects of new increased distance that the PBLs would have to travel to interact with the ECs. Experimental conditions were for the control dish A and dish B no treatments. There were two experimental conditions for the inhibitor studies. The first was dish A no treatment and dish B various agent to check for the previous result of the agent on the ECs. The second was dish A various agent and dish B no treatment to check for the effect of the various agents on the PBLs. PBLs would pass through dish A and be exposed to the various agent and then the effect would be seen in dish B. We found that there was no affect on the PBLs by the various agents and the control no treatment/no treatment (dish B/dish A) condition was no different than the standard control single dish flow system (Figure 3.20 A-C).

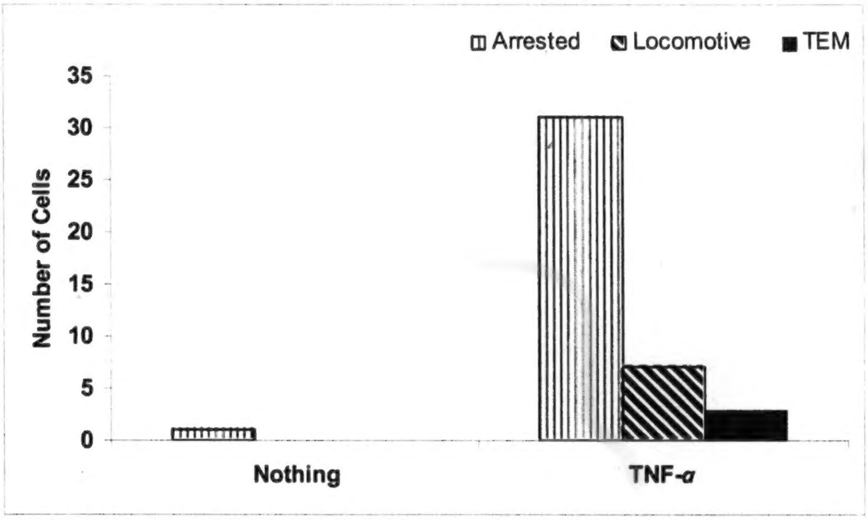

Figure 3.1 TNF-*α* is required to allow lymphocyte interaction with HUVECs. HUVECs were left untreated or pretreated with TNF-*α* (200 U/ml; 20 h) before the assembly of the laminar flow chamber as described in Materials and Methods. Endothelial–adherent lymphocytes were evaluated over the course of 20 min under shear stress of 1 dyne/cm^2. The fraction of arrested, locomotive and transmigrating lymphocytes was determined. Data are representative of three experiments.

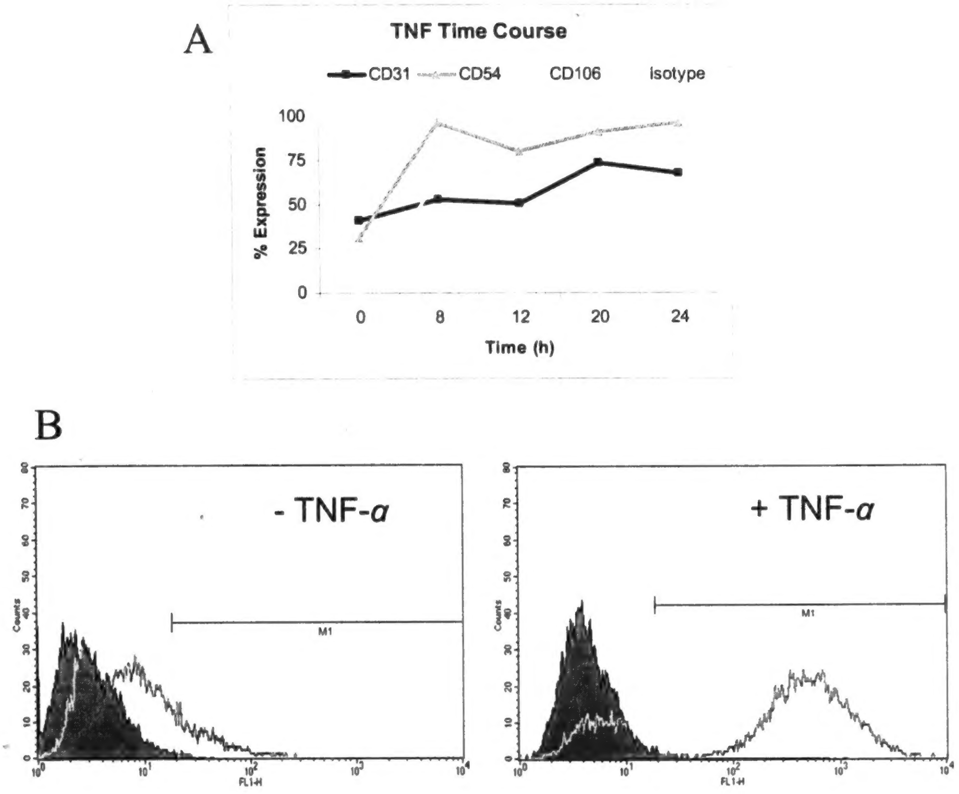

Figure 3.2 HUVECs surface adhesion molecule expression in response to TNF-*α* treatment. (A) TNF-*α* time course experiment. HUVECs were untreated or pretreated with 200 U/ml TNF-*α* for 8, 12, 20 and 24 h. Cells were harvested using trypsin-EDTA and stained for CD31 (black), CD54 (red), CD106 (blue) or isotype control IgG_{2a} (green) with a FITC-conjugated secondary. Analysis was performed as described in Materials and Methods. % Expression was determined by setting M1 marker gates as 1% of isotype control cells. (**B**) Representative data set of TNF-*α* treatment at 20 h or untreated control. Isotype control (purple), CD54 (red) and CD106 (blue) expression levels on HUVECs are displayed. Data are representative of three experiments.

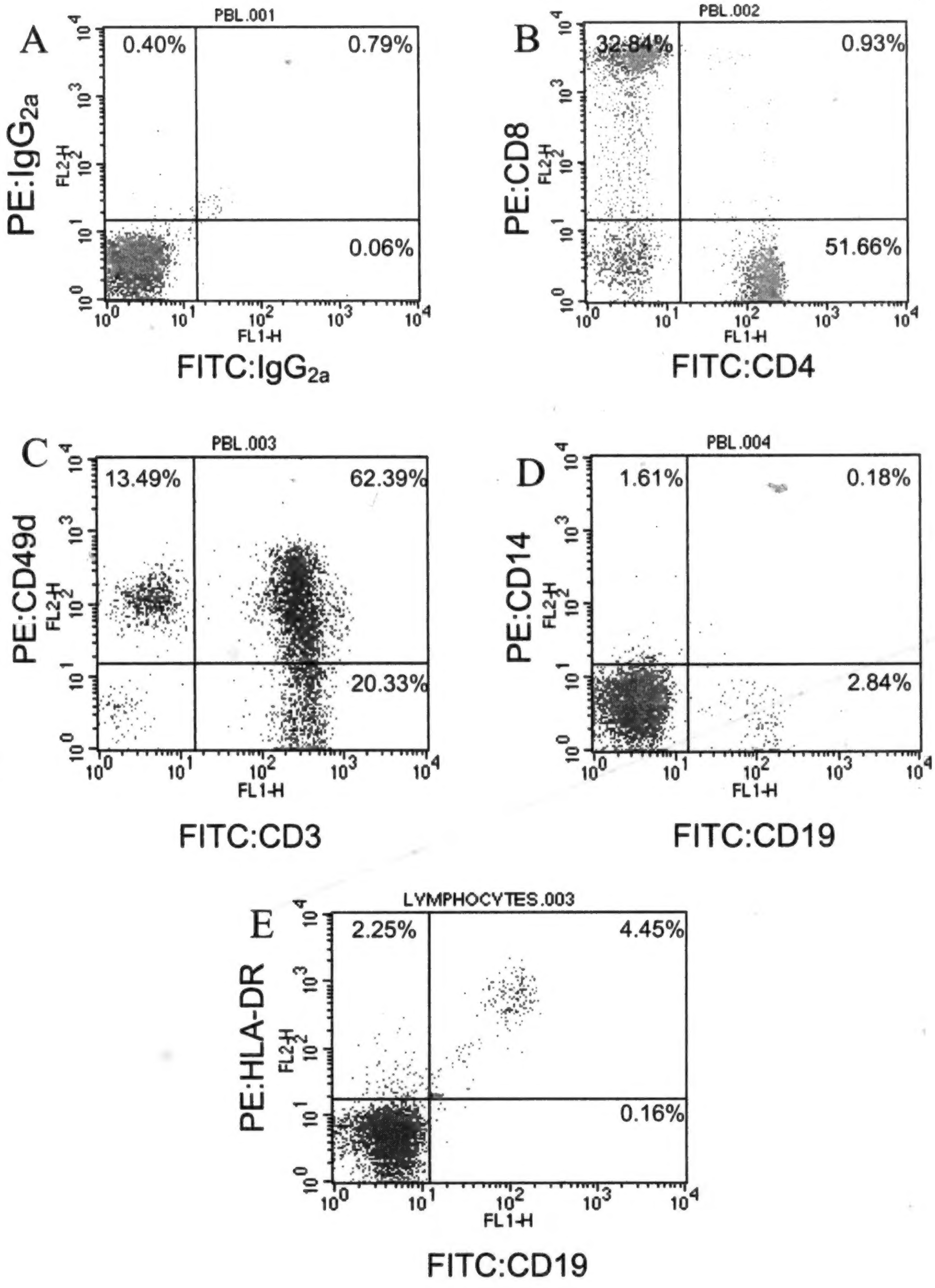
A
PBL.001
PE:IgG2a
FL2-H
0.40%
0.79%
0.06%
FL1-H
FITC:IgG2a
B
PBL.002
PE:CD8
FL2-H
32.84%
0.93%
51.66%
FL1-H
FITC:CD4
C
PBL.003
PE:CD49d
FL2-H
13.49%
62.39%
20.33%
FL1-H
FITC:CD3
D
PBL.004
PE:CD14
FL2-H
1.61%
0.18%
2.84%
FL1-H
FITC:CD19
E
LYMPHOCYTES.003
PE:HLA-DR
FL2-H
2.25%
4.45%
0.16%
FL1-H
FITC:CD19
10^0
10^1
10^2
10^3
10^4

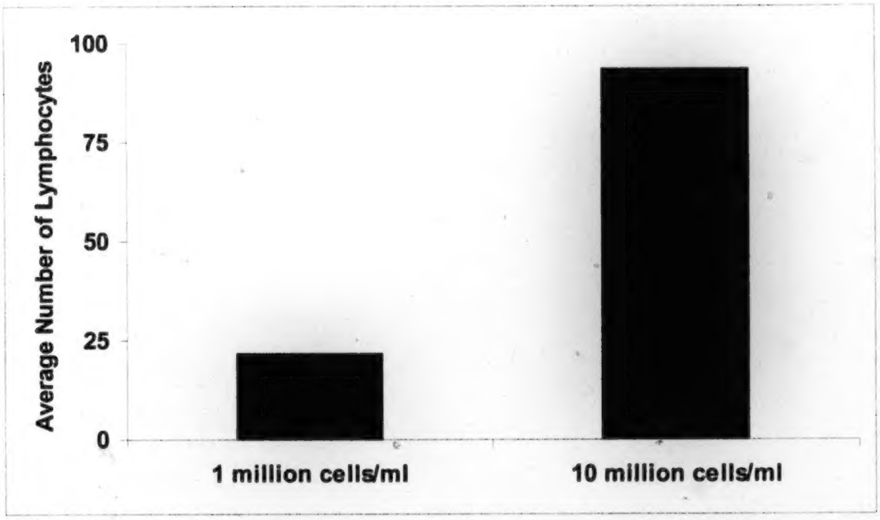

Figure 3.4 Higher concentrations of lymphocytes create increased interactive events between the endothelium and lymphocytes. PBLs were freshly isolated and resuspended in binding media to a concentration of either 1 million cells/ml or 10 million cells/ml. PBLs were then perfused over the TNF-*α* stimulated HUVEC monolayer and the total number of PBLs interacting with the endothelium was recorded. Interacting PBLs included arrested, locomotive and transmigrating cells. Data are representative of three experiments.

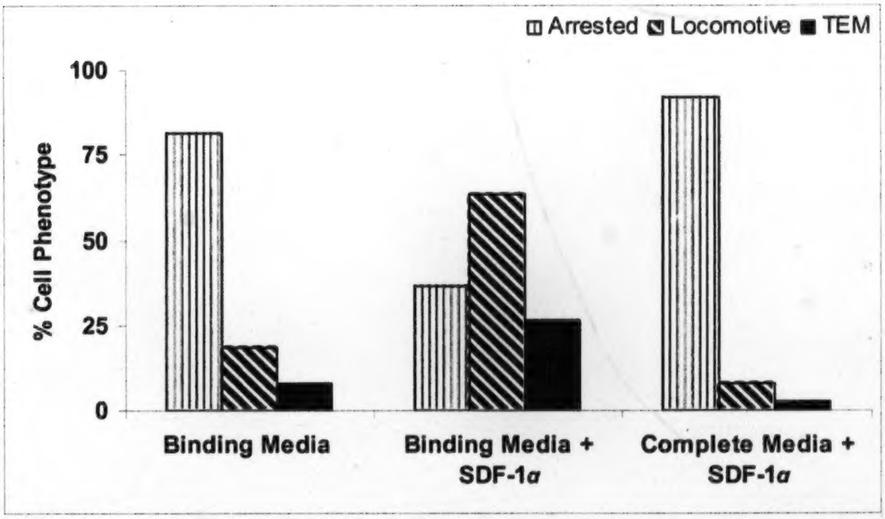

Figure 3.5 SDF-1*α* and complete media affect PBL TEM. HUVEC monolayers were left untreated or pretreated with SDF-1*α* (100 U/ml) for 5 min before the assembly of the laminar flow chamber as described in Materials and Methods. Treatments and perfusion of PBLs was also either performed using binding or complete media as indicated. Endothelial–adherent lymphocytes were evaluated over the course of 20 min under shear stress of 1 dyne/cm^2. The fraction of arrested, locomotive and transmigrating lymphocytes was determined. Data are representative of three experiments.

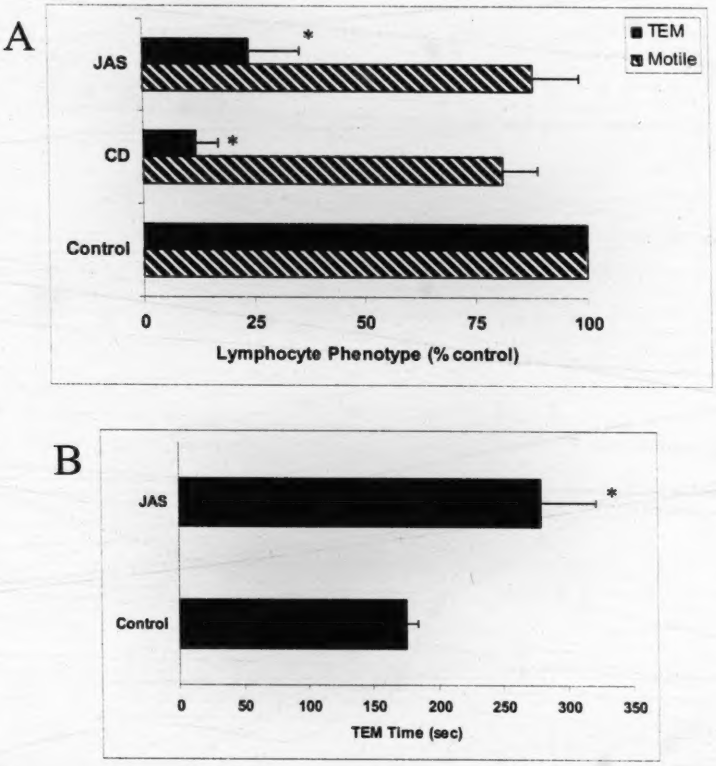

Figure 3.6 Disruption of the endothelial F-actin cytoskeleton inhibits lymphocyte TEM. (A) HUVEC monolayers were left untreated or pretreated with CD (1 µM; 1 h) or JAS (300nM; 1 h) before the assembly of the laminar flow chamber as described in Materials and Methods. Endothelial–adherent lymphocytes were evaluated over the course of 20 min under shear stress of 1 dyne/cm^2. The fraction of motile and transmigrating lymphocytes was determined. Data are mean ± SEM of at least four experiments. *$P < 0.05$. **(B)** The time taken by a lymphocyte to completely travel under the EC monolayer. Data are mean ± SEM of at least four experiments. *$P < 0.05$.

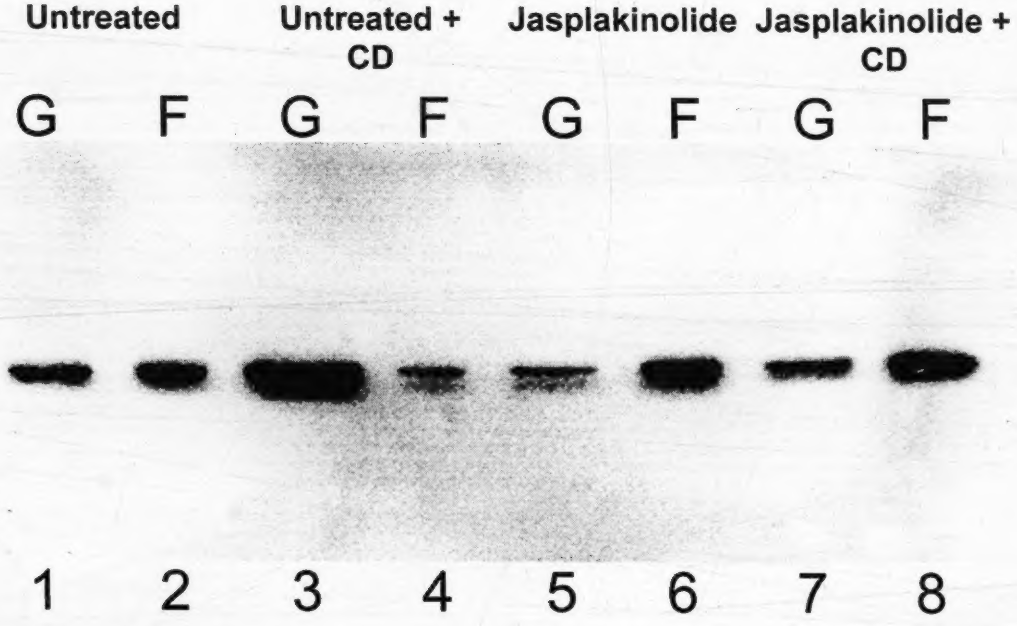

Figure 3.7 JAS stabilizes the endothelial F-actin cytoskeleton. The relative amounts of F-actin versus G-actin in endothelial cell lysates was analyzed as described in Materials and Methods. Untreated EC G-actin (lanes 1 and 3) and F-actin (lanes 2 and 4) or JAS pre-treated EC G-actin (lanes 5 and 7) and F-actin (lanes 6 and 8) levels are shown in response to incubation with (lanes 3, 4, 7 and 8) or without (lanes 1, 2, 5 and 6) CD for 10 min. Immunoblots are representative of three independent experiments.

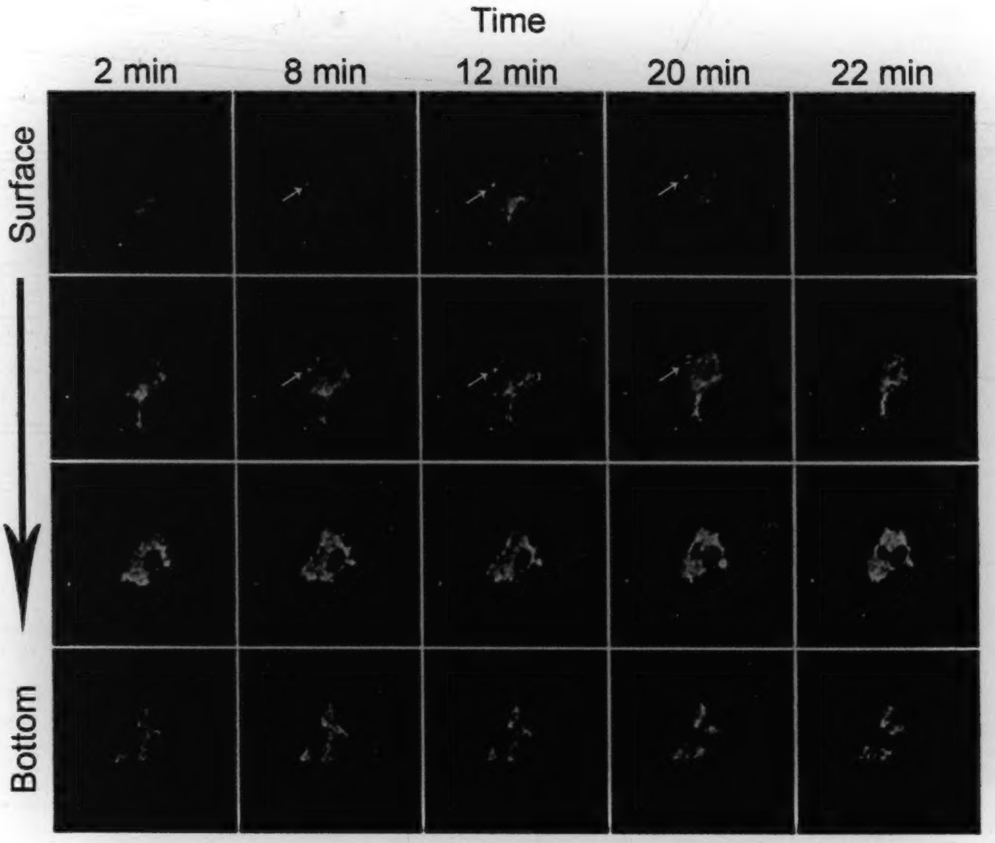
Time
2 min
8 min
12 min
20 min
22 min
Surface
Bottom

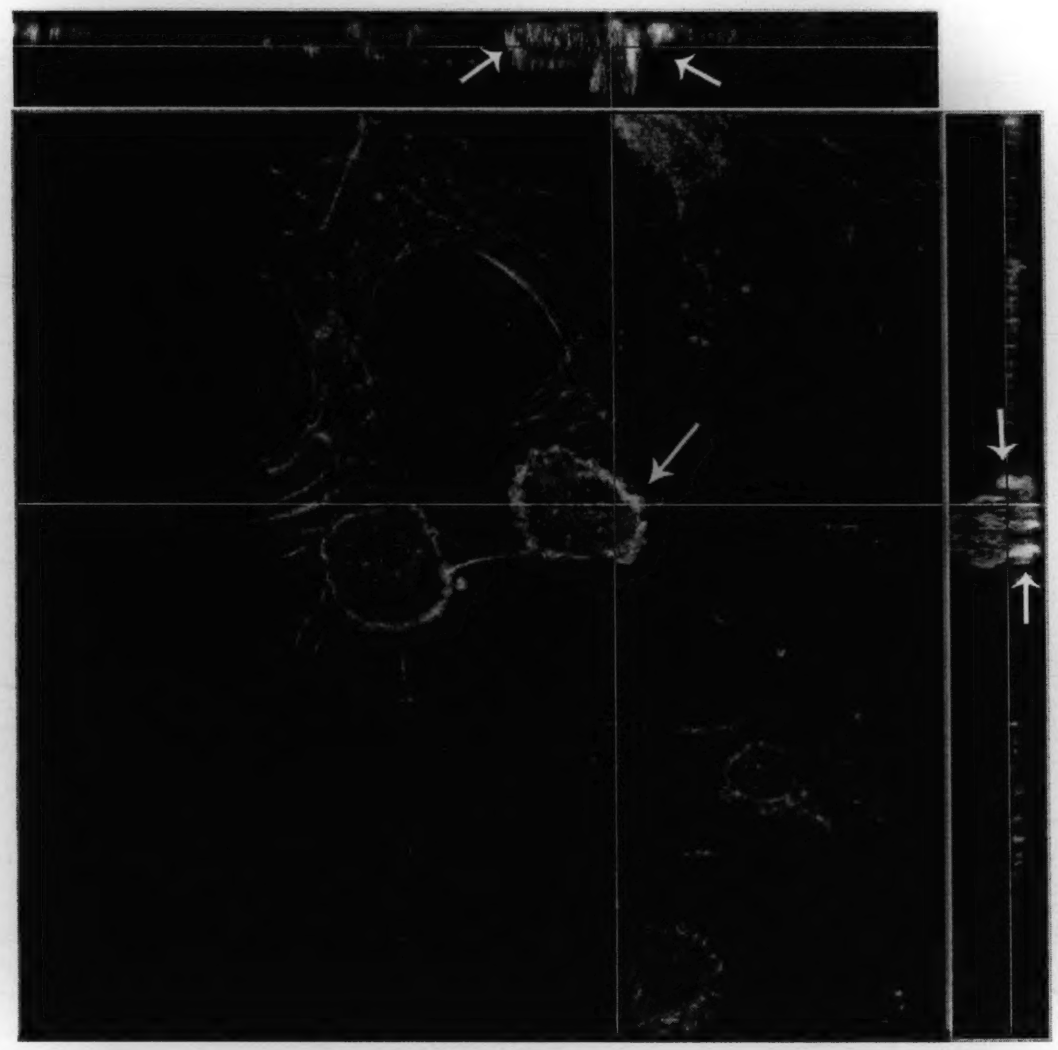

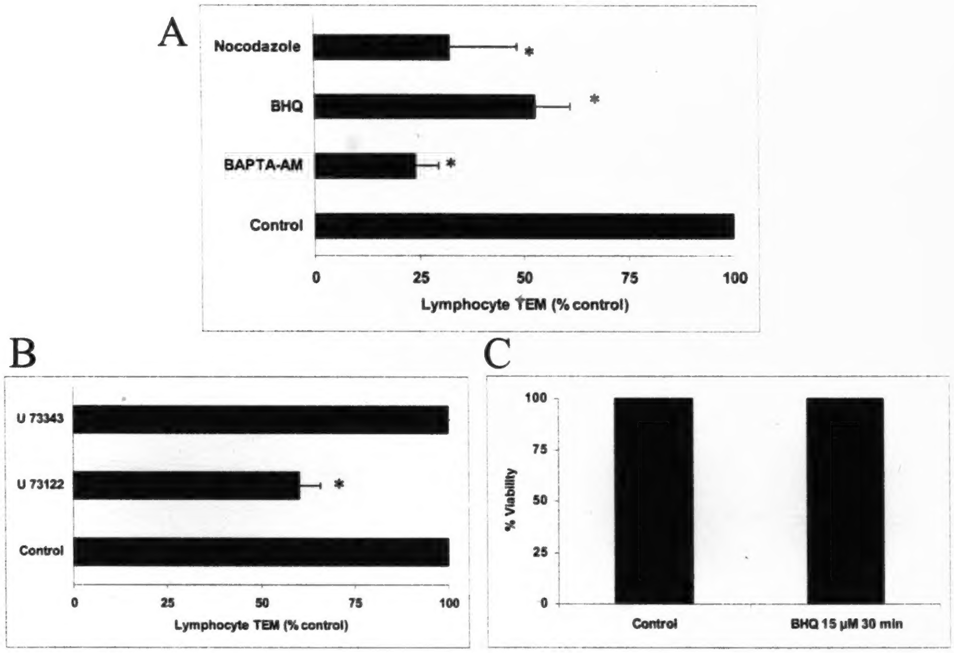

Figure 3.10 Lymphocyte TEM is dependent on endothelial Ca^{2+}. (A-B) HUVEC monolayers were left untreated or pretreated with either BAPTA-AM (20 μM; 30 min), BHQ (15 μM; 30 min), nocodazole (10 μM; 16 h), U 73122 (5 μM; 30 min) or U 73343 (5 μM; 30 min) before the assembly of the laminar flow chamber as described in Materials and Methods. The fraction of transmigrating lymphocytes was determined as in Figure 3.6. Data are the mean ± SEM of at least three experiments. *$^*P < 0.05$* **(C)** XTT cell viability assay was performed as described in Materials and Methods. Control (no treatment) values were adjusted to equal 100%. % viability is measured as absorbance values of treatment compared to the control. Data are expressed as mean ± SEM of three experiments.

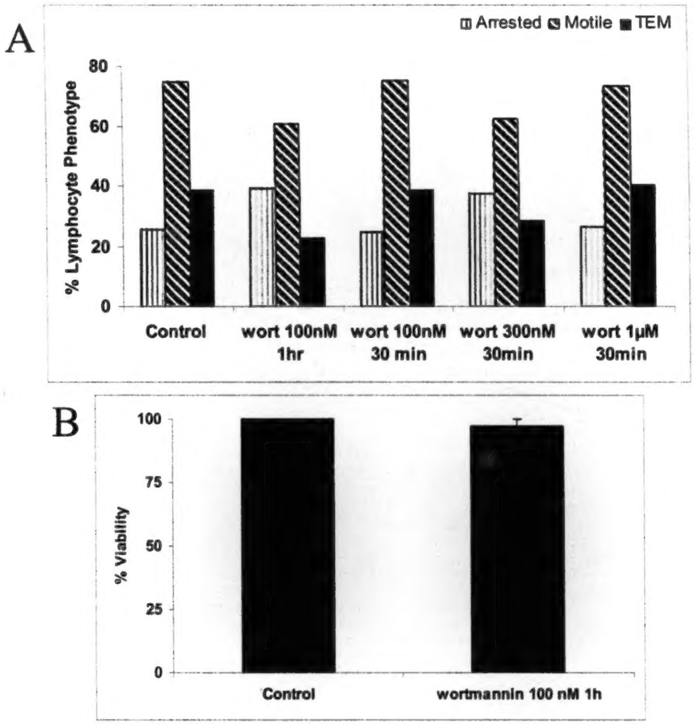

Figure 3.11 Effect of various wortmannin concentrations and incubation times in treated HUVECs on lymphocyte TEM and HUVEC viability. (A) HUVECs were left untreated or pretreated with PIK inhibitor wortmannin with the indicated concentrations and times before the assembly of the laminar flow chamber as described in Materials and Methods. Endothelial–adherent lymphocytes were evaluated over the course of 20 min under shear stress of 1 dyne/cm^2. The fraction of arrested, locomotive and transmigrating lymphocytes was determined. Data is representative of three experiments. **(B)** XTT cell viability assay was performed as described in Materials and Methods. Control (no treatment) values were adjusted to equal 100%. % viability is measured as absorbance values of treatment compared to the control. Data are expressed as mean ± SEM of three experiments.

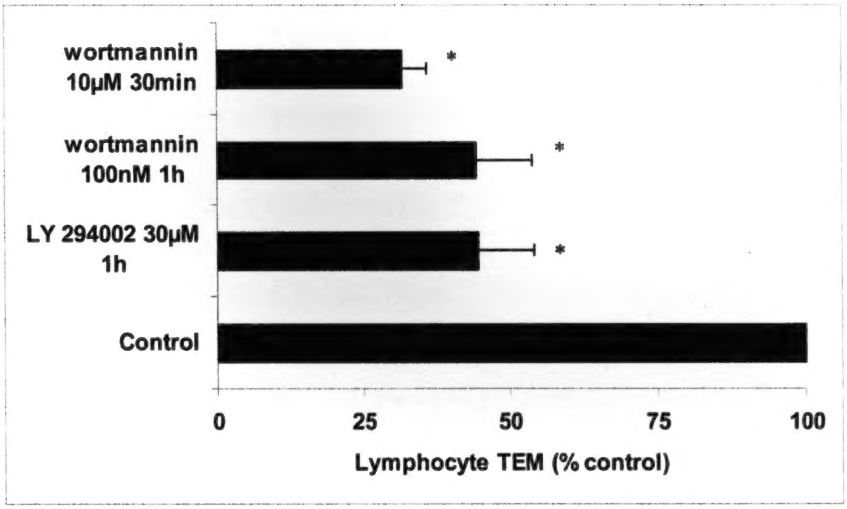

Figure 3.12 Endothelial PIK inhibition decreases lymphocyte TEM. HUVECs were left untreated or pretreated with PIK inhibitors, wortmannin (100 nM; 1 h or 10 µM; 30 min) or LY 294002 (30 µM; 1 h) before the assembly of the laminar flow chamber as described in Materials and Methods. The fraction of transmigrating lymphocytes was determined as in Figure 3.6. Data are mean ± SEM of three experiments. $^{*}P < 0.05$

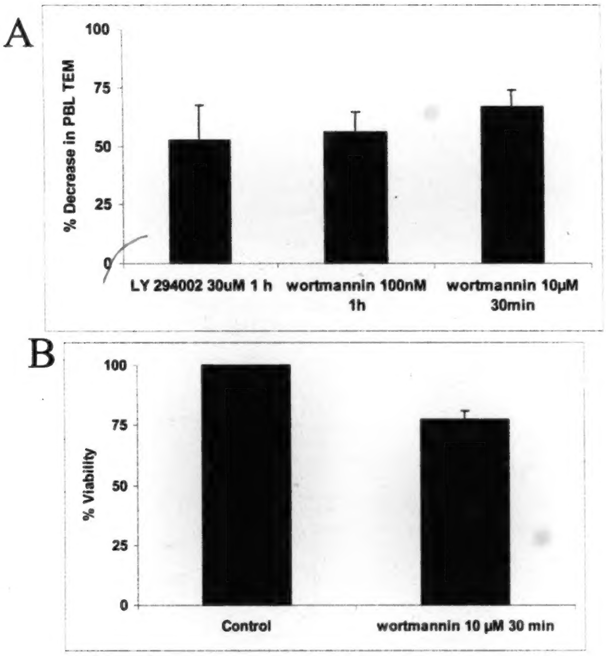

Figure 3.13 Endothelial PI4K inhibits lymphocyte TEM. (A) HUVECs were then left untreated or pretreated with PIK inhibitors, wortmannin (100nM; 1 h and 10µM; 30 min) and LY 294002 (30µM; 1 h) before the assembly of the laminar flow chamber. % decrease was determined by expressing the difference between control and treatment TEM values compared to the control value. Data are mean ± SEM of three experiments. *$P < 0.05$ **(B)** XTT cell viability assay was performed as described in Materials and Methods. Control (no treatment) values were adjusted to equal 100%. % viability is measured as absorbance values of treatment compared to the control. Data are expressed as mean ± SEM of three experiments.

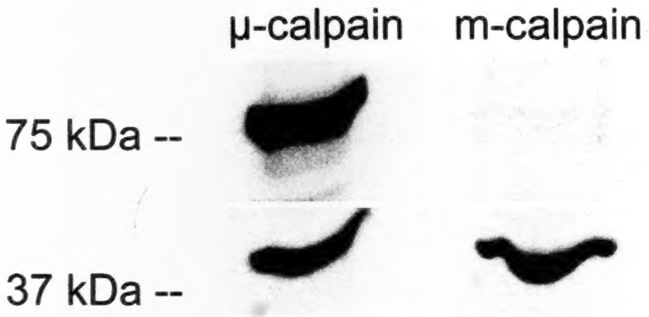

Figure 3.14 Robust expression of μ-calpain in HUVEC lysates. HUVEC lysate were run on 7.5% SDS-Page and transferred to a PVDF membrane. Lysates were then stained for either μ- (~80 kDa) or m-calpain (~80 kDa) and anti-actin loading control (~42 kDa). Immunoblots are representative of three independent experiments.

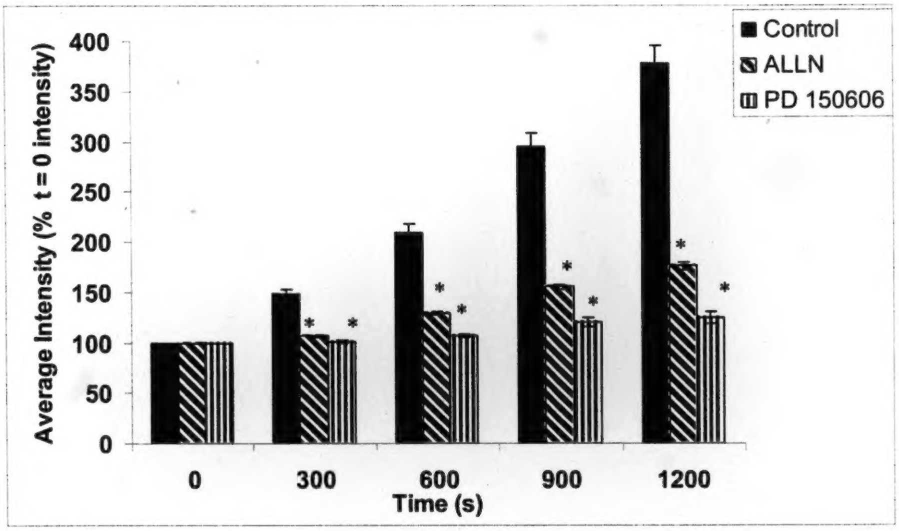

Figure 3.15 HUVECs possess constitutive calpain activity which is inhibited by ALLN and PD 150606. HUVECs were left untreated or pretreated with calpain inhibitors, ALLN (100 µM; 1 h) or PD 150606 (100 µM; 1 h) and BOC (10 µM) was added at t = 0 as described in Materials and Methods. Data are shown as relative to its corresponding treatment at t = 0. Data are mean ± SEM of eight cells. Data are representative of three experiments. *$P < 0.05$.*

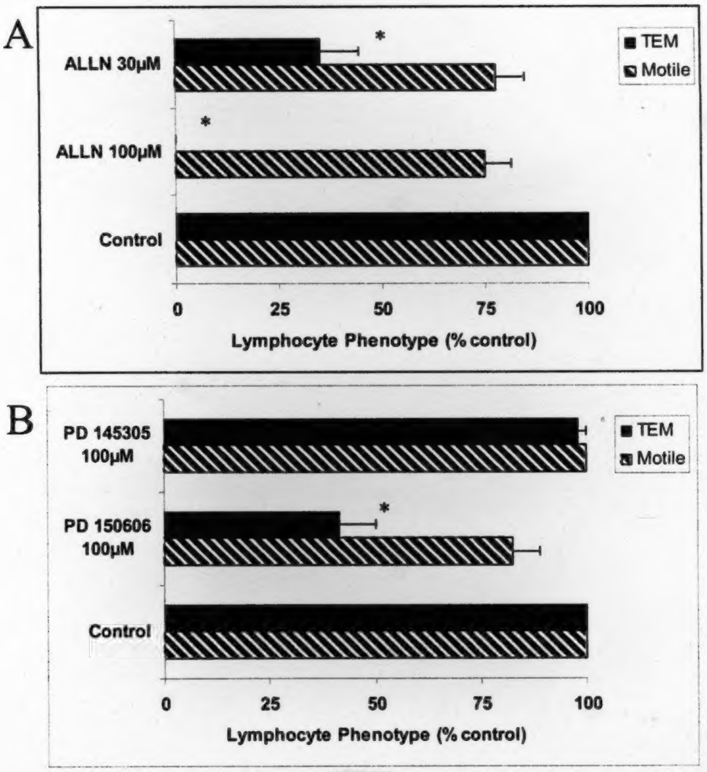

Figure 3.16 Endothelial calpain activity is required for efficient PBL TEM. **(A)** HUVECs were left untreated or pretreated with calpain inhibitors, ALLN (30 μM or 100 μM; 1 h) before the assembly of the laminar flow chamber as described in Materials and Methods. The fraction of transmigrating lymphocytes was determined as in Figure 3.6. Data are mean ± SEM of three experiments. *$P < 0.05$ **(B)** HUVEC monolayers were left untreated or pretreated with PD 1506060 or inactive analog PD 145305 (each 100 μM; 1h) before the assembly of the laminar flow chamber as described in Materials and Methods. The fraction of motile and transmigrating lymphocytes was determined as in Figure 3.6. Data are mean ± SEM of at five experiments. *$P < 0.05$.

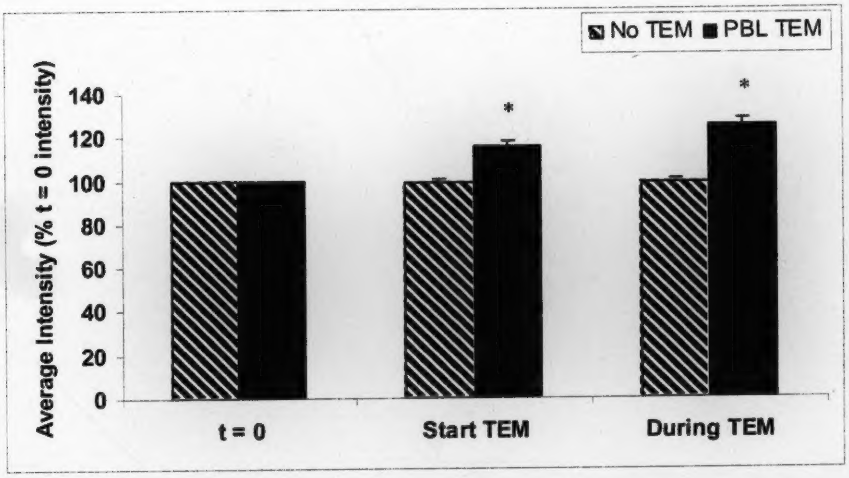

Figure 3.17 Calpain activity is increased in HUVECs that participated in TEM. HUVECs were pretreated with BOC (10 µM; 20 min) before the assembly of the laminar flow chamber as described in Materials and Methods. HUVEC intensity was evaluated at t = 0, the start of PBL TEM and during the transmigration process under shear stress of 1 dyne/cm^2. Data are shown relative to their corresponding zero time point. Data are mean ± SEM of at least twelve ECs. *$P < 0.05$

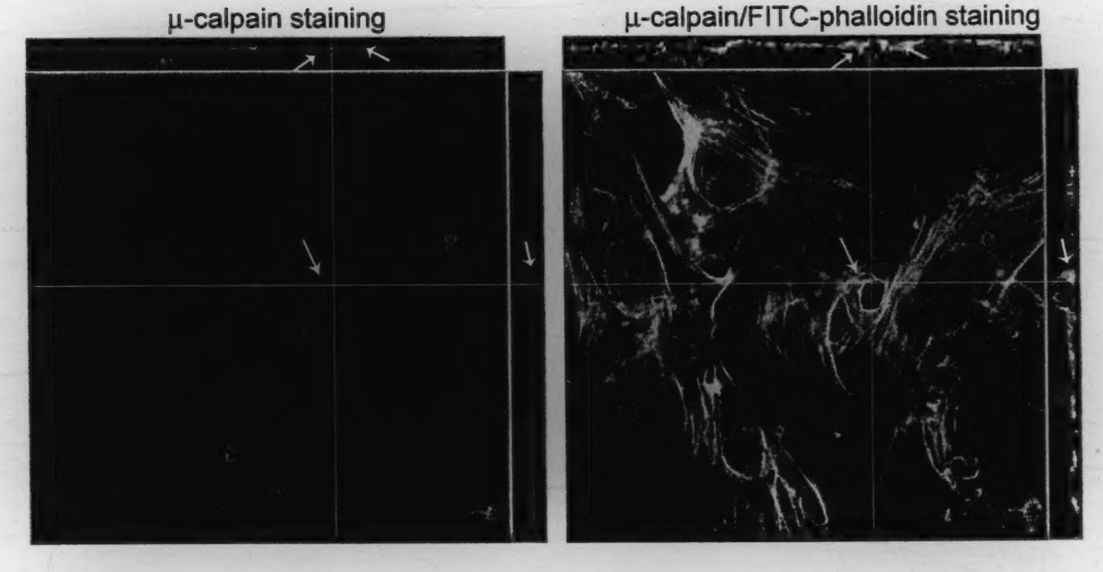

Figure 3.18 Endothelial μ-Calpain appears to localize around transmigrating lymphocytes. Serial confocal fluorescence image of a fixed and permeabilized HUVEC monolayer through which PBLs are seen to transmigrate under laminar shear stress is shown. μ-calpain (red) is visualized using Texas Red secondary conjugated to anti μ-calpain primary antibody. F-actin is visualized using FITC-phalloidin (green). Z plane of the Y-axis (red line) is shown on the right of the figure and the Z plane of the X-axis (green line) is shown on the top of the figure. Top panel shows μ-calpain staining alone and the bottom panel shows combined μ-calpain/FITC-phalloidin staining. Arrows indicate areas with an enhanced μ-calpain signal around a transmigrating PBL. Data are representative of three experiments.

		Control	**ALLN**	**JAS**
t = 0 min	**No Cup**	23%	36%	43%
	Partial Cup	20%	46%	39%
	Complete Cup	57%	18%	18%
	p value		***0.005 vs. control***	***0.002 vs. control***
t = 6 min	**No Cup**	25%	47%	42%
	Partial Cup	16%	32%	34%
	Complete Cup	59%	21%	24%
	p value		***0.003 vs. control***	***0.009 vs. control***

Table 3.1 Calpain inhibitions decreases ICAM cup formation around adherent lymphocytes. HUVEC monolayers were left untreated of pretreated with calpain inhibitor ALLN (100 mM; 1 h) or F-actin stabilizing agent JAS (300 nM; 1 h) before the assembly of the laminar flow chamber as described in Materials and Methods. ICAM cup formation on HUVECs surrounding PBLs at t = 0 min and t = 6 min was determined as described in Materials and Methods. Data are representative of two experiments.

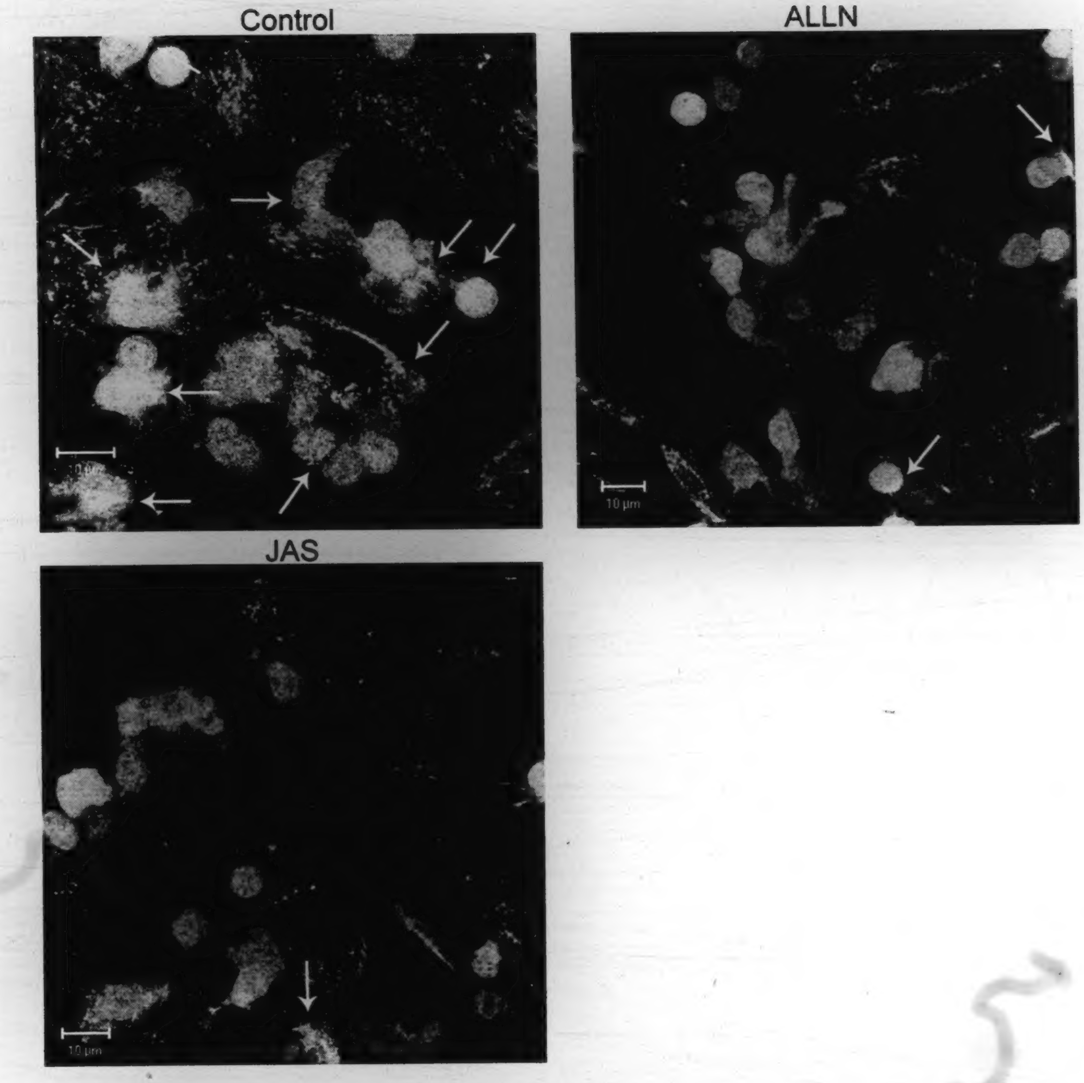

Figure 3.19 Calpain inhibitions decreases ICAM cup formation around adherent lymphocytes. Serial confocal live-cell fluorescence images of ICAM-1 (red) stained HUVECs on which CMFDA-stained PBLs (green) adhere under laminar shear stress conditions as described in Materials and Methods are shown. Z slices of 0.5 µm were collected every 2 min over a 20 min period. Compressed Z plane images are shown for the 6 min time point. Arrows represent areas in which ICAM cup formation is complete. Data are representative of two experiments.

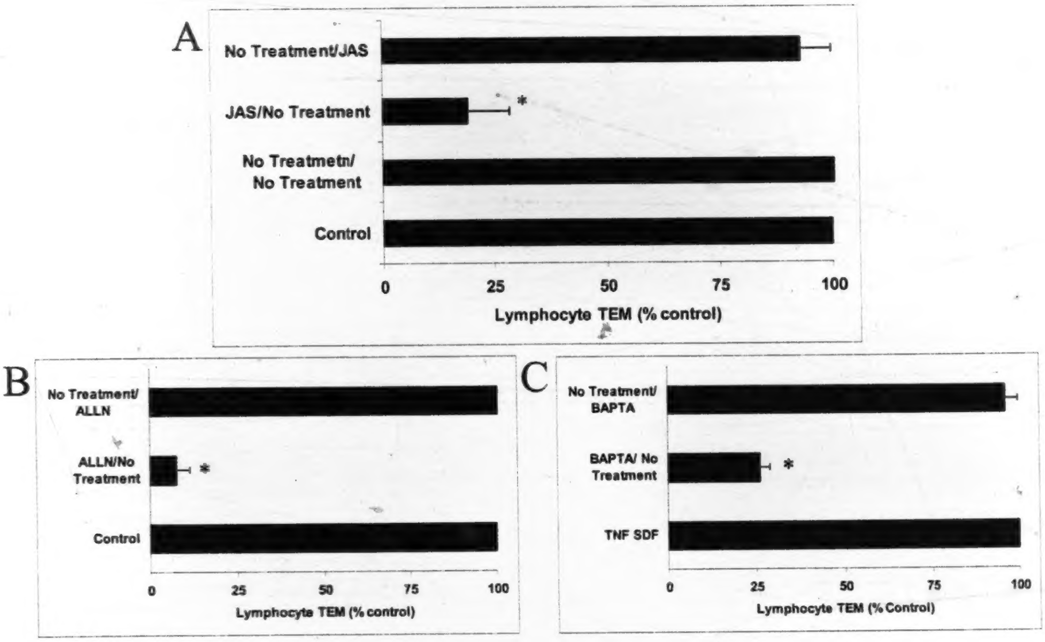

Figure 3.20 Various agents have no affect on PBLs. (A-C) HUVECs were left untreated or pretreated with various agents, JAS (300 nM; 1 h), BAPTA-AM (20 μM; 30 min) or ALLN (100 μM; 1 h) before the assembly of the 2 chamber laminar flow chamber as described in Materials and Methods. Data is show as dish B/dish A. The fraction of transmigrating lymphocytes was determined as in Figure 3.6. Data are mean ± SEM of three experiments. *$P < 0.05$

CHAPTER 4. GENERAL DISCUSSION.

The work presented in this thesis demonstrates that the active participation of the EC is crucial for the process of lymphocyte TEM. Using an experimental model of lymphocyte-EC interaction under shear stress conditions, we found that EC actively remodel their F-actin cytoskeleton to allow PBL TEM to proceed. Inhibition of F-actin remodelling in EC with JAS pretreatment both decreased the fraction of lymphocytes that underwent TEM, and markedly increased the transit time of those lymphocytes that successfully migrated across the endothelium. Furthermore, EC F-actin was seen to condense around the migration pore using living cell fluorescence microscopy. EC pretreated with BAPTA-AM, nocodazole and BHQ also showed a decrease in lymphocyte TEM, confirming previous observations of the involvement of EC Ca^{2+} signalling in neutrophil TEM. Further, pretreatment of EC with calpain inhibitors, ALLN and PD 150606, and PIK inhibitors, wortmannin and LY 294002, showed a significant decrease in the proportion of lymphocytes that underwent TEM. These data, taken together, provide strong evidence that the process of lymphocyte TEM is dependent upon the active remodelling of the EC F-actin cytoskeleton.

In the course of optimizing the experimental conditions we were able to validate previous observation of PBL TEM. First we confirm the need for apical bound chemokines in inducing PBL TEM under shear stress [125]. PBL stimulatory chemokines are normally apically presented on inflamed endothelia in vivo [63]. Pretreatment of HUVEC monolayers with SDF-1α was sufficient in inducing PBL TEM. When SDF-1α treatment is absent from the laminar flow assay system, PBL TEM is significantly reduced (Figure 3.5). Second, we were also to confirm physiological time frames of PBL TEM in this in vitro system. We found on average that the course of PBL TEM took 175 sec ± 9 sec which was near the values that have been reported in intravital microscopy studies and within physiological ranges [125, 261, 262]. This was one of the clear drawbacks from the transwell method of studying TEM, which has now been solved.

Another interesting result found from optimization studies was the differences between binding and complete media on PBL TEM. Originally we used complete media which was comprised of M199 with 10% FBS, penicillin, streptomycin, and glutamine. Binding media (HBSS, 10 mM HEPES at pH 7.4, 2 mg/ml BSA, 1 mM Ca^{2+} and 1 mM Mg^{2+}) was the media used in previous studies [125] differs essentially from complete media in the absence of FBS. The presence of complete media could essentially prevent any PBL from undergoing TEM. It has been previously reported that fetal calf serum decreased transendothelial permeability to macromolecules [263]. It is possible that FBS could also be acting in the same way in our flow assay to decrease PBL TEM. Serum is also known to posses significant levels of sphingosine-1-phosphate (S1P) [264]. S1P has been reported to promote EC barrier integrity by cytoskeletal rearrangement [265, 266]. S1P produced rapid, sustained, and dose-dependent increases in transmonolayer electrical resistance. This effect may have also been one of the factors that was preventing PBL TEM, since we have also seen that certain cytoskeletal rearrangements are required for PBL TEM. However, the involvement of S1P in our system may also be contradictive of what has been seen. FTY720, an immunosuppressant, activates S1P receptors (S1PRs) and leads to increased lymphocyte homing to secondary lymphoid organs [267]. But still, S1PRs are able to both support and inhibit cell migration [268]. Thus, S1P may be the agent that is causing the decrease in PBL TEM. More studies will have to be done to fully understand what is happening. There are likely to be other factors in the complete media that are causing the decrease, therefore future studies isolating these factors will be essential in understanding the complete media's effect.

The transmigration of leukocytes including monocytes, neutrophils, and lymphocytes has been previously examined under laminar flow conditions [7, 269, 270]. However, the majority of these studies emphasized the leukocytes' role in TEM. Looking specifically at the endothelium in our study, we have shown that ECs are an active participant in the diapedesis step of lymphocyte recruitment to the tissue compartment. Depolymerization of endothelial F-actin prevents TEM [5], indicating that endothelial F-actin structures are used to support leukocyte TEM. Moreover, previous work has indicated that ECs remodel their actin cytoskeleton and matrix adhesion structures after lymphocyte adhesion [2, 104]. We have confirmed these results and extended them to demonstrate that the inhibition of remodelling of EC F-actin was sufficient to inhibit TEM under physiological shear stress conditions. We were also able to visualize one feature of F-actin remodelling with the use of the YFP-actin chimeric protein, namely an increase in F-actin around the migration pore. Our data also shows F-actin forming around the leukocyte (Appendix Video B.4). This condensation of F-actin at the margins of the transmigration passage has also been previously seen in monocyte TEM [271]. However, F-actin was only shown to be present in high levels around the migration pore. Our observations extend these results to show the importance of the EC F-actin cytoskeleton in PBL TEM and that EC F-actin is actively remodelled. These data suggest a significant role for F-actin in TEM.

Several models for the role of EC F-actin polymerization in lymphocyte TEM may be considered. First, subplasmalemmal F-actin remodelling may be required to strengthen a "tunnel" at the EC border to allow the lymphocyte to diapedese through the intercellular junction. Alternatively, remodelling of cortical F-actin may be involved in the recruitment of new membrane to the surface of the endothelial cell at the migration pore as recently suggested by Muller [104]. They report that ICAM-1 microvilli-like membrane projections formed around a leukocyte, and were enriched in actin. These structures had no effect on firm adhesion, occur within physiological time frames of TEM, are inhibited by inhibitors that also block TEM, and are associated with leukocytes throughout TEM. These observations indicate a strong link of these structures to TEM, which would also be in agreement with our data. Near the end stages of PBL TEM F-actin condenses around the top of the lymphocyte helping possible to either push the final bit of the PBL through or seal of the rear end so that nothing would be able to leak through. Along with strengthening a “tunnel” for the PBL to pass through, F-actin may also play a more active role in TEM by helping to guide the cell through the endothelium.

The specific mechanism that leads to EC F-actin remodelling is likely governed in part, by a Ca^{2+} flux. The block in lymphocyte TEM appears at an early stage since lymphocytes move across the surface of either JAS-treated or calpain-inhibitor-treated EC monolayers normally, but do not appear to extend processes between EC. In EC a transient increase in the intracellular free calcium is required for TEM of neutrophils [3] and has been linked to endothelial calcium-dependent myosin light chain kinase (MLCK) activity [180]. Our data agree with these findings with regards to lymphocyte TEM. We confirm that intracellular calcium is required in EC and further extend these observations to show that that the sER and SERCA are an integral part of the calcium flux pathway in lymphocyte TEM. PLC is also involved in the generation of the Ca^{2+} signal required by the endothelium to allow PBL TEM to proceed. PLC converts PIP_2 into DAG and IP_3. IP_3 activates the IP_3 receptor on the ER to elicit a Ca^{2+} response. These results indicate that the Ca^{2+} source required in ECs for PBL TEM arises from the sER. Although we have not identified the membrane-proximal event that initiates this signal, others have implicated G-protein coupled receptor stimulation [272], or ligation of adhesion molecules such as CD54 or CD31 [273, 274]. In our model Ca^{2+} stores in the sER are released and would signal downstream effectors that would ultimately be able to produce EC cytoskeletal F-actin remodelling and leukocyte diapedesis. Calcium's role in PBL TEM is as an intermediate in the signalling pathway.

Calpain is a likely target of this signalling pathway in addition to MLCK. It is proposed that an increase in intracellular Ca^{2+} can lead to calpain mediated, localized cytoskeletal reorganization [275]. Calpains are involved in remodelling of the actin cytoskeleton during EC monolayer wound healing and are also found to be active during cell migration [234]. In the migrating cell, calpain proteolytic activity appears to cleave integrin-F-actin linkages at the rear of the cell and this leads to the disruption of cell-matrix interactions [212]. Calpain activity in leukocytes governs integrin-mediated adhesion by disrupting cytoskeletal linkages [71]. Our observations indicate that endothelial calpain activity is required for efficient lymphocyte TEM (Figure 3.16 A, B) and likely participates in F-actin remodelling. EC calpain activity was also increased in the ECs that participated in lymphocyte TEM (Figure 3.17). The increase in intensity was seen globally over the entire HUVEC and was not seen to localize to either the focal adhesion complex or interendothelial junctions. These results are consistent with a role for calpain in acting on F-actin associated molecules during PBL TEM at the surface of the endothelium.

Calpain was also seen to be localized around the migration pore of a transmigrating PBL. The enhanced calpain signal is seen near the surface of the EC and is overlapped by F-actin staining (Figure 3.18 A, B). There is no evidence of increased calpain staining at the focal adhesion complex or at the interendothelial junction. However it is difficult to determine whether EC or PBL calpain is enhanced at the migration pore. These results are consistent with the hypothesis that calpain is functioning at the same level as cortical F-actin remodelling.

There are many possible specific targets of calpain proteolytic activity in ECs that may be involved in supporting lymphocyte TEM. Candidates include adaptor molecules involved in linking F-actin to the interendothelial cell plasma membrane such as ERM family members, vinculin and ezrin [234, 276], VE-cadherin [277], or regulatory molecules such as the Rho GTPases [278]. Our data indicate that it is probable that calpain is actin on ERM proteins to liberate surface ICAM-1 (Figure 3.19 A, B). The ERM proteins function in allowing the cortical cytoskeleton to regulate the membrane localization ICAMs [260, 279, 280]. We speculate that once the ERM proteins are cleaved by calpain, ICAM becomes able to be aggregated on the surface of the endothelium underneath an adherent PBL in the docking structure. ICAM-1 then forms cup like projections that are thought to aid in the TEM step of the leukocyte adhesion cascade [104]. Calpain inhibition significantly decreased the amount the ICAM-1 cup projections around adherent PBLs on the surface of the endothelium. Data showing calpain's involvement with cytoskeletal remodelling and our data indicating the need for both calpain and F-actin remodelling, strongly suggest that calpain does function by altering the EC F-actin cytoskeleton in TEM. More specifically it appears that one of calpain's definite roles may be in creating the ICAM cup projection.

We also looked at which form of calpain in HUVECs is likely to mediate TEM. Previous reports indicate that HUVECs contain low expression of µ-calpain [281]. Also, a report of the mode of cytoskeletal reorganization in migrating HUVECs indicated that m-calpain is the active form. It was seen that in migrating HUVECs activated m-calpain was present mainly in the edges of the cell and there was a decrease in the amounts of cytoskeletal associated proteins [282].

Our data differs from these results. Using Western blot analysis of total cell lysates from HUVECs we found robust expression of µ-calpain (Figure 3.11A). A significant difference in our study as compared to Fujitani et al. [281], was the method used to determine calpain levels. HUVECs were separated on the column and then each fraction was run on SDS-Page. The majority of µ-calpain appeared in only one fraction whereas m-calpain was distributed in four fractions and appeared darker on the blot. However, it is hard to judge which form is present in greater levels since a greater amount of the m-calpain could be present in one fraction so when resolving the fractions unequal amounts of the calpains would have been loaded. Interestingly, they also show using Northern blot analysis that μ-calpain mRNA is present in higher levels than m-calpain mRNA. We believe HUVECs express high levels of μ-calpain (Figure 3.14) and that μ-calpain is the form active in lymphocyte TEM. It seems likely that this is true due to the fact that Ca^{2+} concentrations required to activate μ-calpain are closer to physiological levels than m-calpain [216].

Consistent with a role for a calpain-dependent pathway involved in lymphocyte TEM, we show that EC pretreated with PIK inhibitors do not support efficient lymphocyte TEM. PIP_2 is required for calpain activation in cells [223]. PI4K and phosphatidylinositol phosphate kinases phosphorylate the 4- and 5-hydroxyl groups of phosphatidylinositol respectively to generate PIP_2 [283, 284]. PIP_2 is a substrate for PI3K and when phosphorylated by PI3K PIP_2 is converted to PI 3,4,5-trisphosphate (PIP_3). Accordingly, there appears to be a trend that shows combined PI4K and PI3K inhibition has a greater inhibitory effect on PBL TEM than PI3K inhibition alone, however it is not statistically significant. The pronounced effect of PI4K-inhibitory concentrations of wortmannin is consistent with a critical role for PIP_2 generation in EC. PIP_2 has a regulatory role in the function of a number of proteins, including calpain, involved in the reorganization of F-actin structures [223]. PIP_2 is also a substrate for PLC to elicit a Ca^{2+} signal through IP_3. PI4K inhibition functions to decrease PIP_2 levels produced thus causing decreased calpain activation and Ca^{2+} signalling which then prevents cytoskeletal remodelling and ultimately ends in decreased in PBL TEM.

PI3K also significantly decreased PBL TEM (Figure 3.13). The method of action may not include calpain activation however it is likely that it will result in F-actin remodelling. Previous studies report that F-actin induced by Ras [285, 286], G protein-coupled receptor [287], and integrin [288] required PI3K to be remodelled. Also recently it has been reported that in fibroblast cell migration, PI3K activity alone could lead to remodelling of F-actin [289]. The PI3K inhibitor wortmannin did not inhibit lymphocyte TEM when the lymphocytes were pre-treated with the compound [125]. Therefore the effect of these inhibitors on PI generation appears to be a unique feature of EC signalling in TEM. Nevertheless, overall our data support a model of calcium-dependent calpain-activity involved in the remodelling of EC cortical actin structures at the migration pore.

In summary, the experiments described in this thesis describe an endothelial phenomenon, which facilitates PBL TEM in vitro. The active participation of the EC is critical in the processes of lymphocyte TEM. EC F-actin was observed to condense around the migration pore, perhaps indicating a structural role for the remodelled F-actin structures. Moreover endothelial Ca^{2+}, calpain-, PI3K- and PI4K–dependent events are involved in supporting lymphocyte diapedesis. The simplest interpretation of the data suggest a model in which the endothelial cortical actin cytoskeleton is dynamically remodelled to participate in the formation of the migration pore, in a process involving calpain proteolytic activity of actin-associated molecules.

CONCLUSIONS

I. The endothelium actively participates in lymphocyte TEM.

II. An intact endothelial F-actin cytoskeleton is required for lymphocyte TEM to occur.

III. The intact endothelial F-actin cytoskeleton needs to be remodelled for lymphocyte TEM to occur.

IV. F-actin condenses around the migration pore, possibly strengthening of a "tunnel" for the lymphocyte to transmigrate through.

V. Endothelial Ca^{2+} signalling is a prerequisite in the pathway of lymphocyte TEM, and is generated through PLC activity and sER Ca^{2+} release.

VI. Lymphocyte TEM requires endothelial calpain activity.

VII. Endothelial calpain is required for aggregation of EC ICAM-1 into adhesion cup formation.

VIII. Endothelial PI3K- and PI4K-dependent PI generation aids in lymphocyte TEM.

BIBLIOGRAPHY

1. Hancock, W.W., N.M. Thomson, and R.C. Atkins, *Composition of interstitial cellular infiltrate identified by monoclonal antibodies in renal biopsies of rejecting human renal allografts.* Transplantation, 1983. **35**(5): p. 458-63.
2. Mullaly, S.C., et al., *Stable lymphocyte contact induces remodeling of endothelial cell matrix receptor complexes.* Eur J Immunol, 2002. **32**(5): p. 1493-501.
3. Huang, A.J., et al., *Endothelial cell cytosolic free calcium regulates neutrophil migration across monolayers of endothelial cells.* J Cell Biol, 1993. **120**(6): p. 1371-80.
4. Hixenbaugh, E.A., et al., *Stimulated neutrophils induce myosin light chain phosphorylation and isometric tension in endothelial cells.* Am J Physiol, 1997. **273**(2 Pt 2): p. H981-8.
5. Kielbassa, K., C. Schmitz, and V. Gerke, *Disruption of endothelial microfilaments selectively reduces the transendothelial migration of monocytes.* Exp Cell Res, 1998. **243**(1): p. 129-41.
6. Shaw, S.K., et al., *Real-time imaging of vascular endothelial-cadherin during leukocyte transmigration across endothelium.* J Immunol, 2001. **167**(4): p. 2323-30.
7. Allport, J.R., W.A. Muller, and F.W. Luscinskas, *Monocytes induce reversible focal changes in vascular endothelial cadherin complex during transendothelial migration under flow.* J Cell Biol, 2000. **148**(1): p. 203-16.
8. Sandig, M., E. Negrou, and K.A. Rogers, *Changes in the distribution of LFA-1, catenins, and F-actin during transendothelial migration of monocytes in culture.* J Cell Sci, 1997. **110**(Pt 22): p. 2807-18.
9. Springer, T.A., et al., *Traffic signals for lymphocyte recirculation and leukocyte emigration: the multistep paradigm.* Cell, 1994. **76**(2): p. 301-14.
10. Schenkel, A.R., Z. Mamdouh, and W.A. Muller, *Locomotion of monocytes on endothelium is a critical step during extravasation.* Nat Immunol, 2004. **5**(4): p. 393-400.
11. Gallatin, W.M., I.L. Weissman, and E.C. Butcher, *A cell-surface molecule involved in organ-specific homing of lymphocytes.* Nature, 1983. **304**(5921): p. 30-4.
12. Catalina, M.D., et al., *The route of antigen entry determines the requirement for L-selectin during immune responses.* J Exp Med, 1996. **184**(6): p. 2341-51.
13. Tedder, T.F., D.A. Steeber, and P. Pizcueta, *L-selectin-deficient mice have impaired leukocyte recruitment into inflammatory sites.* J Exp Med, 1995. **181**(6): p. 2259-64.

14. Arbones, M.L., et al., *Lymphocyte homing and leukocyte rolling and migration are impaired in L-selectin-deficient mice.* Immunity, 1994. **1**(4): p. 247-60.

15. Mayadas, T.N., et al., *Leukocyte rolling and extravasation are severely compromised in P selectin-deficient mice.* Cell, 1993. **74**(3): p. 541-54.

16. Fuhlbrigge, R.C., et al., *Sialylated, fucosylated ligands for L-selectin expressed on leukocytes mediate tethering and rolling adhesions in physiologic flow conditions.* J Cell Biol, 1996. **135**(3): p. 837-48.

17. Bargatze, R.F. and E.C. Butcher, *Rapid G protein-regulated activation event involved in lymphocyte binding to high endothelial venules.* J Exp Med, 1993. **178**(1): p. 367-72.

18. Picker, L.J., et al., *Control of lymphocyte recirculation in man. I. Differential regulation of the peripheral lymph node homing receptor L-selectin on T cells during the virgin to memory cell transition.* J Immunol, 1993. **150**(3): p. 1105-21.

19. McCafferty, D.M., et al., *E/P-selectin-deficient mice: an optimal mutation for abrogating antigen but not tumor necrosis factor-alpha-induced immune responses.* Eur J Immunol, 2000. **30**(8): p. 2362-71.

20. Xie, H., et al., *Acquisition of selectin binding and peripheral homing properties by CD4(+) and CD8(+) T cells.* J Exp Med, 1999. **189**(11): p. 1765-76.

21. Bevilacqua, M.P., et al., *Endothelial leukocyte adhesion molecule 1: an inducible receptor for neutrophils related to complement regulatory proteins and lectins.* Science, 1989. **243**(4895): p. 1160-5.

22. Picker, L.J., et al., *Control of lymphocyte recirculation in man. II. Differential regulation of the cutaneous lymphocyte-associated antigen, a tissue-selective homing receptor for skin-homing T cells.* J Immunol, 1993. **150**(3): p. 1122-36.

23. Stenberg, P.E., et al., *A platelet alpha-granule membrane protein (GMP-140) is expressed on the plasma membrane after activation.* J Cell Biol, 1985. **101**(3): p. 880-6.

24. Bonfanti, R., et al., *PADGEM (GMP140) is a component of Weibel-Palade bodies of human endothelial cells.* Blood, 1989. **73**(5): p. 1109-12.

25. McEver, R.P., et al., *GMP-140, a platelet alpha-granule membrane protein, is also synthesized by vascular endothelial cells and is localized in Weibel-Palade bodies.* J Clin Invest, 1989. **84**(1): p. 92-9.

26. Lorant, D.E., et al., *Coexpression of GMP-140 and PAF by endothelium stimulated by histamine or thrombin: a juxtacrine system for adhesion and activation of neutrophils.* J Cell Biol, 1991. **115**(1): p. 223-34.

27. Laszik, Z., et al., *P-selectin glycoprotein ligand-1 is broadly expressed in cells of myeloid, lymphoid, and dendritic lineage and in some nonhematopoietic cells.* Blood, 1996. **88**(8): p. 3010-21.

28. Maly, P., et al., *The alpha(1,3)fucosyltransferase Fuc-TVII controls leukocyte trafficking through an essential role in L-, E-, and P-selectin ligand biosynthesis.* Cell, 1996. **86**(4): p. 643-53.

29. Alon, R., et al., *The integrin VLA-4 supports tethering and rolling in flow on VCAM-1.* J Cell Biol, 1995. **128**(6): p. 1243-53.

30. Moore, K.L., et al., *P-selectin glycoprotein ligand-1 mediates rolling of human neutrophils on P-selectin.* J Cell Biol, 1995. **128**(4): p. 661-71.

31. McEver, R.P. and R.D. Cummings, *Perspectives series: cell adhesion in vascular biology. Role of PSGL-1 binding to selectins in leukocyte recruitment.* J Clin Invest, 1997. **100**(3): p. 485-91.

32. Ushiyama, S., et al., *Structural and functional characterization of monomeric soluble P-selectin and comparison with membrane P-selectin.* J Biol Chem, 1993. **268**(20): p. 15229-37.

33. Ley, K., T.F. Tedder, and G.S. Kansas, *L-selectin can mediate leukocyte rolling in untreated mesenteric venules in vivo independent of E- or P-selectin.* Blood, 1993. **82**(5): p. 1632-8.

34. Jung, U., et al., *Velocity differences between L- and P-selectin-dependent neutrophil rolling in venules of mouse cremaster muscle in vivo.* Am J Physiol, 1996. **271**(6 Pt 2): p. H2740-7.

35. Stein, J.V., et al., *L-selectin-mediated leukocyte adhesion in vivo: microvillous distribution determines tethering efficiency, but not rolling velocity.* J Exp Med, 1999. **189**(1): p. 37-50.

36. Alon, R., D.A. Hammer, and T.A. Springer, *Lifetime of the P-selectin-carbohydrate bond and its response to tensile force in hydrodynamic flow.* Nature, 1995. **374**(6522): p. 539-42.

37. Diacovo, T.G., et al., *Circulating activated platelets reconstitute lymphocyte homing and immunity in L-selectin-deficient mice.* J Exp Med, 1998. **187**(2): p. 197-204.

38. Kunkel, E.J., et al., *Absence of trauma-induced leukocyte rolling in mice deficient in both P-selectin and intercellular adhesion molecule 1.* J Exp Med, 1996. **183**(1): p. 57-65.

39. Labow, M.A., et al., *Characterization of E-selectin-deficient mice: demonstration of overlapping function of the endothelial selectins.* Immunity, 1994. **1**(8): p. 709-20.

40. Kunkel, E.J. and K. Ley, *Distinct phenotype of E-selectin-deficient mice. E-selectin is required for slow leukocyte rolling in vivo.* Circ Res, 1996. **79**(6): p. 1196-204.

41. Ley, K., et al., *Importance of E-selectin for firm leukocyte adhesion in vivo.* Circ Res, 1998. **83**(3): p. 287-94.

42. Milstone, D.S., et al., *Mice lacking E-selectin show normal numbers of rolling leukocytes but reduced leukocyte stable arrest on cytokine-activated microvascular endothelium.* Microcirculation, 1998. **5**(2-3): p. 153-71.

43. Berlin, C., et al., *alpha 4 integrins mediate lymphocyte attachment and rolling under physiologic flow.* Cell, 1995. **80**(3): p. 413-22.

44. Johnston, B., et al., *Differential roles of selectins and the alpha4-integrin in acute, subacute, and chronic leukocyte recruitment in vivo.* J Immunol, 1997. **159**(9): p. 4514-23.

45. Bargatze, R.F., M.A. Jutila, and E.C. Butcher, *Distinct roles of L-selectin and integrins alpha 4 beta 7 and LFA-1 in lymphocyte homing to Peyer's patch-HEV in situ: the multistep model confirmed and refined.* Immunity, 1995. **3**(1): p. 99-108.

46. Zlotnik, A. and O. Yoshie, *Chemokines: a new classification system and their role in immunity.* Immunity, 2000. **12**(2): p. 121-7.

47. Murdoch, C. and A. Finn, *Chemokine receptors and their role in inflammation and infectious diseases.* Blood, 2000. **95**(10): p. 3032-43.

48. Pries, A.R., T.W. Secomb, and P. Gaehtgens, *The endothelial surface layer.* Pflugers Arch, 2000. **440**(5): p. 653-66.

49. Luster, A.D., *Chemokines--chemotactic cytokines that mediate inflammation.* N Engl J Med, 1998. **338**(7): p. 436-45.

50. Cyster, J.G., *Chemokines and cell migration in secondary lymphoid organs.* Science, 1999. **286**(5447): p. 2098-102.

51. Rossi, D. and A. Zlotnik, *The biology of chemokines and their receptors.* Annu Rev Immunol, 2000. **18**: p. 217-42.

52. Mackay, C.R., *Chemokines: immunology's high impact factors.* Nat Immunol, 2001. **2**(2): p. 95-101.

53. Thelen, M., *Dancing to the tune of chemokines.* Nat Immunol, 2001. **2**(2): p. 129-34.

54. Bleul, C.C., et al., *A highly efficacious lymphocyte chemoattractant, stromal cell-derived factor 1 (SDF-1).* J Exp Med, 1996. **184**(3): p. 1101-9.

55. Servant, G., et al., *Polarization of chemoattractant receptor signaling during neutrophil chemotaxis.* Science, 2000. **287**(5455): p. 1037-40.

56. Constantin, G., et al., *Chemokines trigger immediate beta2 integrin affinity and mobility changes: differential regulation and roles in lymphocyte arrest under flow.* Immunity, 2000. **13**(6): p. 759-69.

57. Kantele, J.M., S. Kurk, and M.A. Jutila, *Effects of continuous exposure to stromal cell-derived factor-1 alpha on T cell rolling and tight adhesion to monolayers of activated endothelial cells.* J Immunol, 2000. **164**(10): p. 5035-40.

58. Feil, C. and H.G. Augustin, *Endothelial cells differentially express functional CXC-chemokine receptor-4 (CXCR-4/fusin) under the control of autocrine activity and exogenous cytokines.* Biochem Biophys Res Commun, 1998. **247**(1): p. 38-45.

59. Gupta, S.K., et al., *Chemokine receptors in human endothelial cells. Functional expression of CXCR4 and its transcriptional regulation by inflammatory cytokines.* J Biol Chem, 1998. **273**(7): p. 4282-7.

60. Salcedo, R., et al., *Differential expression and responsiveness of chemokine receptors (CXCR1-3) by human microvascular endothelial cells and umbilical vein endothelial cells.* Faseb J, 2000. **14**(13): p. 2055-64.

61. Salcedo, R. and J.J. Oppenheim, *Role of chemokines in angiogenesis: CXCL12/SDF-1 and CXCR4 interaction, a key regulator of endothelial cell responses.* Microcirculation, 2003. **10**(3-4): p. 359-70.

62. Imai, K., et al., *Selective secretion of chemoattractants for haemopoietic progenitor cells by bone marrow endothelial cells: a possible role in homing of haemopoietic progenitor cells to bone marrow.* Br J Haematol, 1999. **106**(4): p. 905-11.

63. Pablos, J.L., et al., *Stromal-cell derived factor is expressed by dendritic cells and endothelium in human skin.* Am J Pathol, 1999. **155**(5): p. 1577-86.

64. Salvucci, O., et al., *Regulation of endothelial cell branching morphogenesis by endogenous chemokine stromal-derived factor-1.* Blood, 2002. **99**(8): p. 2703-11.

65. Peled, A., et al., *The chemokine SDF-1 stimulates integrin-mediated arrest of CD34(+) cells on vascular endothelium under shear flow.* J Clin Invest, 1999. **104**(9): p. 1199-211.

66. Shirozu, M., et al., *Structure and chromosomal localization of the human stromal cell-derived factor 1 (SDF1) gene.* Genomics, 1995. **28**(3): p. 495-500.

67. Salcedo, R., et al., *Vascular endothelial growth factor and basic fibroblast growth factor induce expression of CXCR4 on human endothelial cells: In vivo neovascularization induced by stromal-derived factor-1alpha.* Am J Pathol, 1999. **154**(4): p. 1125-35.

68. Grabovsky, V., et al., *Subsecond induction of alpha4 integrin clustering by immobilized chemokines stimulates leukocyte tethering and rolling on endothelial vascular cell adhesion molecule 1 under flow conditions.* J Exp Med, 2000. **192**(4): p. 495-506.

69. Chan, J.R., S.J. Hyduk, and M.I. Cybulsky, *Chemoattractants induce a rapid and transient upregulation of monocyte alpha4 integrin affinity for vascular cell adhesion molecule 1 which mediates arrest: an early step in the process of emigration.* J Exp Med, 2001. **193**(10): p. 1149-58.

70. Weber, C., J. Kitayama, and T.A. Springer, *Differential regulation of beta 1 and beta 2 integrin avidity by chemoattractants in eosinophils.* Proc Natl Acad Sci U S A, 1996. **93**(20): p. 10939-44.

71. Stewart, M.P., A. McDowall, and N. Hogg, *LFA-1-mediated adhesion is regulated by cytoskeletal restraint and by a Ca2+-dependent protease, calpain.* J Cell Biol, 1998. **140**(3): p. 699-707.

72. Yauch, R.L., et al., *Mutational evidence for control of cell adhesion through integrin diffusion/clustering, independent of ligand binding.* J Exp Med, 1997. **186**(8): p. 1347-55.

73. Bazzoni, G. and M.E. Hemler, *Are changes in integrin affinity and conformation overemphasized?* Trends Biochem Sci, 1998. **23**(1): p. 30-4.

74. Johnston, B. and E.C. Butcher, *Chemokines in rapid leukocyte adhesion triggering and migration.* Semin Immunol, 2002. **14**(2): p. 83-92.

75. Stewart, M.P., C. Cabanas, and N. Hogg, *T cell adhesion to intercellular adhesion molecule-1 (ICAM-1) is controlled by cell spreading and the activation of integrin LFA-1.* J Immunol, 1996. **156**(5): p. 1810-7.

76. Lawrence, M.B. and T.A. Springer, *Leukocytes roll on a selectin at physiologic flow rates: distinction from and prerequisite for adhesion through integrins.* Cell, 1991. **65**(5): p. 859-73.

77. Campbell, J.J., et al., *Chemokines and the arrest of lymphocytes rolling under flow conditions.* Science, 1998. **279**(5349): p. 381-4.

78. Gerszten, R.E., et al., *MCP-1 and IL-8 trigger firm adhesion of monocytes to vascular endothelium under flow conditions.* Nature, 1999. **398**(6729): p. 718-23.

79. Rainger, G.E., A.C. Fisher, and G.B. Nash, *Endothelial-borne platelet-activating factor and interleukin-8 rapidly immobilize rolling neutrophils.* Am J Physiol, 1997. **272**(1 Pt 2): p. H114-22.

80. Kitayama, J., et al., *The C-C chemokine receptor CCR3 participates in stimulation of eosinophil arrest on inflammatory endothelium in shear flow.* J Clin Invest, 1998. **101**(9): p. 2017-24.

81. Feigelson, S.W., et al., *The Src kinase p56(lck) up-regulates VLA-4 integrin affinity. Implications for rapid spontaneous and chemokine-*

triggered T cell adhesion to VCAM-1 and fibronectin. J Biol Chem, 2001. **276**(17): p. 13891-901.

82. Weber, C., et al., *Sequential regulation of alpha 4 beta 1 and alpha 5 beta 1 integrin avidity by CC chemokines in monocytes: implications for transendothelial chemotaxis.* J Cell Biol, 1996. **134**(4): p. 1063-73.
83. Oxvig, C. and T.A. Springer, *Experimental support for a beta-propeller domain in integrin alpha-subunits and a calcium binding site on its lower surface.* Proc Natl Acad Sci U S A, 1998. **95**(9): p. 4870-5.
84. Emsley, J., et al., *Structural basis of collagen recognition by integrin alpha2beta1.* Cell, 2000. **101**(1): p. 47-56.
85. Hynes, R.O., *Integrins: versatility, modulation, and signaling in cell adhesion.* Cell, 1992. **69**(1): p. 11-25.
86. Humphries, J.D., et al., *Molecular basis of ligand recognition by integrin alpha5beta 1. II. Specificity of arg-gly-Asp binding is determined by Trp157 OF THE alpha subunit.* J Biol Chem, 2000. **275**(27): p. 20337-45.
87. Arnaout, M.A., *Integrin structure: new twists and turns in dynamic cell adhesion.* Immunol Rev, 2002. **186**: p. 125-40.
88. van Kooyk, Y., S.J. van Vliet, and C.G. Figdor, *The actin cytoskeleton regulates LFA-1 ligand binding through avidity rather than affinity changes.* J Biol Chem, 1999. **274**(38): p. 26869-77.
89. Harris, E.S., et al., *The leukocyte integrins.* J Biol Chem, 2000. **275**(31): p. 23409-12.
90. Warnock, R.A., et al., *Molecular mechanisms of lymphocyte homing to peripheral lymph nodes.* J Exp Med, 1998. **187**(2): p. 205-16.
91. Alon, R. and S. Feigelson, *From rolling to arrest on blood vessels: leukocyte tap dancing on endothelial integrin ligands and chemokines at sub-second contacts.* Semin Immunol, 2002. **14**(2): p. 93-104.
92. Oppenheimer-Marks, N., et al., *Differential utilization of ICAM-1 and VCAM-1 during the adhesion and transendothelial migration of human T lymphocytes.* J Immunol, 1991. **147**(9): p. 2913-21.
93. Staunton, D.E., M.L. Dustin, and T.A. Springer, *Functional cloning of ICAM-2, a cell adhesion ligand for LFA-1 homologous to ICAM-1.* Nature, 1989. **339**(6219): p. 61-4.
94. Makgoba, M.W., et al., *ICAM-1 a ligand for LFA-1-dependent adhesion of B, T and myeloid cells.* Nature, 1988. **331**(6151): p. 86-8.
95. Walzog, B., et al., *A role for beta(2) integrins (CD11/CD18) in the regulation of cytokine gene expression of polymorphonuclear neutrophils during the inflammatory response.* Faseb J, 1999. **13**(13): p. 1855-65.
96. Jung, U., et al., *Transit time of leukocytes rolling through venules controls cytokine-induced inflammatory cell recruitment in vivo.* J Clin Invest, 1998. **102**(8): p. 1526-33.
97. Dobrina, A., et al., *Mechanisms of eosinophil adherence to cultured vascular endothelial cells. Eosinophils bind to the cytokine-induced ligand vascular cell adhesion molecule-1 via the very late activation antigen-4 integrin receptor.* J Clin Invest, 1991. **88**(1): p. 20-6.
98. Kubes, P., et al., *A novel beta 1-dependent adhesion pathway on neutrophils: a mechanism invoked by dihydrocytochalasin B or endothelial transmigration.* Faseb J, 1995. **9**(11): p. 1103-11.

99. Koni, P.A., et al., *Conditional vascular cell adhesion molecule 1 deletion in mice: impaired lymphocyte migration to bone marrow.* J Exp Med, 2001. **193**(6): p. 741-54.

100. Berlin-Rufenach, C., et al., *Lymphocyte migration in lymphocyte function-associated antigen (LFA)-1-deficient mice.* J Exp Med, 1999. **189**(9): p. 1467-78.

101. Dustin, M.L., O. Carpen, and T.A. Springer, *Regulation of locomotion and cell-cell contact area by the LFA-1 and ICAM-1 adhesion receptors.* J Immunol, 1992. **148**(9): p. 2654-63.

102. Weber, C. and T.A. Springer, *Interaction of very late antigen-4 with VCAM-1 supports transendothelial chemotaxis of monocytes by facilitating lateral migration.* J Immunol, 1998. **161**(12): p. 6825-34.

103. Henderson, R.B., et al., *The use of lymphocyte function-associated antigen (LFA)-1-deficient mice to determine the role of LFA-1, Mac-1, and alpha4 integrin in the inflammatory response of neutrophils.* J Exp Med, 2001. **194**(2): p. 219-26.

104. Carman, C.V., et al., *Endothelial cells proactively form microvilli-like membrane projections upon intercellular adhesion molecule 1 engagement of leukocyte LFA-1.* J Immunol, 2003. **171**(11): p. 6135-44.

105. Muller, W.A., *Leukocyte-endothelial-cell interactions in leukocyte transmigration and the inflammatory response.* Trends Immunol, 2003. **24**(6): p. 327-34.

106. Feng, D., et al., *Neutrophils emigrate from venules by a transendothelial cell pathway in response to FMLP.* J Exp Med, 1998. **187**(6): p. 903-15.

107. Dejana, E., M. Corada, and M.G. Lampugnani, *Endothelial cell-to-cell junctions.* Faseb J, 1995. **9**(10): p. 910-8.

108. Muller, W.A., et al., *A human endothelial cell-restricted, externally disposed plasmalemmal protein enriched in intercellular junctions.* J Exp Med, 1989. **170**(2): p. 399-414.

109. Newman, P.J., et al., *PECAM-1 (CD31) cloning and relation to adhesion molecules of the immunoglobulin gene superfamily.* Science, 1990. **247**(4947): p. 1219-22.

110. Muller, W.A., et al., *PECAM-1 is required for transendothelial migration of leukocytes.* J Exp Med, 1993. **178**(2): p. 449-60.

111. Liao, F., et al., *Migration of monocytes across endothelium and passage through extracellular matrix involve separate molecular domains of PECAM-1.* J Exp Med, 1995. **182**(5): p. 1337-43.

112. Liao, F., et al., *Soluble domain 1 of platelet-endothelial cell adhesion molecule (PECAM) is sufficient to block transendothelial migration in vitro and in vivo.* J Exp Med, 1997. **185**(7): p. 1349-57.

113. Duncan, G.S., et al., *Genetic evidence for functional redundancy of Platelet/Endothelial cell adhesion molecule-1 (PECAM-1): CD31-deficient mice reveal PECAM-1-dependent and PECAM-1-independent functions.* J Immunol, 1999. **162**(5): p. 3022-30.

114. Schenkel, A.R., et al., *CD99 plays a major role in the migration of monocytes through endothelial junctions.* Nat Immunol, 2002. **3**(2): p. 143-50.

115. Martin-Padura, I., et al., *Junctional adhesion molecule, a novel member of the immunoglobulin superfamily that distributes at intercellular junctions*

and modulates monocyte transmigration. J Cell Biol, 1998. **142**(1): p. 117-27.

116. Williams, L.A., et al., *Identification and characterisation of human Junctional Adhesion Molecule (JAM).* Mol Immunol, 1999. **36**(17): p. 1175-88.
117. Johnson-Leger, C.A., et al., *Junctional adhesion molecule-2 (JAM-2) promotes lymphocyte transendothelial migration.* Blood, 2002. **100**(7): p. 2479-86.
118. Ostermann, G., et al., *JAM-1 is a ligand of the beta(2) integrin LFA-1 involved in transendothelial migration of leukocytes.* Nat Immunol, 2002. **3**(2): p. 151-8.
119. Burns, A.R., et al., *Neutrophil transendothelial migration is independent of tight junctions and occurs preferentially at tricellular corners.* J Immunol, 1997. **159**(6): p. 2893-903.
120. Burns, A.R., et al., *Analysis of tight junctions during neutrophil transendothelial migration.* J Cell Sci, 2000. **113 (Pt 1)**: p. 45-57.
121. Roth, S.J., et al., *Characterization of transendothelial chemotaxis of T lymphocytes.* J Immunol Methods, 1995. **188**(1): p. 97-116.
122. Ding, Z., K. Xiong, and T.B. Issekutz, *Regulation of chemokine-induced transendothelial migration of T lymphocytes by endothelial activation: differential effects on naive and memory T cells.* J Leukoc Biol, 2000. **67**(6): p. 825-33.
123. Middleton, J., et al., *Transcytosis and surface presentation of IL-8 by venular endothelial cells.* Cell, 1997. **91**(3): p. 385-95.
124. Baekkevold, E.S., et al., *The CCR7 ligand elc (CCL19) is transcytosed in high endothelial venules and mediates T cell recruitment.* J Exp Med, 2001. **193**(9): p. 1105-12.
125. Cinamon, G., V. Shinder, and R. Alon, *Shear forces promote lymphocyte migration across vascular endothelium bearing apical chemokines.* Nat Immunol, 2001. **2**(6): p. 515-22.
126. Von Andrian, U.H., et al., *L-selectin function is required for beta 2-integrin-mediated neutrophil adhesion at physiological shear rates in vivo.* Am J Physiol, 1992. **263**(4 Pt 2): p. H1034-44.
127. Mancuso, F., R.J. Flower, and M. Perretti, *Leukocyte transmigration, but not rolling or adhesion, is selectively inhibited by dexamethasone in the hamster post-capillary venule. Involvement of endogenous lipocortin 1.* J Immunol, 1995. **155**(1): p. 377-86.
128. Fujimori, H., et al., *Intravital demonstration of modulation of T lymphocyte migration by CINC/gro in rat Peyer's patches.* Digestion, 2001. **63 Suppl 1**: p. 97-102.
129. Cinamon, G. and R. Alon, *A real time in vitro assay for studying leukocyte transendothelial migration under physiological flow conditions.* J Immunol Methods, 2003. **273**(1-2): p. 53-62.
130. Cooper, D., et al., *Transendothelial migration of neutrophils involves integrin-associated protein (CD47).* Proc Natl Acad Sci U S A, 1995. **92**(9): p. 3978-82.
131. Parkos, C.A., et al., *CD47 mediates post-adhesive events required for neutrophil migration across polarized intestinal epithelia.* J Cell Biol, 1996. **132**(3): p. 437-50.

132. Kitayama, J., et al., *Shear stress affects migration behavior of polymorphonuclear cells arrested on endothelium.* Cell Immunol, 2000. **203**(1): p. 39-46.

133. Weber, K.S., et al., *Differential immobilization and hierarchical involvement of chemokines in monocyte arrest and transmigration on inflamed endothelium in shear flow.* Eur J Immunol, 1999. **29**(2): p. 700-12.

134. Cuvelier, S.L. and K.D. Patel, *Shear-dependent eosinophil transmigration on interleukin 4-stimulated endothelial cells: a role for endothelium-associated eotaxin-3.* J Exp Med, 2001. **194**(12): p. 1699-709.

135. Cinamon, G., et al., *Novel chemokine functions in lymphocyte migration through vascular endothelium under shear flow.* J Leukoc Biol, 2001. **69**(6): p. 860-6.

136. Wu, Y., et al., *HoxB5 is an upstream transcriptional switch for differentiation of the vascular endothelium from precursor cells.* Mol Cell Biol, 2003. **23**(16): p. 5680-91.

137. Cines, D.B., et al., *Endothelial cells in physiology and in the pathophysiology of vascular disorders.* Blood, 1998. **91**(10): p. 3527-61.

138. Michiels, C., *Endothelial cell functions.* J Cell Physiol, 2003. **196**(3): p. 430-43.

139. Stevenson, B.R. and B.H. Keon, *The tight junction: morphology to molecules.* Annu Rev Cell Dev Biol, 1998. **14**: p. 89-109.

140. Corada, M., et al., *Vascular endothelial-cadherin is an important determinant of microvascular integrity in vivo.* Proc Natl Acad Sci U S A, 1999. **96**(17): p. 9815-20.

141. Dejana, E., *Endothelial adherens junctions: implications in the control of vascular permeability and angiogenesis.* J Clin Invest, 1996. **98**(9): p. 1949-53.

142. Ridley, A.J., et al., *Cell migration: integrating signals from front to back.* Science, 2003. **302**(5651): p. 1704-9.

143. Lee, T.Y. and A.I. Gotlieb, *Microfilaments and microtubules maintain endothelial integrity.* Microsc Res Tech, 2003. **60**(1): p. 115-27.

144. VandenBerg, E., et al., *The role of the cytoskeleton in cellular adhesion molecule expression in tumor necrosis factor-stimulated endothelial cells.* J Cell Biochem, 2004. **91**(5): p. 926-37.

145. Ettenson, D.S. and A.I. Gotlieb, *In vitro large-wound re-endothelialization. Inhibition of centrosome redistribution by transient inhibition of transcription after wounding prevents rapid repair.* Arterioscler Thromb, 1993. **13**(9): p. 1270-81.

146. Downing, K.H. and E. Nogales, *Tubulin and microtubule structure.* Curr Opin Cell Biol, 1998. **10**(1): p. 16-22.

147. Lee, J.S. and A.I. Gotlieb, *Microtubule-actin interactions may regulate endothelial integrity and repair.* Cardiovasc Pathol, 2002. **11**(3): p. 135-40.

148. Waterman-Storer, C.M. and E. Salmon, *Positive feedback interactions between microtubule and actin dynamics during cell motility.* Curr Opin Cell Biol, 1999. **11**(1): p. 61-7.

149. Joshi, H.C., *Microtubule dynamics in living cells.* Curr Opin Cell Biol, 1998. **10**(1): p. 35-44.

150. Cassimeris, L., *Accessory protein regulation of microtubule dynamics throughout the cell cycle.* Curr Opin Cell Biol, 1999. **11**(1): p. 134-41.

151. Hesse, M., T.M. Magin, and K. Weber, *Genes for intermediate filament proteins and the draft sequence of the human genome: novel keratin genes and a surprisingly high number of pseudogenes related to keratin genes 8 and 18.* J Cell Sci, 2001. **114**(Pt 14): p. 2569-75.

152. Helfand, B.T., L. Chang, and R.D. Goldman, *Intermediate filaments are dynamic and motile elements of cellular architecture.* J Cell Sci, 2004. **117**(Pt 2): p. 133-41.

153. Wong, M.K. and A.I. Gotlieb, *The reorganization of microfilaments, centrosomes, and microtubules during in vitro small wound reendothelialization.* J Cell Biol, 1988. **107**(5): p. 1777-83.

154. Colangelo, S., et al., *Alterations in endothelial F-actin microfilaments in rabbit aorta in hypercholesterolemia.* Arterioscler Thromb Vasc Biol, 1998. **18**(1): p. 52-6.

155. Ridley, A.J. and A. Hall, *The small GTP-binding protein rho regulates the assembly of focal adhesions and actin stress fibers in response to growth factors.* Cell, 1992. **70**(3): p. 389-99.

156. Kanzaki, M. and J.E. Pessin, *Insulin-stimulated GLUT4 translocation in adipocytes is dependent upon cortical actin remodeling.* J Biol Chem, 2001. **276**(45): p. 42436-44.

157. Condeelis, J., *Life at the leading edge: the formation of cell protrusions.* Annu Rev Cell Biol, 1993. **9**: p. 411-44.

158. Sheterline, P., J. Clayton, and J. Sparrow, *Actin.* Protein Profile, 1995. **2**(1): p. 1-103.

159. Pollard, T.D. and G.G. Borisy, *Cellular motility driven by assembly and disassembly of actin filaments.* Cell, 2003. **112**(4): p. 453-65.

160. Pollard, T.D., *Polymerization of ADP-actin.* J Cell Biol, 1984. **99**(3): p. 769-77.

161. dos Remedios, C.G., et al., *Actin binding proteins: regulation of cytoskeletal microfilaments.* Physiol Rev, 2003. **83**(2): p. 433-73.

162. Bamburg, J.R., *Proteins of the ADF/cofilin family: essential regulators of actin dynamics.* Annu Rev Cell Dev Biol, 1999. **15**: p. 185-230.

163. Goldschmidt-Clermont, P.J., et al., *Mechanism of the interaction of human platelet profilin with actin.* J Cell Biol, 1991. **113**(5): p. 1081-9.

164. Ionescu, C.V., et al., *Neutrophils induce sequential focal changes in endothelial adherens junction components: role of elastase.* Microcirculation, 2003. **10**(2): p. 205-20.

165. Gao, X., et al., *Reversibility of increased microvessel permeability in response to VE-cadherin disassembly.* Am J Physiol Lung Cell Mol Physiol, 2000. **279**(6): p. L1218-25.

166. Coughlin, S.R., *Thrombin signalling and protease-activated receptors.* Nature, 2000. **407**(6801): p. 258-64.

167. Kouklis, P., et al., *Cdc42 regulates the restoration of endothelial barrier function.* Circ Res, 2004. **94**(2): p. 159-66.

168. van Nieuw Amerongen, G.P., et al., *Activation of RhoA by thrombin in endothelial hyperpermeability: role of Rho kinase and protein tyrosine kinases.* Circ Res, 2000. **87**(4): p. 335-40.

169. Vouret-Craviari, V., et al., *Regulation of the actin cytoskeleton by thrombin in human endothelial cells: role of Rho proteins in endothelial barrier function.* Mol Biol Cell, 1998. **9**(9): p. 2639-53.

170. Tiruppathi, C., et al., *Role of Ca2+ signaling in the regulation of endothelial permeability.* Vascul Pharmacol, 2002. **39**(4-5): p. 173-85.

171. Del Maschio, A., et al., *Polymorphonuclear leukocyte adhesion triggers the disorganization of endothelial cell-to-cell adherens junctions.* J Cell Biol, 1996. **135**(2): p. 497-510.

172. Hermant, B., et al., *Identification of proteases involved in the proteolysis of vascular endothelium cadherin during neutrophil transmigration.* J Biol Chem, 2003. **278**(16): p. 14002-12.

173. Cepinskas, G., M. Sandig, and P.R. Kvietys, *PAF-induced elastase-dependent neutrophil transendothelial migration is associated with the mobilization of elastase to the neutrophil surface and localization to the migrating front.* J Cell Sci, 1999. **112 (Pt 12)**: p. 1937-45.

174. Carden, D., et al., *Neutrophil elastase promotes lung microvascular injury and proteolysis of endothelial cadherins.* Am J Physiol, 1998. **275**(2 Pt 2): p. H385-92.

175. Allport, J.R., et al., *Neutrophils from MMP-9- or neutrophil elastase-deficient mice show no defect in transendothelial migration under flow in vitro.* J Leukoc Biol, 2002. **71**(5): p. 821-8.

176. Carragher, N.O., et al., *Degraded collagen fragments promote rapid disassembly of smooth muscle focal adhesions that correlates with cleavage of pp125(FAK), paxillin, and talin.* J Cell Biol, 1999. **147**(3): p. 619-30.

177. Adamson, P., et al., *Lymphocyte migration through brain endothelial cell monolayers involves signaling through endothelial ICAM-1 via a rho-dependent pathway.* J Immunol, 1999. **162**(5): p. 2964-73.

178. Etienne-Manneville, S., et al., *ICAM-1-coupled cytoskeletal rearrangements and transendothelial lymphocyte migration involve intracellular calcium signaling in brain endothelial cell lines.* J Immunol, 2000. **165**(6): p. 3375-83.

179. Su, W.H., et al., *Endothelial [Ca(2+)](i) signaling during transmigration of polymorphonuclear leukocytes.* Blood, 2000. **96**(12): p. 3816-22.

180. Saito, H., et al., *Endothelial myosin light chain kinase regulates neutrophil migration across human umbilical vein endothelial cell monolayer.* J Immunol, 1998. **161**(3): p. 1533-40.

181. Kielbassa-Schnepp, K., et al., *Endothelial intracellular Ca2+ release following monocyte adhesion is required for the transendothelial migration of monocytes.* Cell Calcium, 2001. **30**(1): p. 29-40.

182. Resnick, N., et al., *Fluid shear stress and the vascular endothelium: for better and for worse.* Prog Biophys Mol Biol, 2003. **81**(3): p. 177-99.

183. Fujiwara, K., et al., *Is PECAM-1 a mechanoresponsive molecule?* Cell Struct Funct, 2001. **26**(1): p. 11-7.

184. Dejana, E., et al., *The molecular organization of endothelial junctions and their functional role in vascular morphogenesis and permeability.* Int J Dev Biol, 2000. **44**(6): p. 743-8.

185. Dejana, E., R. Spagnuolo, and G. Bazzoni, *Interendothelial junctions and their role in the control of angiogenesis, vascular permeability and leukocyte transmigration.* Thromb Haemost, 2001. **86**(1): p. 308-15.

186. Shay-Salit, A., et al., *VEGF receptor 2 and the adherens junction as a mechanical transducer in vascular endothelial cells.* Proc Natl Acad Sci U S A, 2002. **99**(14): p. 9462-7.

187. Ingber, D., *In search of cellular control: signal transduction in context.* J Cell Biochem Suppl, 1998. **30-31**: p. 232-7.

188. Muller, J.M., W.M. Chilian, and M.J. Davis, *Integrin signaling transduces shear stress--dependent vasodilation of coronary arterioles.* Circ Res, 1997. **80**(3): p. 320-6.

189. Bhullar, I.S., et al., *Fluid shear stress activation of IkappaB kinase is integrin-dependent.* J Biol Chem, 1998. **273**(46): p. 30544-9.

190. Chen, K.D., et al., *Mechanotransduction in response to shear stress. Roles of receptor tyrosine kinases, integrins, and Shc.* J Biol Chem, 1999. **274**(26): p. 18393-400.

191. Takahashi, M. and B.C. Berk, *Mitogen-activated protein kinase (ERK1/2) activation by shear stress and adhesion in endothelial cells. Essential role for a herbimycin-sensitive kinase.* J Clin Invest, 1996. **98**(11): p. 2623-31.

192. Jo, H., et al., *Differential effect of shear stress on extracellular signal-regulated kinase and N-terminal Jun kinase in endothelial cells. Gi2- and Gbeta/gamma-dependent signaling pathways.* J Biol Chem, 1997. **272**(2): p. 1395-401.

193. Gudi, S.R., C.B. Clark, and J.A. Frangos, *Fluid flow rapidly activates G proteins in human endothelial cells. Involvement of G proteins in mechanochemical signal transduction.* Circ Res, 1996. **79**(4): p. 834-9.

194. Imberti, B., et al., *Shear stress-induced cytoskeleton rearrangement mediates NF-kappaB-dependent endothelial expression of ICAM-1.* Microvasc Res, 2000. **60**(2): p. 182-8.

195. Levesque, M.J. and R.M. Nerem, *The elongation and orientation of cultured endothelial cells in response to shear stress.* J Biomech Eng, 1985. **107**(4): p. 341-7.

196. Schnittler, H.J., et al., *Role of actin filaments in endothelial cell-cell adhesion and membrane stability under fluid shear stress.* Pflugers Arch, 2001. **442**(5): p. 675-87.

197. Noria, S., et al., *Assembly and reorientation of stress fibers drives morphological changes to endothelial cells exposed to shear stress.* Am J Pathol, 2004. **164**(4): p. 1211-23.

198. Sun, D., et al., *Endothelial microtubule disruption blocks flow-dependent dilation of arterioles.* Am J Physiol Heart Circ Physiol, 2001. **280**(5): p. H2087-93.

199. Langille, B.L., *Morphologic responses of endothelium to shear stress: reorganization of the adherens junction.* Microcirculation, 2001. **8**(3): p. 195-206.

200. Hsieh, H.J., N.Q. Li, and J.A. Frangos, *Pulsatile and steady flow induces c-fos expression in human endothelial cells.* J Cell Physiol, 1993. **154**(1): p. 143-51.

201. Khachigian, L.M., et al., *Egr-1 is activated in endothelial cells exposed to fluid shear stress and interacts with a novel shear-stress-response element in the PDGF A-chain promoter.* Arterioscler Thromb Vasc Biol, 1997. **17**(10): p. 2280-6.

202. Resnick, N., et al., *Platelet-derived growth factor B chain promoter contains a cis-acting fluid shear-stress-responsive element.* Proc Natl Acad Sci U S A, 1993. **90**(10): p. 4591-5.

203. Nagel, T., et al., *Shear stress selectively upregulates intercellular adhesion molecule-1 expression in cultured human vascular endothelial cells.* J Clin Invest, 1994. **94**(2): p. 885-91.

204. Shyy, J.Y., et al., *The cis-acting phorbol ester "12-O-tetradecanoylphorbol 13-acetate"-responsive element is involved in shear stress-induced monocyte chemotactic protein 1 gene expression.* Proc Natl Acad Sci U S A, 1995. **92**(17): p. 8069-73.

205. Topper, J.N., et al., *Identification of vascular endothelial genes differentially responsive to fluid mechanical stimuli: cyclooxygenase-2, manganese superoxide dismutase, and endothelial cell nitric oxide synthase are selectively up-regulated by steady laminar shear stress.* Proc Natl Acad Sci U S A, 1996. **93**(19): p. 10417-22.

206. Ohno, M., et al., *Fluid shear stress induces endothelial transforming growth factor beta-1 transcription and production. Modulation by potassium channel blockade.* J Clin Invest, 1995. **95**(3): p. 1363-9.

207. Malek, A.M., A.L. Greene, and S. Izumo, *Regulation of endothelin 1 gene by fluid shear stress is transcriptionally mediated and independent of protein kinase C and cAMP.* Proc Natl Acad Sci U S A, 1993. **90**(13): p. 5999-6003.

208. Ando, J., et al., *Shear stress inhibits adhesion of cultured mouse endothelial cells to lymphocytes by downregulating VCAM-1 expression.* Am J Physiol, 1994. **267**(3 Pt 1): p. C679-87.

209. McCormick, S.M., et al., *DNA microarray reveals changes in gene expression of shear stressed human umbilical vein endothelial cells.* Proc Natl Acad Sci U S A, 2001. **98**(16): p. 8955-60.

210. Chen, B.P., et al., *DNA microarray analysis of gene expression in endothelial cells in response to 24-h shear stress.* Physiol Genomics, 2001. **7**(1): p. 55-63.

211. Goll, D.E., et al., *The calpain system.* Physiol Rev, 2003. **83**(3): p. 731-801.

212. Huttenlocher, A., et al., *Regulation of cell migration by the calcium-dependent protease calpain.* J Biol Chem, 1997. **272**(52): p. 32719-22.

213. Dourdin, N., et al., *Reduced cell migration and disruption of the actin cytoskeleton in calpain-deficient embryonic fibroblasts.* J Biol Chem, 2001. **276**(51): p. 48382-8.

214. Perrin, B.J. and A. Huttenlocher, *Calpain.* Int J Biochem Cell Biol, 2002. **34**(7): p. 722-5.

215. Tompa, P., et al., *Domain III of calpain is a ca2+-regulated phospholipid-binding domain.* Biochem Biophys Res Commun, 2001. **280**(5): p. 1333-9.

216. Johnson, G.V. and R.P. Guttmann, *Calpains: intact and active?* Bioessays, 1997. **19**(11): p. 1011-8.

217. Molinari, M. and E. Carafoli, *Calpain: a cytosolic proteinase active at the membranes.* J Membr Biol, 1997. **156**(1): p. 1-8.

218. Goll, D.E., et al., *Is calpain activity regulated by membranes and autolysis or by calcium and calpastatin?* Bioessays, 1992. **14**(8): p. 549-56.

219. Becker, P.L., et al., *Regulation of calcium concentration in voltage-clamped smooth muscle cells.* Science, 1989. **244**(4901): p. 211-4.

220. Berlin, J.R. and M. Konishi, *Ca2+ transients in cardiac myocytes measured with high and low affinity Ca2+ indicators.* Biophys J, 1993. **65**(4): p. 1632-47.

221. Harkins, A.B., N. Kurebayashi, and S.M. Baylor, *Resting myoplasmic free calcium in frog skeletal muscle fibers estimated with fluo-3.* Biophys J, 1993. **65**(2): p. 865-81.

222. Pontremoli, S., et al., *Role of phospholipids in the activation of the Ca2+-dependent neutral proteinase of human erythrocytes.* Biochem Biophys Res Commun, 1985. **129**(2): p. 389-95.

223. Saido, T.C., et al., *Positive regulation of mu-calpain action by polyphosphoinositides.* J Biol Chem, 1992. **267**(34): p. 24585-90.

224. Carragher, N.O., et al., *v-Src-induced modulation of the calpain-calpastatin proteolytic system regulates transformation.* Mol Cell Biol, 2002. **22**(1): p. 257-69.

225. Glading, A., et al., *Epidermal growth factor receptor activation of calpain is required for fibroblast motility and occurs via an ERK/MAP kinase signaling pathway.* J Biol Chem, 2000. **275**(4): p. 2390-8.

226. Glading, A., et al., *Membrane proximal ERK signaling is required for M-calpain activation downstream of epidermal growth factor receptor signaling.* J Biol Chem, 2001. **276**(26): p. 23341-8.

227. Shiraha, H., et al., *IP-10 inhibits epidermal growth factor-induced motility by decreasing epidermal growth factor receptor-mediated calpain activity.* J Cell Biol, 1999. **146**(1): p. 243-54.

228. Rock, M.T., et al., *Beta1 integrin-mediated T cell adhesion and cell spreading are regulated by calpain.* Exp Cell Res, 2000. **261**(1): p. 260-70.

229. Rock, M.T., W.H. Brooks, and T.L. Roszman, *Calcium-dependent signaling pathways in T cells. Potential role of calpain, protein tyrosine phosphatase 1b, and p130Cas in integrin-mediated signaling events.* J Biol Chem, 1997. **272**(52): p. 33377-83.

230. Hokin, L.E. and M.R. Hokin, *The Incorporation of 32p from Triphosphate into Polyphosphoinositides (Gamma-32p)Adenosine and Phosphatidic Acid in Erythrocyte Membranes.* Biochim Biophys Acta, 1964. **84**: p. 563-75.

231. Whipps, D.E., et al., *Effects of glucagon and Ca2+ on the metabolism of phosphatidylinositol 4-phosphate and phosphatidylinositol 4,5-bisphosphate in isolated rat hepatocytes and plasma membranes.* Biochem J, 1987. **241**(3): p. 835-45.

232. Kulkarni, S., et al., *Calpain mediates integrin-induced signaling at a point upstream of Rho family members.* J Biol Chem, 1999. **274**(30): p. 21265-75.

233. Bialkowska, K., et al., *Evidence that beta3 integrin-induced Rac activation involves the calpain-dependent formation of integrin clusters that are distinct from the focal complexes and focal adhesions that form as Rac and RhoA become active.* J Cell Biol, 2000. **151**(3): p. 685-96.

234. Potter, D.A., et al., *Calpain regulates actin remodeling during cell spreading.* J Cell Biol, 1998. **141**(3): p. 647-62.

235. Glading, A., D.A. Lauffenburger, and A. Wells, *Cutting to the chase: calpain proteases in cell motility.* Trends Cell Biol, 2002. **12**(1): p. 46-54.

236. Carragher, N.O. and M.C. Frame, *Calpain: a role in cell transformation and migration.* Int J Biochem Cell Biol, 2002. **34**(12): p. 1539-43.

237. Palecek, S.P., et al., *Physical and biochemical regulation of integrin release during rear detachment of migrating cells.* J Cell Sci, 1998. **111 (Pt 7)**: p. 929-40.

238. Bretscher, A., D. Reczek, and M. Berryman, *Ezrin: a protein requiring conformational activation to link microfilaments to the plasma membrane in the assembly of cell surface structures.* J Cell Sci, 1997. **110 (Pt 24)**: p. 3011-8.

239. Shuster, C.B. and I.M. Herman, *Indirect association of ezrin with F-actin: isoform specificity and calcium sensitivity.* J Cell Biol, 1995. **128**(5): p. 837-48.

240. Petruzzelli, L., M. Takami, and H.D. Humes, *Structure and function of cell adhesion molecules.* Am J Med, 1999. **106**(4): p. 467-76.

241. Olave, I.A., S.L. Reck-Peterson, and G.R. Crabtree, *Nuclear actin and actin-related proteins in chromatin remodeling.* Annu Rev Biochem, 2002. **71**: p. 755-81.

242. Gimbrone, M.A., Jr., *Culture of vascular endothelium.* Prog Hemost Thromb, 1976. **3**: p. 1-28.

243. Murray, A.G., et al., *Porcine aortic endothelial cells activate human T cells: direct presentation of MHC antigens and costimulation by ligands for human CD2 and CD28.* Immunity, 1994. **1**(1): p. 57-63.

244. Rosser, B.G., S.P. Powers, and G.J. Gores, *Calpain activity increases in hepatocytes following addition of ATP. Demonstration by a novel fluorescent approach.* J Biol Chem, 1993. **268**(31): p. 23593-600.

245. Madge, L.A. and J.S. Pober, *TNF signaling in vascular endothelial cells.* Exp Mol Pathol, 2001. **70**(3): p. 317-25.

246. Luscinskas, F.W., et al., *L- and P-selectins, but not CD49d (VLA-4) integrins, mediate monocyte initial attachment to TNF-alpha-activated vascular endothelium under flow in vitro.* J Immunol, 1996. **157**(1): p. 326-35.

247. Muller, A.M., et al., *Expression of the endothelial markers PECAM-1, vWf, and CD34 in vivo and in vitro.* Exp Mol Pathol, 2002. **72**(3): p. 221-9.

248. Scholz, D. and J. Schaper, *Platelet/endothelial cell adhesion molecule-1 (PECAM-1) is localized over the entire plasma membrane of endothelial cells.* Cell Tissue Res, 1997. **290**(3): p. 623-31.

249. Kurosaki, T., *Regulation of B-cell signal transduction by adaptor proteins.* Nat Rev Immunol, 2002. **2**(5): p. 354-63.

250. Baldini, M., et al., *A Polymorphism* in the 5' flanking region of the CD14 gene is associated with circulating soluble CD14 levels and with total serum immunoglobulin E.* Am J Respir Cell Mol Biol, 1999. **20**(5): p. 976-83.

251. Monneret, G., et al., *Analytical requirements for measuring monocytic human lymphocyte antigen DR by flow cytometry: application to the monitoring of patients with septic shock.* Clin Chem, 2002. **48**(9): p. 1589-92.

252. Givens, T.S., et al., *Regeneration and tolerance factor: a correlate of human immunodeficiency virus-associated T-cell activation.* Clin Diagn Lab Immunol, 1999. **6**(6): p. 872-7.

253. Hentzen, E.R., et al., *Sequential binding of CD11a/CD18 and CD11b/CD18 defines neutrophil capture and stable adhesion to intercellular adhesion molecule-1.* Blood, 2000. **95**(3): p. 911-20.

254. Lum, A.F., et al., *Dynamic regulation of LFA-1 activation and neutrophil arrest on intercellular adhesion molecule 1 (ICAM-1) in shear flow.* J Biol Chem, 2002. **277**(23): p. 20660-70.

255. Pfau, S., et al., *Lymphocyte adhesion-dependent calcium signaling in human endothelial cells.* J Cell Biol, 1995. **128**(5): p. 969-78.

256. Meyers, R. and L.C. Cantley, *Cloning and characterization of a wortmannin-sensitive human phosphatidylinositol 4-kinase.* J Biol Chem, 1997. **272**(7): p. 4384-90.

257. Wong, K. and L.C. Cantley, *Cloning and characterization of a human phosphatidylinositol 4-kinase.* J Biol Chem, 1994. **269**(46): p. 28878-84.

258. Yano, H., et al., *Inhibition of histamine secretion by wortmannin through the blockade of phosphatidylinositol 3-kinase in RBL-2H3 cells.* J Biol Chem, 1993. **268**(34): p. 25846-56.

259. Okada, T., et al., *Blockage of chemotactic peptide-induced stimulation of neutrophils by wortmannin as a result of selective inhibition of phosphatidylinositol 3-kinase.* J Biol Chem, 1994. **269**(5): p. 3563-7.

260. Barreiro, O., et al., *Dynamic interaction of VCAM-1 and ICAM-1 with moesin and ezrin in a novel endothelial docking structure for adherent leukocytes.* J Cell Biol, 2002. **157**(7): p. 1233-45.

261. Stein, J.V., et al., *The CC chemokine thymus-derived chemotactic agent 4 (TCA-4, secondary lymphoid tissue chemokine, 6Ckine, exodus-2) triggers lymphocyte function-associated antigen 1-mediated arrest of rolling T lymphocytes in peripheral lymph node high endothelial venules.* J Exp Med, 2000. **191**(1): p. 61-76.

262. Luu, N.T., G.E. Rainger, and G.B. Nash, *Kinetics of the different steps during neutrophil migration through cultured endothelial monolayers treated with tumour necrosis factor-alpha.* J Vasc Res, 1999. **36**(6): p. 477-85.

263. Lum, H., et al., *Serum albumin decreases transendothelial permeability to macromolecules.* Microvasc Res, 1991. **42**(1): p. 91-102.

264. Yatomi, Y., et al., *Sphingosine 1-phosphate, a bioactive sphingolipid abundantly stored in platelets, is a normal constituent of human plasma and serum.* J Biochem (Tokyo), 1997. **121**(5): p. 969-73.

265. Garcia, J.G., et al., *Sphingosine 1-phosphate promotes endothelial cell barrier integrity by Edg-dependent cytoskeletal rearrangement.* J Clin Invest, 2001. **108**(5): p. 689-701.

266. Dudek, S.M., et al., *Pulmonary endothelial cell barrier enhancement by sphingosine 1-phosphate: Roles for cortactin and myosin light chain kinase.* J Biol Chem, 2004.

267. Kimura, T., et al., *The sphingosine 1-phosphate (S1P) receptor agonist FTY720 supports CXCR4-dependent migration and bone marrow homing of human CD34+ progenitor cells.* Blood, 2004.

268. Okamoto, H., et al., *Inhibitory regulation of Rac activation, membrane ruffling, and cell migration by the G protein-coupled sphingosine-1-phosphate receptor EDG5 but not EDG1 or EDG3.* Mol Cell Biol, 2000. **20**(24): p. 9247-61.

269. Gopalan, P.K., et al., *Preferential sites for stationary adhesion of neutrophils to cytokine-stimulated HUVEC under flow conditions.* J Leukoc Biol, 2000. **68**(1): p. 47-57.

270. Kitayama, J., et al., *Alpha 6 beta 1 integrin (VLA-6) mediates leukocyte tether and arrest on laminin under physiological shear flow.* Cell Immunol, 2000. **199**(2): p. 97-103.

271. Sandig, M., E. Negrou, and K.A. Rogers, *Changes in the distribution of LFA-1, catenins, and F-actin during transendothelial migration of monocytes in culture.* J Cell Sci, 1997. **110 (Pt 22)**: p. 2807-18.

272. Adamson, P., et al., *Lymphocyte trafficking through the blood-brain barrier is dependent on endothelial cell heterotrimeric G-protein signaling.* Faseb J, 2002. **16**(10): p. 1185-94.

273. Lehmann, J.C., et al., *Overlapping and selective roles of endothelial intercellular adhesion molecule-1 (ICAM-1) and ICAM-2 in lymphocyte trafficking.* J Immunol, 2003. **171**(5): p. 2588-93.

274. Gurubhagavatula, I., et al., *Engagement of human PECAM-1 (CD31) on human endothelial cells increases intracellular calcium ion concentration and stimulates prostacyclin release.* J Clin Invest, 1998. **101**(1): p. 212-22.

275. Cooray, P., et al., *Focal adhesion kinase (pp125FAK) cleavage and regulation by calpain.* Biochem J, 1996. **318 (Pt 1)**: p. 41-7.

276. Liu, X. and R.G. Schnellmann, *Calpain mediates progressive plasma membrane permeability and proteolysis of cytoskeleton-associated paxillin, talin, and vinculin during renal cell death.* J Pharmacol Exp Ther, 2003. **304**(1): p. 63-70.

277. Rios-Doria, J., et al., *The role of calpain in the proteolytic cleavage of E-cadherin in prostate and mammary epithelial cells.* J Biol Chem, 2003. **278**(2): p. 1372-9.

278. Kulkarni, S., D.E. Goll, and J.E. Fox, *Calpain cleaves RhoA generating a dominant-negative form that inhibits integrin-induced actin filament assembly and cell spreading.* J Biol Chem, 2002. **277**(27): p. 24435-41.

279. Serrador, J.M., et al., *Moesin interacts with the cytoplasmic region of intercellular adhesion molecule-3 and is redistributed to the uropod of T lymphocytes during cell polarization.* J Cell Biol, 1997. **138**(6): p. 1409-23.

280. Heiska, L., et al., *Association of ezrin with intercellular adhesion molecule-1 and -2 (ICAM-1 and ICAM-2). Regulation by phosphatidylinositol 4, 5-bisphosphate.* J Biol Chem, 1998. **273**(34): p. 21893-900.

281. Fujitani, K., et al., *Identification of mu-, m-calpains and calpastatin and capture of mu-calpain activation in endothelial cells.* J Cell Biochem, 1997. **66**(2): p. 197-209.

282. Ariyoshi, H., et al., *Localized activation of m-calpain in migrating human umbilical vein endothelial cells stimulated by shear stress.* J Cell Biochem, 2001. **81**(1): p. 184-92.

283. Rana, R.S. and L.E. Hokin, *Role of phosphoinositides in transmembrane signaling.* Physiol Rev, 1990. **70**(1): p. 115-64.

284. Anderson, R.A., et al., *Phosphatidylinositol phosphate kinases, a multifaceted family of signaling enzymes.* J Biol Chem, 1999. **274**(15): p. 9907-10.

285. Rodriguez-Viciana, P., et al., *Phosphatidylinositol-3-OH kinase as a direct target of Ras.* Nature, 1994. **370**(6490): p. 527-32.

286. Rodriguez-Viciana, P., et al., *Role of phosphoinositide 3-OH kinase in cell transformation and control of the actin cytoskeleton by Ras.* Cell, 1997. **89**(3): p. 457-67.

287. Ma, A.D., et al., *Cytoskeletal reorganization by G protein-coupled receptors is dependent on phosphoinositide 3-kinase gamma, a Rac guanosine exchange factor, and Rac.* Mol Cell Biol, 1998. **18**(8): p. 4744-51.

288. Mercurio, A.M. and I. Rabinovitz, *Towards a mechanistic understanding of tumor invasion--lessons from the alpha6beta 4 integrin.* Semin Cancer Biol, 2001. **11**(2): p. 129-41.

289. Qian, Y., et al., *PI3K induced actin filament remodeling through Akt and p70S6K1: implication of essential role in cell migration.* Am J Physiol Cell Physiol, 2004. **286**(1): p. C153-63.

290. Lane, R.D., D.M. Allan, and R.L. Mellgren, *A comparison of the intracellular distribution of mu-calpain, m-calpain, and calpastatin in proliferating human A431 cells.* Exp Cell Res, 1992. **203**(1): p. 5-16.

291. Flatau, G., et al., *Toxin-induced activation of the G protein p21 Rho by deamidation of glutamine.* Nature, 1997. **387**(6634): p. 729-33.

292. Brest, P., et al., *Rho GTPase is activated by cytotoxic necrotizing factor 1 in peripheral blood T lymphocytes: potential cytotoxicity for intestinal epithelial cells.* Infect Immun, 2003. **71**(3): p. 1161-9.

APPENDIX

APPENDIX A: FUTURE EXPERIMENTS

A.1 RATIONALE

The data presented answers many questions about the role of the EC cytoskeleton in mediating PBL TEM however, many new questions arise. Importantly, what other molecules are involved in the signalling pathways to F-actin remodelling in guiding PBL TEM? One candidate pathway we have considered is the Rho GTPase signalling pathway. Calpain has been implicated in cell spreading upstream of Rho-mediated signalling [213], and therefore Rho GTPases are an excellent candidate for further investigation. In pilot studies we have looked at ROCK; a serine/threonine kinase effecter of Rho A. ROCK becomes activated when it selectively binds to the active Rho. Activated ROCK interacts with the actin cytoskeleton to promote stress-fibre formation and assembly of focal contacts [290]. It appears that the Rho family will be the next logical target to explore in deciphering the pathway of EC F-actin remodelling required for efficient PBL TEM.

A.2 PRELIMINARY RESULTS

A.2.1 EC ROCK's Involvement in Lymphocyte TEM

The Rho signaling pathway was attacked to see its involvement in PBL TEM. We used Y27632, a selective inhibitor of ROCK; a serine/threonine kinase effecter of Rho A, in our parallel plate laminar flow adhesion assay. HUVECs pretreated with Y27632 show a modest decrease in PBL TEM (Figure A.1). Error bars are significantly large but the trend shown appears to be a dose dependent decrease in PBL TEM.

A.2.2 CNF-1 Rho Mobility Shift Assay

To further our study of the Rho pathway in PBL TEM, we plan on testing the effect of CNF-1 on HUVECs. CNF-1 permanent locks Rho GTP-binding proteins in their active state by the deamidation of Rho Glu^{63} residue [291]. The deamidation of Rho Glu^{63} by CNF-1 is accompanied by a decrease in the electrophoretic mobility of the protein during SDS PAGE [292]. Various concentrations of CNF-1 were used to treat HUVECs for 16 h. This was attempted to discover which concentrations would be optimal for use in our flow assay. CNF-1 treatments from 0.1 – 5.0 nM all lead to the decrease in electrophoretic mobility or an upward shift on the western blot (Figure A.2). However, HUVEC monolayers were increasingly less confluent with higher concentrations of CNF-1 treatment.

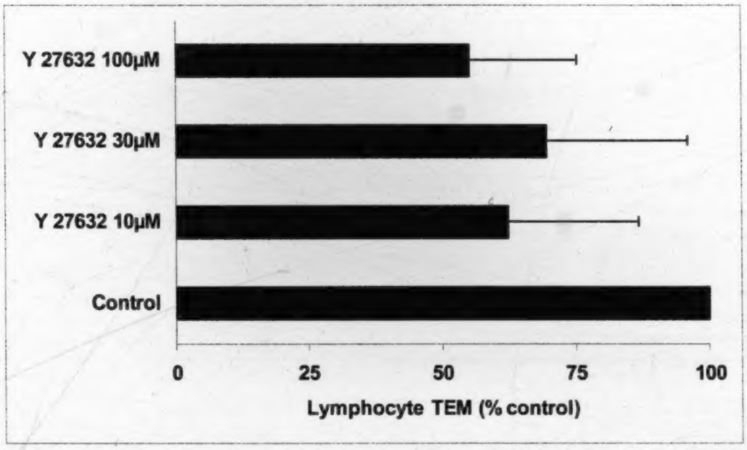

Figure A.1 Endothelial ROCK inhibition decreases lymphocyte TEM. HUVECs were then left untreated or pretreated with Y 27632, a selective inhibitor of the serine/threonine kinase effecter of Rho A, ROCK. HUVECs were treated for 30 min prior to the assembly of the laminar flow chamber as described in Materials and Methods. The fraction of transmigrating lymphocytes was determined as in Figure 3.6. Data are mean ± SEM of three experiments.

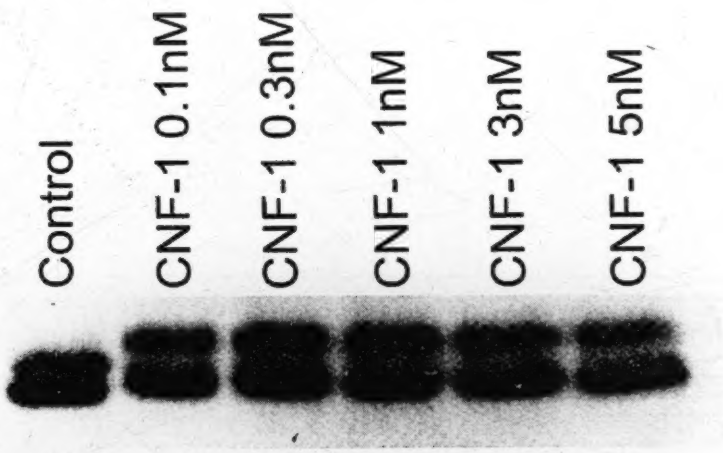

Figure A.2 CNF-1 stimulated Rho A activation. HUVECs were left untreated of pretreated for 16 h with the indicated concentrations of CNF-1. HUVEC cells were lysed and the lysate was run on 7.5% SDS-Page and transferred to a PVDF membrane. Lysates were then stained with anti-Rho A (24 kDa). Immunoblots are representative of three independent experiments.

APPENDIX B: ANALYSIS VIDEOS (CD – QUICKTIME REQUIRED)

Video B.1 Lymphocyte are able adhere to the HUVEC monolayer but efficient TEM is absent. HUVECs were TNF-*α* stimulated as described in Materials and Methods. Lymphocytes attach to the surface and remain stationary. Very few lymphocytes transmigrate through the HUVEC monolayer. Lymphocytes that turn from phase bright to phase dark are considered transmigrating.

Video B.2 Efficient PBL TEM requires SDF-1*α* pretreatment of HUVECs. HUVECs were TNF-*α* and SDF-1*α* stimulated as described in Materials and Methods. Lymphocytes become locomotive and migrate in all directions on the HUVEC monolayer. Lymphocytes that turn from phase bright to phase dark are considered transmigrating.

Video B.3 Stabilization of the endothelial F-actin cytoskeleton inhibits lymphocyte TEM. (A) HUVECs were TNF-*α* and SDF-1*α* stimulated as described in Materials and Methods. Lymphocytes become locomotive and migrate in all directions on the HUVEC monolayer. Lymphocytes that turn from phase bright to phase dark are considered transmigrating. **(B)** HUVECs were pretreated with JAS (300 nM; 1 h) before the assembly of the laminar flow chamber as described in Materials and Methods. Lymphocytes are able to become locomotive and migrate on the HUVEC monolayer, however lymphocyte TEM is inhibited.

Video B.4 EC F-Actin localizes to areas of lymphocyte TEM. Confocal fluorescence imaging was used to acquire images of YFP-Actin (green) expressing HUVECs through which CMTMR stained PBLs (red) are transmigrating. Z slices of 0.2 µm were collected every 2 min over a 40 min period. Actin condenses to the migration pore. Video show a slice midway through the cell. Data are representative of three experiments.

Video B.5 Cytoplasmic clumping around the migration pore is absent. Confocal fluorescence imaging was used to acquire images of CMFDA stained HUVECs (green) through which CMTMR stained PBLs (red) are transmigrating. Z slices of 0.2 µm were collected every 2 min over a 40 min period. There is no increase in fluorescence around the migration pore. Video show a slice midway through the cell. Data are representative of three experiments.

Video B.6 Endothelial calpain activity is required for efficient lymphocyte TEM. (A) HUVECs were TNF-*α* and SDF-1*α* stimulated as described in Materials and Methods. Lymphocytes become locomotive and migrate in all directions on the HUVEC monolayer. Lymphocytes that turn from phase bright to phase dark are considered transmigrating. **(B)** HUVECs were pretreated with PD 1506060 (100 µM; 1h) before the assembly of the laminar flow chamber as described in Materials and Methods. Lymphocytes are able to become locomotive and migrate on the HUVEC monolayer, however lymphocyte TEM is inhibited.